



***In vivo* imaging and optogenetic approach to study the
formation of olfactory memory and locomotor behaviour
in *Drosophila melanogaster***

Dissertation zur Erlangung des
naturwissenschaftlichen Doktorgrades
der Julius-Maximilians-Universität Würzburg

vorgelegt von

Alexander Kapustjansky
aus Winnica, Ukraine

Würzburg, 2011

Eingereicht am:

Mitglieder der Promotionskommission:

Vorsitzender:

Gutachter : Prof. Dr. Erich Buchner

Gutachter: Prof. Dr. Wolfgang Rössler

Tag des Promotionskolloquiums:

Doktorurkunde ausgehändigt am:

Erklärung

Erklärung gemäß § 4 Absatz 3 der Promotionsordnung der Fakultät für Biologie der Bayerischen Julius-Maximilians-Universität zu Würzburg von 15. März 1999.

Hiermit erkläre ich, die vorgelegte Dissertation selbständig angefertigt zu haben und keine anderen als die von mir angegebenen Quellen und Hilfsmittel benutzt zu haben. Alle aus der Literatur entnommenen Stellen sind als solche kenntlich gemacht. Des Weiteren erkläre ich, dass die vorliegende Arbeit weder in gleicher noch in ähnlicher Form bereits in einem anderem Prüfungsverfahren vorgelegt hat. Zuvor habe ich keine akademischen Grade erworben oder zu erwerben versucht.

Würzburg, den

.....

Alexander Kapustjansky

INDEX

1. SUMMARY	2
2. ZUSAMMENFASSUNG.....	4
3. INTRODUCTION.....	6
3.1. DROSOPHILA	6
3.2. GENETIC TOOLS.....	7
3.3. OPTOGENETICS	8
3.4. LEARNING AND MEMORY	12
3.5. LOCOMOTOR CONTROL AND ORIENTATION.....	16
3.6. AIMS OF THIS STUDY	19
4. METHODS.....	20
4.1. IMAGING	20
4.2. LOCOMOTOR CONTROL.....	38
4.3. SHOCKBOX.....	43
5. RESULTS	47
5.1. CAMP IMAGING	47
5.2. IMAGING AND OPTICAL ACTIVATION OF NEURONS IN WALKING FLIES.....	60
5.3. CONDITIONING IN THE "SHOCK BOX"	71
6. DISCUSSION	80
6.1. CAMP IMAGING	80
6.2. IMAGING AND OPTICAL ACTIVATION OF NEURONS IN WALKING FLIES.....	86
6.3. CONDITIONING IN THE "SHOCK BOX"	89
7. LITERATURE.....	92
8. CURRICULUM VITAE	97
9. ACKNOWLEDGEMENTS.....	99

1. Summary

Understanding of complex interactions and events in a nervous system, leading from the molecular level up to certain behavioural patterns calls for interdisciplinary interactions of various research areas. The goal of the presented work is to achieve such an interdisciplinary approach to study and manipulate animal behaviour and its underlying mechanisms.

Optical *in vivo* imaging is a new constantly evolving method, allowing one to study not only the local but also wide reaching activity in the nervous system. Due to ease of its genetic accessibility *Drosophila melanogaster* represents an extraordinary experimental organism to utilize not only imaging but also various optogenetic techniques to study the neuronal underpinnings of behaviour.

In this study four genetically encoded sensors were used to investigate the temporal dynamics of cAMP concentration changes in the horizontal lobes of the mushroom body, a brain area important for learning and memory, in response to various physiological and pharmacological stimuli. Several transgenic lines with various genomic insertion sites for the sensor constructs Epac1, Epac2, Epac2K390E and HCN2 were screened for the best signal quality, one line was selected for further experiments. The *in vivo* functionality of the sensor was assessed via pharmacological application of 8-bromo-cAMP as well as Forskolin, a substance stimulating cAMP producing adenylyl cyclases. This was followed by recording of the cAMP dynamics in response to the application of dopamine and octopamine, as well as to the presentation of electric shock, odorants or a simulated olfactory signal, induced by acetylcholine application to the observed brain area. In addition the interaction between the shock and the simulated olfactory signal by simultaneous presentation of both stimuli was studied. Preliminary results are supporting a coincidence detection mechanism at the level of the adenylyl cyclase as postulated by the present model for classical olfactory conditioning.

In a second series of experiments an effort was made to selectively activate a subset of neurons via the optogenetic tool Channelrhodopsin (ChR2). This was achieved by recording the behaviour of the fly in a walking ball paradigm. A new method was developed to analyse the walking behaviour of the animal whose brain was made optically accessible via a dissection technique, as used for imaging, thus allowing one to target selected brain areas. Using the Gal4-UAS system the protocerebral bridge, a substructure of the central complex, was highlighted by expressing the ChR2 tagged by fluorescent protein EYFP. First behavioural recordings of such specially prepared animals were made.

Summary

Lastly a new experimental paradigm for single animal conditioning was developed (Shock Box). Its design is based on the established Heat Box paradigm, however in addition to spatial and operant conditioning available in the Heat Box, the design of the new paradigm allows one to set up experiments to study classical and semioperant olfactory conditioning, as well as semioperant place learning and operant no idleness experiments. First experiments involving place learning were successfully performed in the new apparatus.

2. Zusammenfassung

Das Verständnis für die komplexen Interaktionen und Zusammenhänge, die von der molekularen Ebene bis zum Auftreten von bestimmten Verhaltensmustern führen, erfordert die interdisziplinäre Zusammenarbeit unterschiedlicher Forschungsrichtungen. Das Ziel der vorgelegten Arbeit war es einen solchen interdisziplinären Ansatz für die Erforschung und die Manipulation von Verhalten und ihm zu Grunde liegenden Mechanismen zu verwirklichen.

Optisches *in vivo Imaging* ist eine neue, sich ständig weiterentwickelnde Methode, welche es ermöglicht, nicht nur lokale sondern auch weitläufige Aktivitäten innerhalb des Nervensystem zu untersuchen. *Drosophila melanogaster* stellt aufgrund der leichten genetischen Zugänglichkeit einen herausragenden experimentellen Organismus dar, bei welchem neben optischem Imaging eine ganze Reihe optogenetischer Methoden angewandt werden kann, um die neuronalen Grundlagen des Verhaltens zu erforschen.

Im Rahmen dieser Arbeit wurde mit Hilfe von vier genetisch kodierten Sensoren *in vivo* die Dynamik der cAMP Konzentration in den horizontalen Loben des Pilzkörpers, bei Applikation unterschiedlicher physiologischer und pharmazeutischer Stimuli untersucht. Dabei wurden mehrere transgene Fliegenlinien mit Sensorkonstrukten Epac1, Epac2, Epac2K390E und HCN2 an unterschiedlichen genomischen Insertionsorten, hinsichtlich ihrer Signalqualität untersucht, eine der Linien wurde für weitere Experimente ausgewählt. Zunächst wurde an dieser die *in vivo* Tauglichkeit des Sensors gezeigt, indem die Konzentration von cAMP durch pharmakologische Applikationen von 8-Bromo-cAMP und Forskolin, einer Substanz welche die Aktivität von cAMP produzierenden Adenylatcyclasen stimuliert, appliziert wurden. Anschließend wurde eine Untersuchung der cAMP Dynamik als Antwort auf einen elektrischen Schock, unterschiedliche Düfte, sowie einen durch Applikation von Acetylcholin simulierten Duftstimulus durchgeführt. Vorläufige Ergebnisse bestärken das aktuelle Modell der klassischen olfaktorischen Konditionierung durch die Koinzidenzdetektion auf der Ebene der Adenylatcyclase.

In einem weiteren Experiment wurde der Versuch einer optogenetischen neuronalen Aktivierung unternommen, dabei wurde basierend auf einem Laufball Paradigma eine Methode entwickelt, das Laufverhalten der Fliegen zu analysieren während ihr Gehirn durch eine Imaging-Präparation freigelegt wurde, um gezielt bestimmte durch fluoreszierende Proteine markierte Gehirnbereiche

Zusammenfassung

anzuregen. Erste Aufzeichnungen des Laufverhaltens bei Aktivierung der protocerebralen Brücke, einer Substruktur des Zentralkomplexes, wurden durchgeführt.

Schließlich wurde eine neue Apparatur (Shock Box) für die Konditionierung von Einzeltieren entwickelt und gebaut, das Design beruht auf dem der sogenannten Heat Box, ermöglicht jedoch klassische und semioperante olfaktorische Konditionierung zusätzlich zu der in der Heat Box möglichen räumlichen und operanten Konditionierung. Die ersten Versuche für räumliches Lernen wurden in der Apparatur durchgeführt.

3. Introduction

The 20th century has seen some of the greatest breakthroughs and important steps towards understanding of the inner workings and processes of such a complex system as a brain, which guides, generates and processes information, from which behaviour arises.

Memory is often an integral part of goal oriented behaviour and plays a crucial role in both classical associative or operant learning. First and major steps towards investigation of conditioning and learning were made in vertebrates. However, already in the beginning of the last century invertebrates, insects in particular, proved to be suitable model organisms for behavioural studies revolving around learning and memory.

Modern day approach allows us to combine various biological disciplines such as the neurobiology, socio-biology, physiology, molecular biology and genetics, to gain a deeper understanding not only of individual steps and mechanism, but also of the greater picture of the formation and execution of behavioural patterns.

3.1. *Drosophila*

Being a classical model organism in genetics, the fruit fly *Drosophila melanogaster* came into prominence due to extensive work of Thomas Hunt Morgan and his colleagues around 1910, who observed the first known *Drosophila* mutant and expanded the work of Gregor Mendel by describing X-chromosome linked inheritance. Currently *Drosophila* poses as a crucial organism in research of human diseases, as approximately 75% of known human disease genes have a recognisable match in the genome of fruit flies (Adams 2000, Reiter et. al., 2001).

Featuring between 100.000-200.000 neurons the brain of *Drosophila* could be considered comparatively small and simple especially when compared to the complex brains of the vertebrates featuring more neurons by several orders of magnitude (Ito et al., 1998). Thus the tasks of mapping neuronal networks and understanding their interactions are much less daunting in such a model organism. A wide repertoire of behaviours ranging from simple phototaxis and geotaxis, to more complex locomotor and optomotor behaviour, to intricate behavioural patterns such as courtship behaviour, aggression, and olfactory behaviour, has been successfully described and studied in *Drosophila* opening a wide field for detailed future studies.

3.2. Genetic tools

Further advantages of the fruit fly lie primarily on the genetic level, with its short life cycle, relatively small genome size (Adams, 2000) , easy genetic accessibility, and the broad palette of genetic tools available. Thus non invasive manipulation of distinct parts of the brain and nervous system and even individual neurons is possible, providing a unique opportunity for neuronal, physiological and behavioural studies.

Selective expression

One of the most important and powerful genetic tools in *Drosophila* is the Gal4-UAS gene expression system (Fig 1.), consisting of the Gal4 driver construct and the UAS effector construct which can be separately maintained in different fly strains, with the desired gene expression taking place upon their crossing. Gal4 is a galactose transcription factor native to the yeast *Saccharomyces cerevisiae*, it contains three domains, a DNA-binding domain specifically recognised by the “upstream activating sequence” UAS, , a transcriptional activator domain, which can activate any gene being under the control of the UAS and a regulatory domain binding the galactose- sensitive inhibitory protein Gal80 (Fischer, 1988). For studies of developmental and immediate effects of protein synthesis Gal80ts a temperature sensitive repressor of Gal4 can be utilized. Recently an additional system (LexA) was developed, allowing for simultaneous selective expression of two transgenes in the same animal (Lai, Lee, 2006).

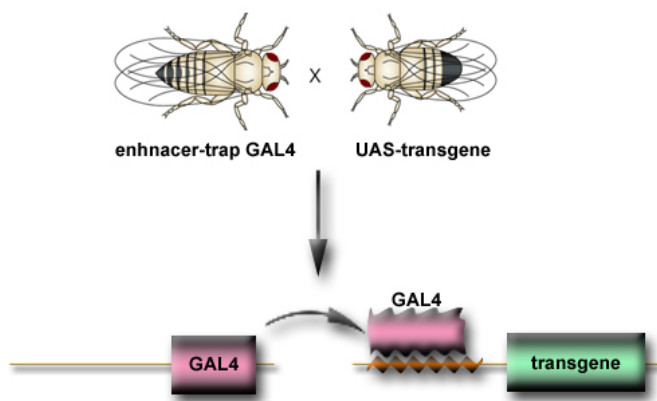


Figure 1: GAL4-UAS-System (Modified from Duffy, 2002)

3.3. Optogenetics

A prospective field in modern neurobiology, optogenetics is a blend of optical and genetic techniques which allows often non invasive monitoring and manipulation of various processes within an organism, and the nervous system in particular (Knöpfel, 2006). Emerging in the last decade this field of studies not only supplements but often substitutes the classical electrophysiological approaches to study a multitude of neuronal processes. The breadth of its application ranging from visualisation of intracellular processes to control and manipulation of behaviour (Miesenböck, 2004).

Visualisation

It took 30 years after the isolation of GFP from the light emitting organ of *Aequorea victoria*, to genetically characterise its encoding DNA. This event became the most important step in the transgenic approach to intracellular molecule visualisation and the invention of various fluorescent reporter proteins (Tsien, 1998). Although blue-cyan and yellowish green variants of GFP have been developed it took yet another group of marine organisms *Arthosoa* (coral animals) to introduce GFP-like fluorescent proteins encompassing the long wave band of the emission spectrum. Presently there is a large number of fluorescent proteins (Griesbeck, 2004), widely used in live imaging and immunohistochemistry (Fig.2)

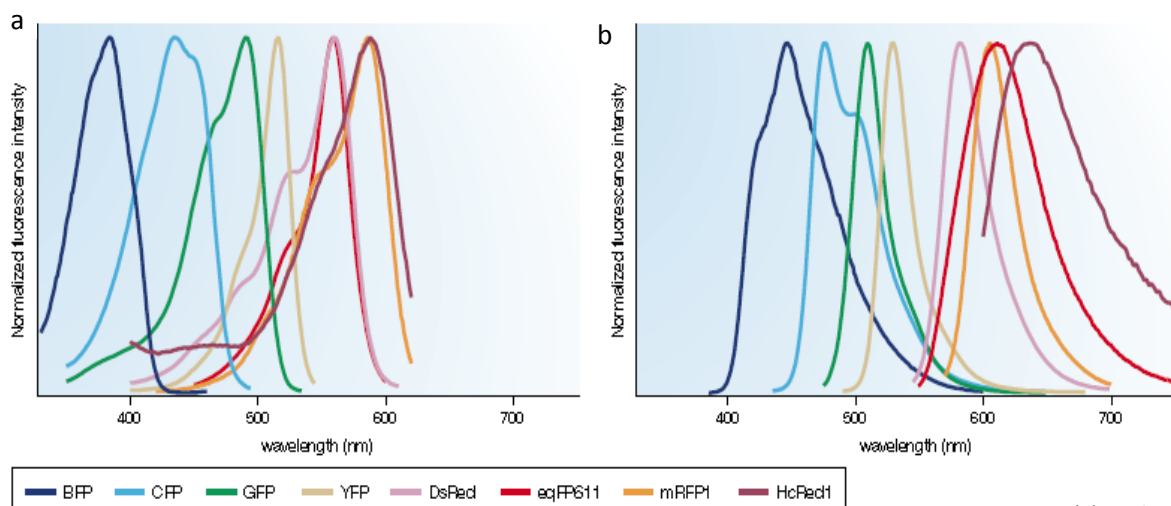


Figure 2: Excitation (a) and emission (b) spectra of various fluorescent proteins (Miyawaki 2003)

Monomeric Sensors

Monomeric fluorescent reporters provide an excellent option for live monitoring of various intercellular events. Allowing for a wide range of experiments to study processes like protein recovery ratios, investigation of diffusional movements as well as measurement of molecular cascade speeds and tracking of individual molecules (Knöpfel et al., 2010). Monomeric sensors found a broad

Introduction

area of application within the discipline of neurobiology in form of genetically encoded calcium indicators (GECI), presenting a modern approach to recording and monitoring of neuronal activity patterns. The quality and reliability of the currently available Calcium sensors steadily increases, promising new venues of noninvasive recording on par with electrophysiological data in the near future (Mank, 2006). One of the most prominent sensor designs based on a circularly permuted GFP variant is illustrated in Fig.3.

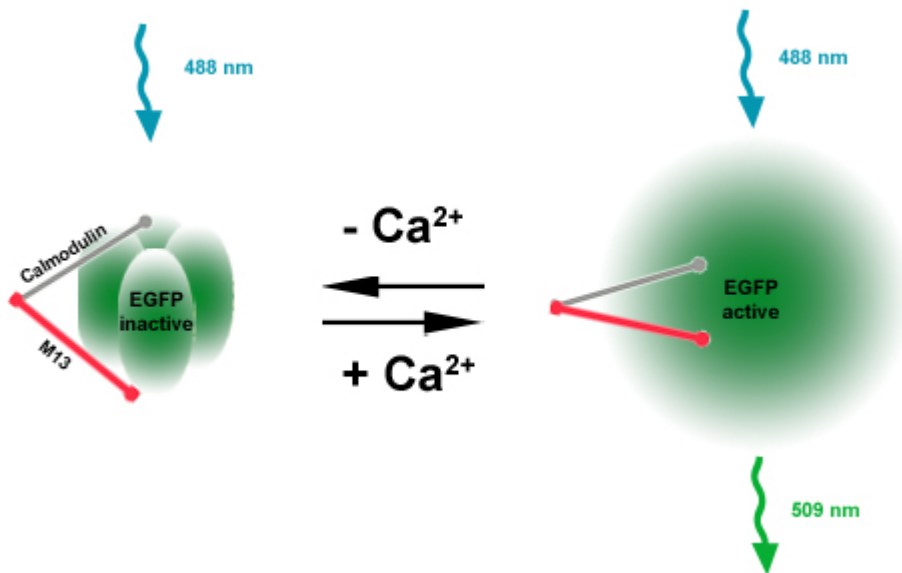


Figure 3: Working principle of the GCAMP-Sensor

Upon binding of Ca²⁺ to calmodulin, the inactive EGFP undergoes a conformational change and starts to emit fluorescence when excited by blue light (modified from Miyawaki 2003)

Ratiometric Sensors

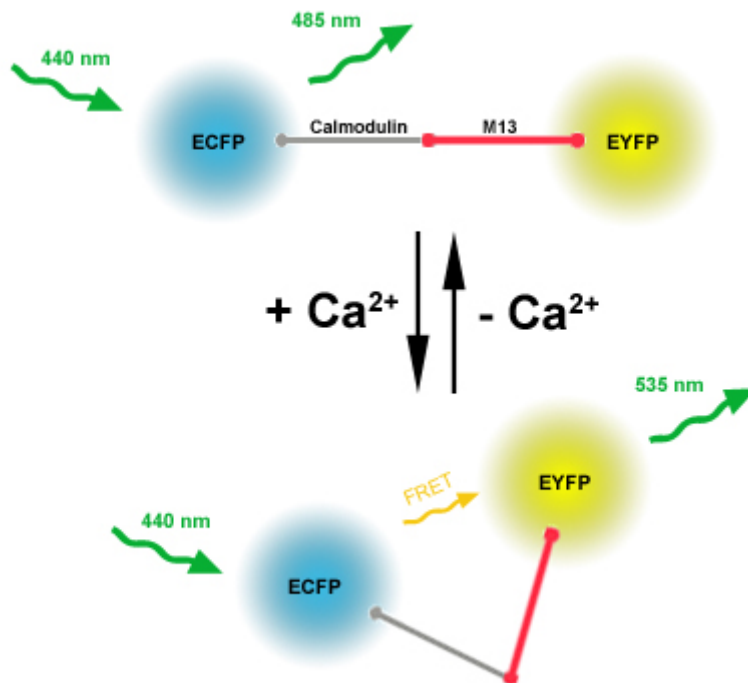


Figure 4: Working principle of the Cameleon 2.1 sensor

The fluorophores are fused to a complex of the Ca^{2+} binding domain of calmodulin and the M13 peptide. Upon binding of calcium the complex undergoes a conformation change leading to spatial bending of the molecule, bringing the fluorophores into a distance suitable for occurrence of FRET (modified from Miyawaki 2003)

In contrast to monomeric sensors, ratiometric reporters are far less prone to movement artifacts, and therefore better suited for imaging of tissues and organs *in-vivo* (Riemensperger et al., 2005). Their working principle is based on Förster resonance energy transfer (FRET) between two chromophores situated less than 10 nm from each other. Under these conditions the energy is transferred via nonradiative dipole-dipole coupling, from the electron excited donor to the acceptor chromophore. In cases where the transfer happens between two fluorophores the term fluorescence resonance energy transfer is sometimes used, however even such cases the transfer is always nonradiative.

A typical ratiometric fluorescent reporter consists of two fluorophores fused to a binding site for the molecule in question. Upon binding a conformation change in the sensor molecule is initialised bringing the fluorophores closer to each other or moving them farther apart, leading either to an increase or decrease in FRET, respectively (Miyawaki et al., 1999). The principle of operation of the ratiometric sensor Chameleon 2.1 is shown in Fig.4.

Photoactivation

The technique of photoactivation provides, unparalleled flexibility and control in noninvasive manipulation of neurons. One of the main molecular tools utilized in photoactivation studies is Channelrhodopsin-2 (Nagel et al 2003, Schroll et al., 2006) (Fig 5.). Being a sub-family of opsin proteins, channelrhodopsins can function as light gated Ion channels. Although three channelrhodopsins are currently known (Channelrhodopsin-1 (ChR1), Channelrhodopsin-2 (ChR2), and Volvox Channelrhodopsin (VChR1)), all of them function as unspecific cation channels (Nagel et al., 2003). Akin to G-Protein coupled receptors, channelrhodopsins consist of 7 transmembrane domains, however in contrast to metabotropic G-Protein coupled receptors opening channels via second messengers, channelrhodopsins form ion channels directly hence having an ionotropic function. The chromophore retinal (a derivate of vitamin A) is situated between the transmebrane domains and is prone to light induced isomerisation from an all-trans to a cis-trans state. This confirmation change causes the channel to open and leads to a cation influx and depolarization of the cell, expressing channelrhodopsin.

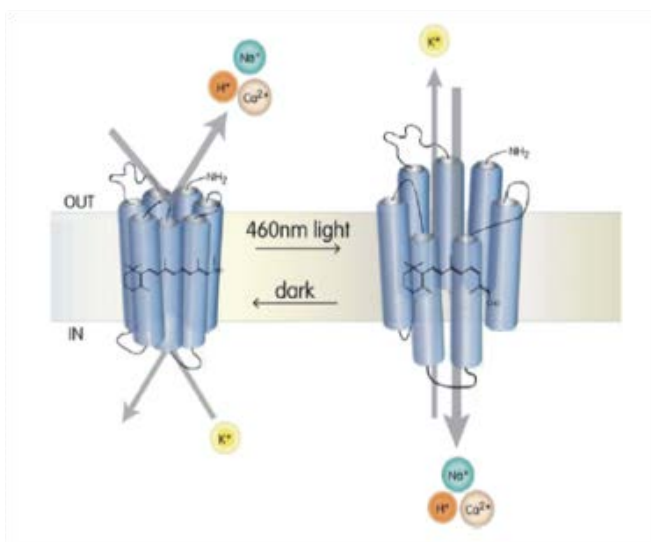


Figure 5: Working principle of channelrhodopsin-2, showing the formation of ion channel via light induced confirmation change in the rhetinal (Modified from Flannery and Greenberg 2006)

3.4. Learning and Memory

Two most prominent types of learning are the classical associative conditioning and the goal oriented operant conditioning. However a living organism always has some biological predispositions.

One of the first described scientific forays into the research field of learning and conditioning is accounted to A.Kreidl, an Austrian scientist, who reported the phenomenon of fishes being able to associate an acoustic signal with the availability of food (Kreidl 1895). In the beginning of the 20th century Ivan Pavlov a Russian scientist, published a comprehensive study concerning the ability of dogs to be trained to associate two different stimuli (Pavlov 1927). In parallel, particularly in the experiments by Karl von Frisch similar ability for associative learning was described for invertebrates (bees), this study laid the groundwork for the field of vision and visual learning research in invertebrates (von Frisch 1914).

First reported by Thorndike (Thorndike 1898) for cats trying to escape puzzle boxes and extensively researched by in the mid 20th century by the group of B.Skinner, the scientific community was provided with yet another form of learning phenomenon: the operant learning (Skinner, 1950). To display this type of learning the experimental animal is not constantly exposed to an unalterable pair of stimuli during training, but rather has to deduct the course of action necessary for either avoiding punishment, or receiving a reward, from its repertoire of available behaviours (which is limited by constraints of the experimental environment).

Yet although the behavioral components of both operant and associative learning were studied to a great extent in various animal models, first comprehensive insights into the neuronal functionality behind these phenomena were gained by the group of scientists associated with E.Kandel, who described for the sea slug *Aplysia*, the neuronal functionality leading to both classical and operant conditioning (Kandel et al., 2000).

Model organisms with a comparatively simple neuronal architecture are ideally suited for studies regarding neuronal and molecular mechanisms underlying learning behavior and memory formation, as was effectively demonstrated by Kandel (Kandel, 1976). *Drosophila melanogaster* with its unparalleled genetic accessibility and numerous readymade tools for manipulation of neuronal activity, proved to be an excellent experimental animal for such studies, allowing for over half a century of successful and ongoing research and constantly expanding scientific activity in this field. A

Introduction

second advantage of *Drosophila* is the scalable complexity of the nervous system studied, as most genetic and neuronal tools are viable not only in the adult animal, but also in larvae, possessing a drastically simplified neuronal architecture (Fig. 6), yet still displaying learning ability in associative conditioning situations comparable to those of the adult flies (e.g. associative learning based on chemosensation).

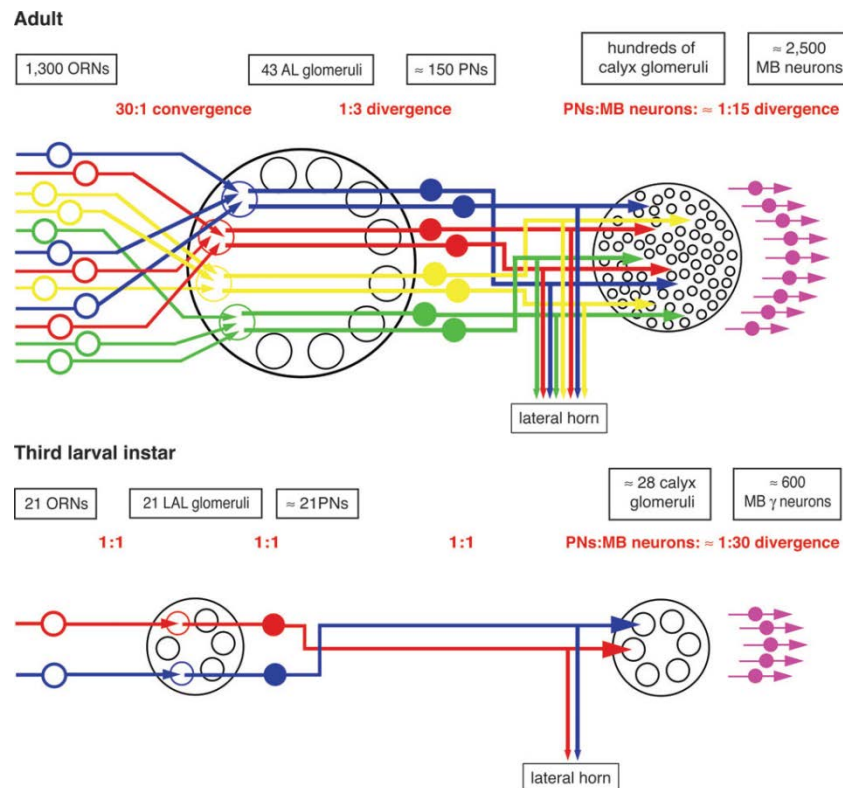


Figure 6: Model of olfactory memory pathway in *Drosophila*

Diagram visualising both the principal structural and network similarities, as well as the differences in the level of structural complexity, between adult and larva in *Drosophila*. Including figures for convergence and divergence of the number of neurons involved (Gerber, Stocker 2008)

High chemosensory/olfactory sensitivity is common in insects, thus providing a suitable conditioned stimulus (CS) which can be easily paired with a punitive (e.g. electric shock) or a rewarding (e.g. food availability/quality) unconditioned stimulus (US), due to this fact a comparatively simple yet reliable experimental design (Tully, Quinn 1985) which is with a few modifications still used in the present day, allows for easy assessment of associative learning and memory performance in *Drosophila*.

Type I adenylyl cyclase rutabaga was shown to be expressed in a high amount in the Kenyon cells of the mushroom bodies. It was reported that the ability to display associative learning and memory is

Introduction

impaired in both rutabaga mutants *rut²⁰⁸⁰* and *rut¹*. A group of scientists associated with Martin Heisenberg devised a model for the neuronal and molecular mechanisms of short term memory displaying functional parallels to the findings in Aplysia.

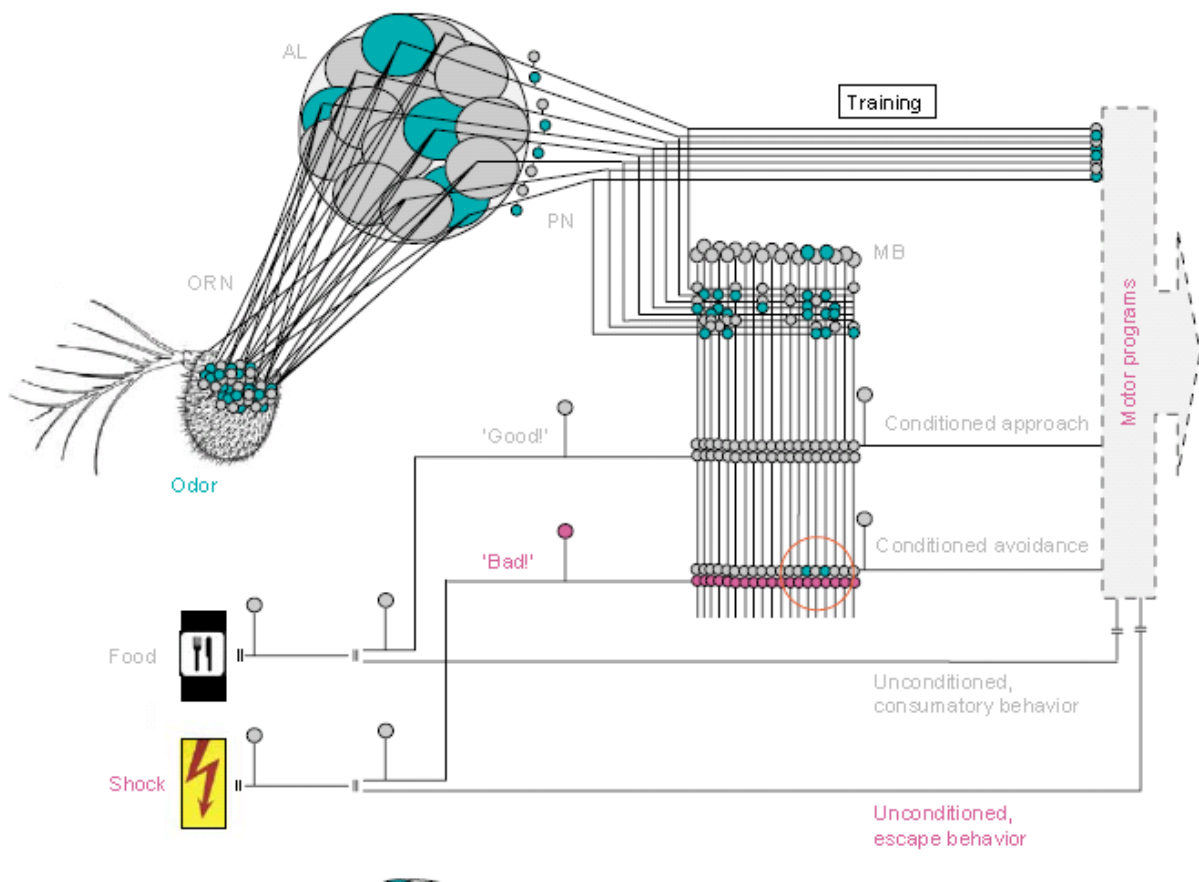


Figure 7: Model of olfactory memory pathway in *Drosophila*

A minimal model for *Drosophila* olfactory learning. A highly simplified diagram showing the olfactory pathways. Olfactory receptor neurons (ORN) project to the antennal lobe (AL), leading to a specific combinatorial activity pattern. From there, uniglomerular projection neurons (PN) relay to the lateral horn and to premotor centers (box labeled 'Motor programs'), as well as to the mushroom body (MB) calyx. Output from the mushroom bodies then projects to a variety of target regions including premotor areas. (Gerber, Tanimoto, Heisenberg 2004)

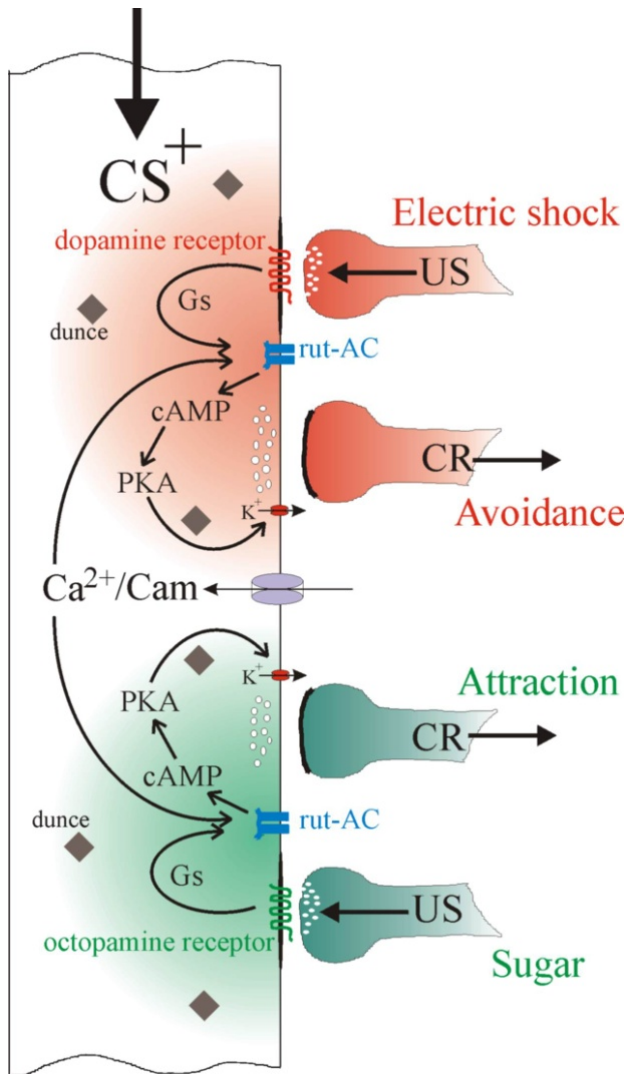


Figure 8: Working Model of the STM acquisition phase in *Drosophila* (courtesy of M.Heisenberg unpublished)

In this model the Kenyon cells of the mushroom bodies pose as a site of coincidence detection of the conditioned and the unconditioned stimulus (Heisenberg 2003). Hereby the CS is mediated to the mushroom body calyx via the olfactory pathway (consisting of the olfactory receptor neurons and the projection neurons), whereas the US is mediated to the Kenyon cells via the aminergic neuronal network, with dopamine playing a crucial role in the case of aversive, and octopamine in the case of appetitive learning (Schwärzel et. al, 2003). The neurotransmitter mediating the US binds to a G-Protein coupled receptor (Bockaert & Pin, 1999), which in turn leads to the stimulation of the rutabaga adenylyl cyclase and therefore production of cAMP. In the model the intracellular Ca^{2+} /Calmodulin interaction also leads to cyclase stimulation (Zars et. al, 2000). In the case where both the arrival of the CS-signal and US-Signal coincide, a synergistic (nonlinear signal summation) hyperstimulation of the cyclase leads to a production of high amounts of cAMP. In turn cAMP among other things, leads to the activation of Protein Kinase A (PKA), thus leading to various phosphorylation events in the synaptic region, which can be the cause for synaptic plasticity, due to altered synaptic signaling.

3.5. Locomotor control and orientation

The insect analogon of the spinal cord in vertebrates is found in certain nerve centres in the thorax. While those are enough to support coordinated locomotion (Cruse et al., 2007), the insect's brain seems to be required to make its movements oriented. The central complex seems to be one of the structures highly involved in control of such orientation behaviour (Strauss, Pichler, 1998; Neuser et al., 2008).

The central complex is a distinct and prominent structure in the central brain, which can be found in all insect species. It is subdivided into four parts: protocerebral bridge, fan-shaped body, ellipsoid body and nodule (Fig. 8), the exact anatomy of those parts differs between various insect species, with a closed ellipsoid body ring being most prominent in Dipterans.

The central complex constitutes a bilaterally symmetrical matrix of three neuron types interconnecting the four neuropilar regions, the small field neurons mostly running dorso-ventrally, the large field neurons running perpendicularly to these, and the central complex intrinsic pontine neurons. All those neuron types usually come in homologous sets of 8 or 16 neurons (Hanesch et al., 1989).

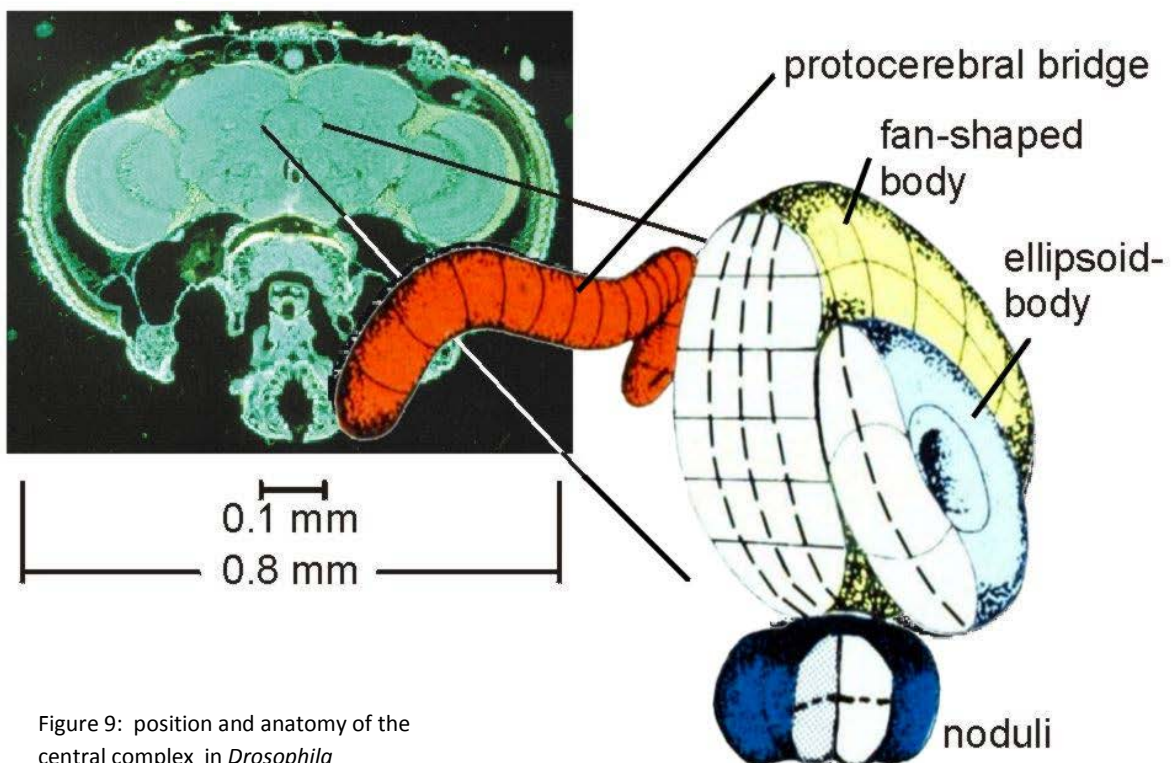


Figure 9: position and anatomy of the central complex in *Drosophila melanogaster* (Strauss et al.)

Introduction

While the ellipsoid body seems to play a critical role in spatial memory and reorientation of the animal towards a memorised stimulus (Neuser et al., 2008), the protocerebral bridge (PB) seems to play a crucial role in immediate locomotor control and maintenance but not the initiation of walking activity in flies (Martin et al., 1999) and is important for directional control while approaching objects, via adjustment of step length. The bridge consists of a symmetrical array of 16 glomeruli with 1 being the innermost and 8 being the outermost on each side. The current working model (Fig. 9) for PB function assumes that a visual target is represented on the same side of the bridge, on which the image projects onto the retina and that the azimuth position of the objects is represented by the activated glomerulus. In the model frontal object positions are represented by neuronal activity in the innermost glomeruli, while the outermost glomerulus 8 represents position in the rear of the visual field. In a fly walking towards a certain stimulus, differences in glomerular activity of the protocerebral bridge lead to a control of step length on the contralateral side in the case of glomeruli 1-7 and on the ipsilateral in the case of glomeruli 8. Therefore localised neuronal activity within the protocerebral bridge can be used by the animal to perform course corrections and turns towards an object in the frontal part of the visual field, or to turn away from objects represented in its rear part.

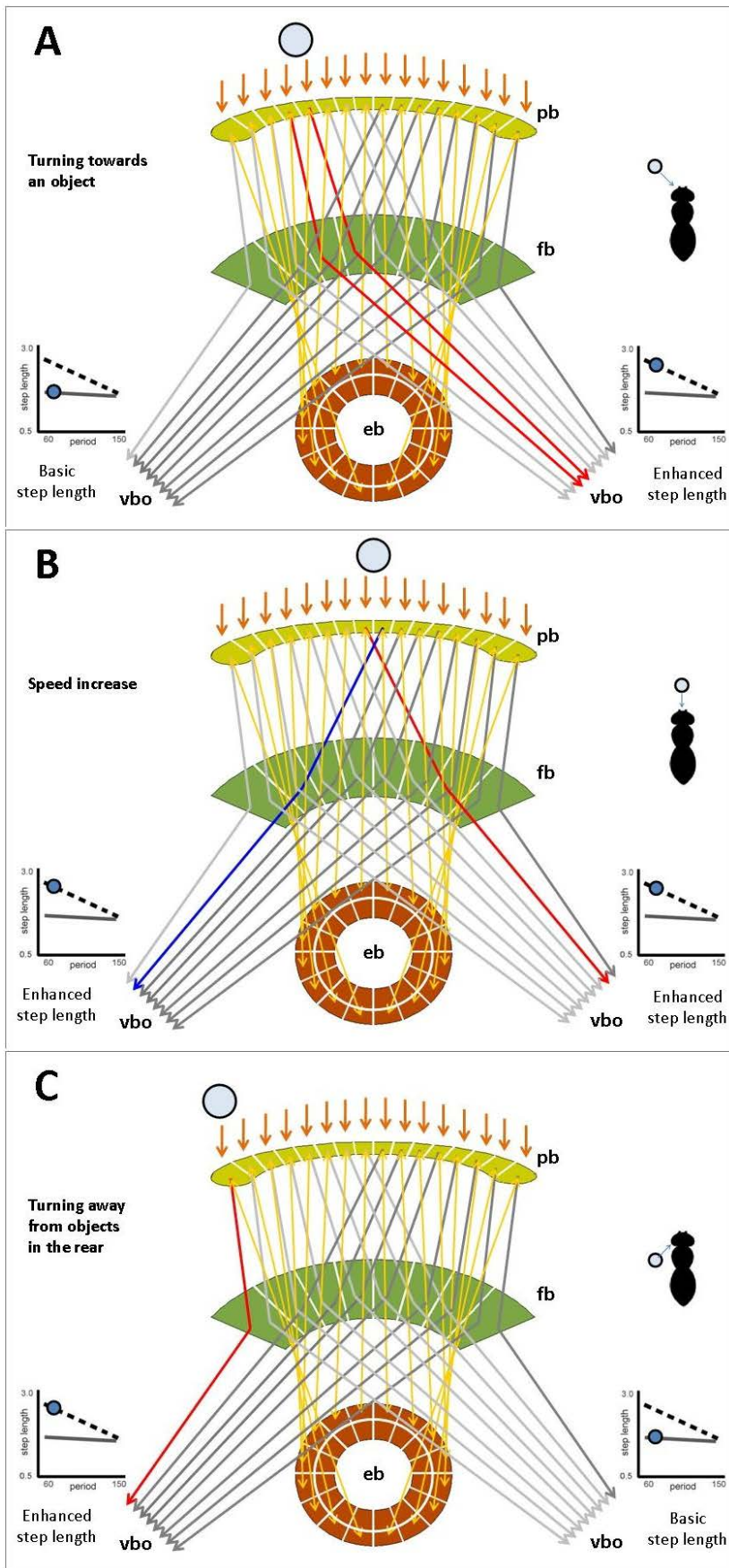


Figure 10: Functional protocerebral bridge model.

A: An object is represented at the left side of the bridge, transferred via the horizontal fiber system to the ventral body, where the step length of the contralateral legs is increased. The fly turns towards the object

B: Representation of an object at the middle of the bridge leads to an increase in step length of the legs on both sides of the body. The fly increases its walking speed towards the object.

C: The outermost bridge glomeruli 8 project ipsilaterally rather than contralaterally. Objects beyond 100° and more rear are represented there. The step length of ipsilateral legs is increased and the fly turns away from such an object

(Strauss et al., 2010)

3.6. Aim of this study

The main goal of this study was the creation and establishment of a combination of various optogenetic techniques and behavioural paradigms necessary to investigate the neuronal and molecular mechanisms and interactions underlying and leading to various behavioural processes. By such a combination it would be possible not only to look into various steps of information processing within the brain but also to the direct output of that processing into motor control and monitored behaviour. A more specific aim was the detection of distinct changes in neuronal activity patterns following the events of conditioning. Therefore it was crucial to find possible ways to combine the monitoring of both the physiological and behavioural changes within an individual animal and to link them, bypassing such biases as group effects, and expanding the amount of available behavioural information beyond the scope of binary yes/no, left/right answers.

In the first part of this study the of *in-vivo* suitability and performance of a novel array of genetically encoded fluorescent reporters of cAMP was to be evaluated. Also, cAMP dynamics in the mushroom bodies during the formation of short term olfactory memory had to be investigated, in order to find out whether the currently proposed working model of the coincidence detection by the cAMP producing adenylyl cyclases fits to the dynamics measured with the new array of genetically encoded cAMP sensors.

In the second part a combinative approach to optical *in-vivo* imaging and light or temperature activation of neurons should be developed. By such an approach one might not only simultaneously and specifically target, and stimulate, distinct parts of the neuronal architecture, but also record both the behavioural responses of the animal and the physiological responses on the neuronal level.

Aim of the third part of this study was the design and creation of a novel multipurpose behavioural assay, as an improvement and combination of several previously available paradigms (e.g. Heat Box, T-Maze) in a single experimental setup. Thereby one might be able to generate detailed data of individual behaviour and learning performance in a wide set of possible experiments including both operant and classical learning situations.

4. Methods

4.1. Imaging

Epifluorescent microscopy in a wide field microscope and several genetically encoded fluorescent reporters were used to visualise the cAMP dynamics in the mushroom bodies of *Drosophila melanogaster*. Custom built stimuli application machinery was created to allow for coupling of aversive electroshock stimuli with application of odours. The effects of individual and simultaneous applications, as well as the responses of the sensors to pharmacological applications were studied. Various fly lines featuring different sensor constructs with distinct insertion sites were tested for their suitability for further experiments. Furthermore the effects of combining multiple sensor copies in a single fly line were investigated.

Fly rearing

To create the food 212 g cornmeal was added to 750 ml water and brought to boiling temperature, then left for maceration over night. 40 ml molasses and 40 ml malt were added to the macerated corn mash. The mixture was again brought to boiling temperature, with 18,5 g dry yeast, 7,0 g agar and 10g soy meal solved in 150 ml water and added to it. After cooling down to 80°C one tee spoon of methyl-4-hydroxybenzoate was added to the mash as fungicide. Still liquid mash was poured in the food vials 2cm high.

Drosophila stocks were kept in small acrylic glass vials, on aforementioned food medium under standardised light-dark cycle (12h/12h) at either 18°C or 25°C. Stocks were transferred to fresh vials after 12-14 days at 25°C and after 3-4 Weeks on 18°C.

Fly Stocks

The sensor tables specify the sensor construct before the point and the numerator of the insertion line after the point (Epac1.1 means insertion line 1 for the sensor construct Epac1-camps). The UAS-Sensor construct is abbreviated by “S”

Epac1-camps	
Epac 1.1	$\frac{w^-}{w^-}; \frac{S}{CyO}; \frac{+}{+}$ or $\frac{w^-}{w^-}; \frac{+}{+}; \frac{S}{TM3}$
Epac 1.2	$\frac{w^-}{w^-}; \frac{S}{CyO}; \frac{+}{+}$ or $\frac{w^-}{w^-}; \frac{+}{+}; \frac{S}{TM3}$
Epac 1.3	$\frac{w^-}{w^-}; \frac{S}{CyO}; \frac{+}{+}$ or $\frac{w^-}{w^-}; \frac{+}{+}; \frac{S}{TM3}$
Epac 1.4	$\frac{w^-}{w^-}; \frac{S}{CyO}; \frac{+}{+}$ or $\frac{w^-}{w^-}; \frac{+}{+}; \frac{S}{TM3}$
Epac 1.5	$\frac{w^-}{w^-}; \frac{S}{CyO}; \frac{+}{+}$ or $\frac{w^-}{w^-}; \frac{+}{+}; \frac{S}{TM3}$

MB247-Gal4	$\frac{w^-}{w^-}; \frac{+}{+}; \frac{MB247 - GAL4}{MB247 - GAL4}$
PKA FRET	$\frac{w^-}{w^-}; \frac{+}{+}; \frac{PKAFRET}{TM3}$
Double Balancer	$\frac{w^-}{w^-}; \frac{Sp}{CyO}; \frac{TM2}{TM6}$

Methods

Epac2-camps	
Epac 2.1	$\frac{w^-}{w^-}; \frac{S}{CyO}; \frac{+}{+}$ or $\frac{w^-}{w^-}; \frac{+}{+}; \frac{S}{TM3}$
Epac 2.2	$\frac{w^-}{w^-}; \frac{S}{CyO}; \frac{+}{+}$ or $\frac{w^-}{w^-}; \frac{+}{+}; \frac{S}{TM3}$
Epac 2.3	$\frac{w^-}{w^-}; \frac{S}{CyO}; \frac{+}{+}$ or $\frac{w^-}{w^-}; \frac{+}{+}; \frac{S}{TM3}$
Epac 2.4	$\frac{w^-}{w^-}; \frac{S}{CyO}; \frac{+}{+}$ or $\frac{w^-}{w^-}; \frac{+}{+}; \frac{S}{TM3}$
Epac 2.5	$\frac{w^-}{w^-}; \frac{S}{CyO}; \frac{+}{+}$ or $\frac{w^-}{w^-}; \frac{+}{+}; \frac{S}{TM3}$
Epac 2.6	$\frac{w^-}{w^-}; \frac{S}{CyO}; \frac{+}{+}$ or $\frac{w^-}{w^-}; \frac{+}{+}; \frac{S}{TM3}$
Epac 2.7	$\frac{w^-}{w^-}; \frac{S}{CyO}; \frac{+}{+}$ or $\frac{w^-}{w^-}; \frac{+}{+}; \frac{S}{TM3}$
Epac 2.8	$\frac{w^-}{w^-}; \frac{S}{CyO}; \frac{+}{+}$ or $\frac{w^-}{w^-}; \frac{+}{+}; \frac{S}{TM3}$
Epac 2.9	$\frac{w^-}{w^-}; \frac{S}{CyO}; \frac{+}{+}$ or $\frac{w^-}{w^-}; \frac{+}{+}; \frac{S}{TM3}$
Epac 2.10	$\frac{w^-}{w^-}; \frac{S}{CyO}; \frac{+}{+}$ or $\frac{w^-}{w^-}; \frac{+}{+}; \frac{S}{TM3}$

Methods

Epac2K390E-camps	
Epac 2 K390E.1	$\frac{w^-}{w^-}; \frac{S}{CyO}; \frac{+}{+}$ or $\frac{w^-}{w^-}; \frac{+}{+}; \frac{S}{TM3}$
Epac 2 K390E.2	$\frac{w^-}{w^-}; \frac{S}{CyO}; \frac{+}{+}$ or $\frac{w^-}{w^-}; \frac{+}{+}; \frac{S}{TM3}$
Epac 2. K390E.3	$\frac{w^-}{w^-}; \frac{S}{CyO}; \frac{+}{+}$ or $\frac{w^-}{w^-}; \frac{+}{+}; \frac{S}{TM3}$
Epac 2 K390E.4	$\frac{w^-}{w^-}; \frac{S}{CyO}; \frac{+}{+}$ or $\frac{w^-}{w^-}; \frac{+}{+}; \frac{S}{TM3}$
Epac 2 K390E.5	$\frac{w^-}{w^-}; \frac{S}{CyO}; \frac{+}{+}$ or $\frac{w^-}{w^-}; \frac{+}{+}; \frac{S}{TM3}$
Epac 2 K390E.6	$\frac{w^-}{w^-}; \frac{S}{CyO}; \frac{+}{+}$ or $\frac{w^-}{w^-}; \frac{+}{+}; \frac{S}{TM3}$
Epac 2 K390E.7	$\frac{w^-}{w^-}; \frac{S}{CyO}; \frac{+}{+}$ or $\frac{w^-}{w^-}; \frac{+}{+}; \frac{S}{TM3}$
Epac 2 K390E.8	$\frac{w^-}{w^-}; \frac{S}{CyO}; \frac{+}{+}$ or $\frac{w^-}{w^-}; \frac{+}{+}; \frac{S}{TM3}$
Epac 2 K390E.9	$\frac{w^-}{w^-}; \frac{S}{CyO}; \frac{+}{+}$ or $\frac{w^-}{w^-}; \frac{+}{+}; \frac{S}{TM3}$
Epac 2 K390E.10	$\frac{w^-}{w^-}; \frac{S}{CyO}; \frac{+}{+}$ or $\frac{w^-}{w^-}; \frac{+}{+}; \frac{S}{TM3}$

Methods

HCN2-camps	
HCN2.1	$\frac{w^-}{w^-}; \frac{S}{CyO}; \frac{+}{+}$ or $\frac{w^-}{w^-}; \frac{+}{+}; \frac{S}{TM3}$
HCN2.2	$\frac{w^-}{w^-}; \frac{S}{CyO}; \frac{+}{+}$ or $\frac{w^-}{w^-}; \frac{+}{+}; \frac{S}{TM3}$
HCN2.3	$\frac{w^-}{w^-}; \frac{S}{CyO}; \frac{+}{+}$ or $\frac{w^-}{w^-}; \frac{+}{+}; \frac{S}{TM3}$
HCN2.4	$\frac{w^-}{w^-}; \frac{S}{CyO}; \frac{+}{+}$ or $\frac{w^-}{w^-}; \frac{+}{+}; \frac{S}{TM3}$
HCN2.5	$\frac{w^-}{w^-}; \frac{S}{CyO}; \frac{+}{+}$ or $\frac{w^-}{w^-}; \frac{+}{+}; \frac{S}{TM3}$

Fly Crosses

For the standard experiment flies of a particular sensor line were crossed directly to the GAL-4 driver line. The indicated F1 animals were used for the experiments

single copy:	$P: \frac{w^-; +}{Y; +}; \frac{MB247 - GAL4}{MB247 - GAL4} \times \frac{w^-; S; +}{w^-; CyO; +} \text{ or } \frac{w^-; +; S}{w^-; +; TM3}$
	$F_1: \frac{w^-; S; +}{w^-; +}; \frac{+}{MB247 - GAL4} \text{ or } \frac{w^-; +; S}{w^-; +}; \frac{S}{MB247 - GAL4}$

To establish fly lines with multiple sensor copies, selected sensor lines were crossed to a double balancer line in a following crossing scheme

Cross I.1:	$P: \frac{w^-; Sp; TM2}{Y; CyO; TM6} \times \frac{w^-; S; +}{w^-; CyO; +}$
	$F_1: \frac{w^-; Sp; TM2}{Y; S; +}$

Cross I.2:	$P: \frac{w^-; Sp; TM2}{Y; CyO; TM6} \times \frac{w^-; +; S}{w^-; +; TM3}$
	$F_1: \frac{w^-; +; S}{w^-; CyO; TM6}$

Cross II:	$P: \frac{w^-; Sp; TM2}{Y; S; +} \times \frac{w^-; +; S}{w^-; CyO; TM6}$
-----------	--

Methods

$F_1:$	$\frac{w^-}{w^-}; \frac{S}{CyO}; \frac{S}{TM2}$
--------	---

Cross III:	$P: \frac{w^-}{Y}; \frac{S}{CyO}; \frac{S}{TM2} \times \frac{w^-}{w^-}; \frac{S}{CyO}; \frac{S}{TM2}$
$F_1:$	$\frac{w^-}{w^-}; \frac{S}{S}; \frac{S}{S}$

Selected progeny of the multiple copies crossing was crossed directly to the GAL-4 driver for the comparison experiments:

multiple copies:	$P: \frac{w^-}{Y}; \frac{+}{+}; \frac{MB247}{MB247} \times \frac{w^-}{w^-}; \frac{S}{S}; \frac{S}{S}$
$F_1:$	$\frac{w^-}{w^-}; \frac{S}{+}; \frac{S}{MB247 - GAL4}$

In-vivo dissection

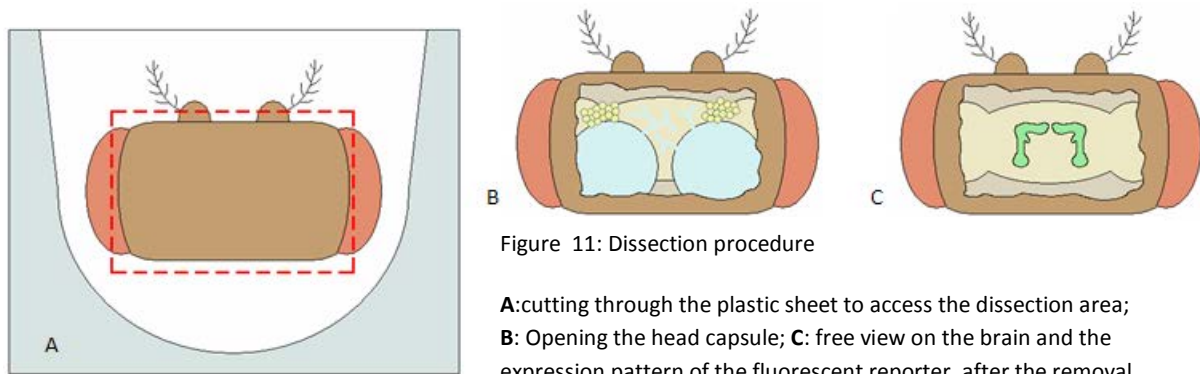


Figure 11: Dissection procedure

A:cutting through the plastic sheet to access the dissection area; **B:** Opening the head capsule; **C:** free view on the brain and the expression pattern of the fluorescent reporter, after the removal of obstructions (air sacs, fat tissue, trachea)

Cameleon construct

Based on previous work, the visualisation of calcium dynamics while imaging the brain of *Drosophila* was achieved by utilizing the Ca^{2+} sensor Cameleon 2.1 (Myawaki et. al, 1999). The sensor consists of four subunits, the fluorophores EYFP and ECFP (emission wavelength-shifted derivatives of GFP), the calcium binding domain of Calmodulin and the Calmodulin-target-peptide. The sensor's functionality is based on the FRET (Fluorescence resonance energy transfer) effect. FRET can occur over small distances between two fluorophores. In the absence of Ca^{2+} ECFP excited by light of 436 nm emits fluorescence of 480 nm. Light of this wavelength in principle is able to excite EYFP, which emits light of 535 nm wavelength, but the absorption of the fluorescent light is very inefficient. Upon binding of Ca^{2+} , the sensor protein undergoes a conformational change, bringing both EYFP and ECFP fluorophores within a distance where an efficient FRET can occur, thus decreasing 480nm fluorescence and increasing the amount of 535 nm fluorescence emitted by the sensor construct. In case, when both the yellow and the cyan fluorescences are recorded, a ratio of the two emission strengths can be calculated, the ratio's value increases with the increase of the calcium concentration in the cells marked by the Cameleon sensor. The ratiometric nature of the sensor makes it possible to discriminate and correct movement and recording artefacts, where the amount of light emitted by both fluorophores would change in the same direction without affecting the ratio, e.g. if the tissue of interest leaves the recorded field, whereas the change in the ratio can in most cases be attributed to a change in the intracellular Ca^{2+} concentration. This fact is particularly advantageous for in-vivo recording of the fly brain, where the pulsation of antennal hearts can lead to movement of the brain.

Epac- and HCN2-camps constructs

Several different ratiometric sensors were utilised to investigate the cAMP dynamics. Three types of sensors were used: Epac1-camps, Epac2-camps, Epac2K390E-camps and HCN2 camps. Those reporters feature single cAMP binding domains, derived either from human and murine Epac protein or murine HCN2 channel, fused to EYFP- and ECFP-proteins (Nikolaev et al., 2004, Nikolaev et al., 2006). These sensors are based on a similar principle as the Cameleon 2.1 Sensor. The binding of cAMP, however, here leads to a drop in FRET, as the conformation change of the molecule upon cAMP binding moves the fluorophores farther apart, thus decreasing the FRET effect (Fig. 12).

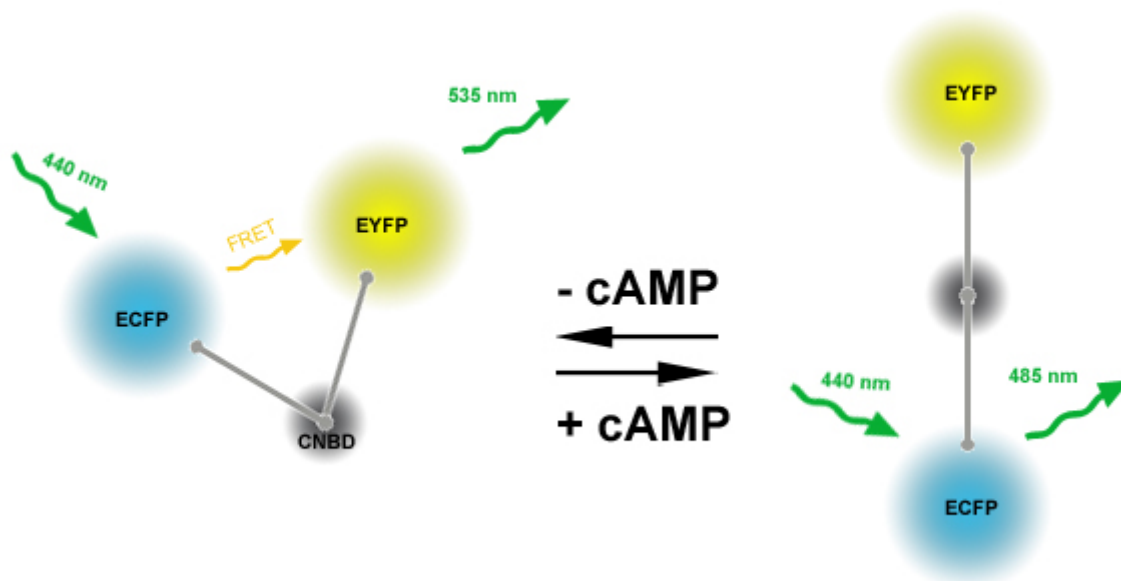


Figure12: Working principle of the Epac-camps and HCN2-camps sensors (modified from Nikolayev et al., 2006)

Imaging Setup

The complete system (Visitron Systems, Puchheim, Germany) consists of a Xenon arc Lamp (75W, Visitron Systems, Puchheim, Germany), Visichrom High-Speed Polychromator System (Visitron Systems, Puchheim, Germany), a CCD-Camera (CoolSnap HQ, Resolution: 1280 x 960 Pixel, Roper Scientific, Tucson, USA), a beam splitter consisting of a 455–470nm dichroic filter and two emission filters 485/40nm and 535/30nm (Optical Insights, Santa Fe, USA), an additional dichroic filter 505–515nm (Chroma, Brattleboro, VT, USA), an epifluorescence microscope (Axioskop 2FS plus, Zeiss, Jena, Germany), shock and odour application devices (Biocenter workshop), and a computer (Lynx, Reutlingen, Germany) (Fig. 13).

The monochromator grating allows one to select part of the spectrum produced by the xenon arc lamp. Before hitting the head of the fly, light of the chosen wavelength is reflected by the dichroic filter and passes through the objective. In turn, light emitted by the specimen passes the low pass filter of the dichroic and is separated into EYFP and ECFP fluorescences via the beam splitter and two emission filters, before it reaches the chip of the CCD Camera. The chip consists of a matrix of lightsensitive cells, each of them producing a charge proportional to the amount of light hitting it. While saving the charge information during read-out, the chip is occluded by a shutter to avoid data corruption. Recorded data is processed into images and recorded by the Metafluor software (Universal Imaging, Downington, PA, USA). Further processing is done in the Metamorph software (Universal Imaging, Downington, PA, USA).

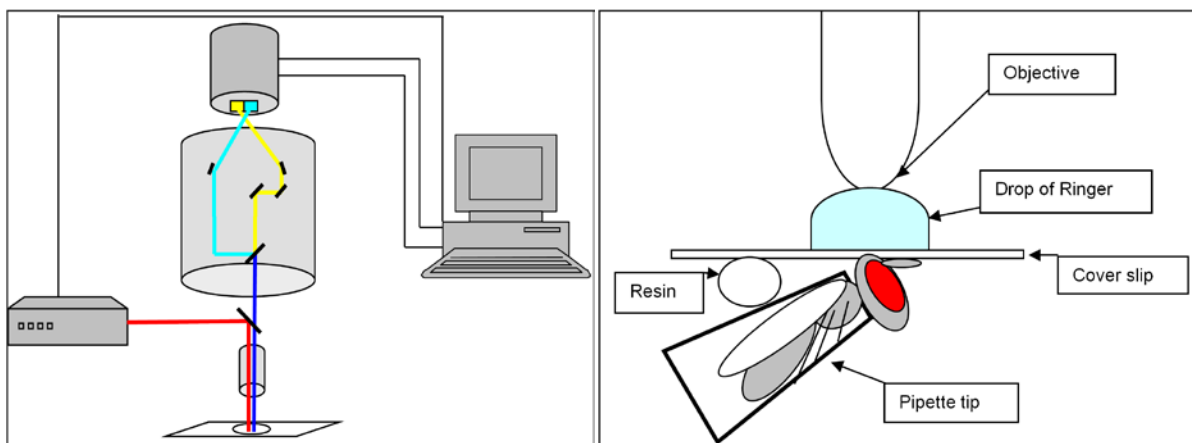


Figure13: Imaging setup and positioning of the experimental animal in the setup (Modified from Fiala et. al 2003)

Olfactometer

Flies were presented with different odours via a device called the Olfactometer (Fig. 14). In it, the odours are dispersed from one of 10 odour containers (plastic vials für scintillation counters, diameter 27 mm, Carl Roth GmbH, Karlsruhe, Germany) via an air pump (Power Air Pump 400, Rondex, Dennerle GmbH, Münchweiler) and presented to the fly through a plastic pipette (Length: 230 mm, Carl Roth GmbH, Karlsruhe, Germany) . The output selection is controlled via magnetic valves (The Lee Company, Essex, CT, USA). The odour is blown over the fly antennae from a distance of approx. 2mm, a constant air stream is maintained in the imaging area in order to restrict the odour presence around the fly to the application events. Application procedure is controlled via the Metafluor Software.

Pure odours were dissolved in mineral oil (Sigma-Aldrich, USA) directly in their odour container and mixed with a vortexing device (Assistent Reamix).

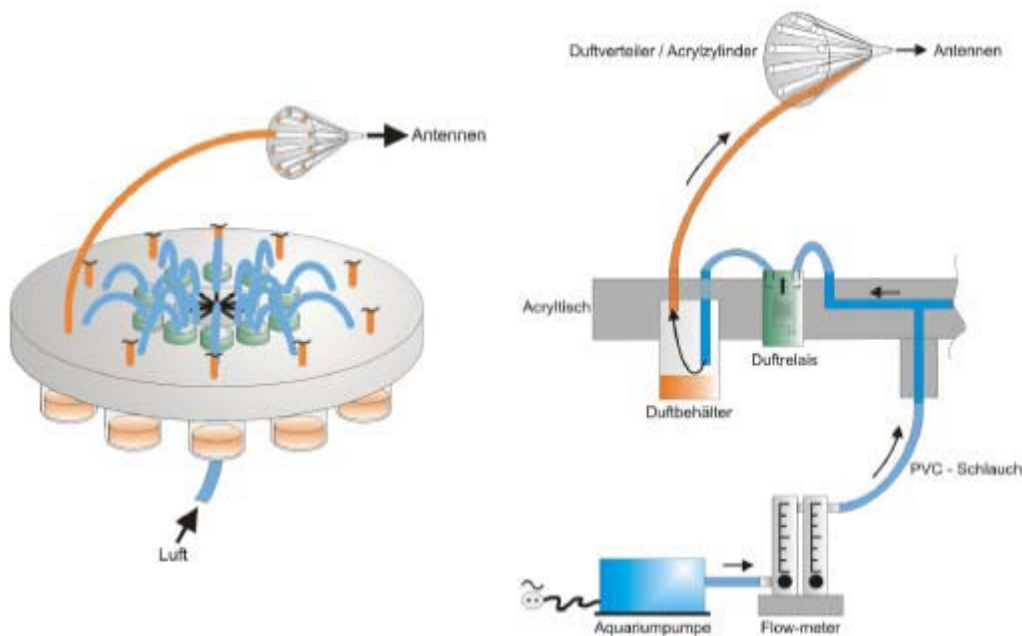


Figure 14: Olfactometer (Spall 2004)

Application of pharmaceuticals

The different steps of fixing the fly for imaging in combination with drug application are shown in Fig.15. Thin translucent foil (transparent flower wrap foil) is fixed to a perforated cover slip by nail polish (Plastic cover slips, Ted Pella Inc., USA) the pipette tip with fly is fixed on the cover slip by plasticine, subsequently the flies head is glued to the foil by dental glue (Protemp II, 3M ESPE AG, Germany)

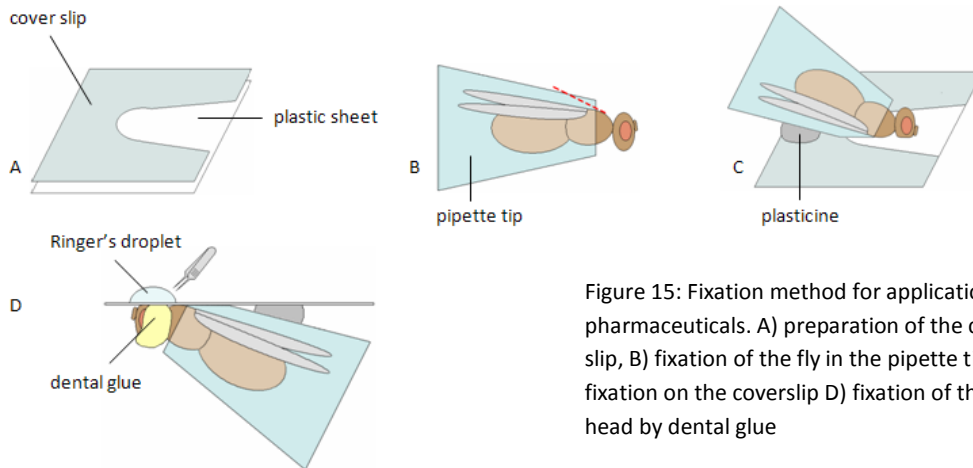


Figure 15: Fixation method for application of pharmaceuticals. A) preparation of the cover slip, B) fixation of the fly in the pipette tip, C) fixation on the coverslip D) fixation of the head by dental glue

Shock apparatus

The apparatus (Fig. 16) consisted of a fly holder cut from acrylic glass. Within it the fly is tightly held, to prevent body movements, the head position of the fly is adjusted by a slider. Embedded in the holder below the fly are two parallel platinum wires used to deliver the current to the legs and abdomen of the animal. The apparatus is connected to a shock device, capable to present 1 sec pulses of 90V DC to the fly.

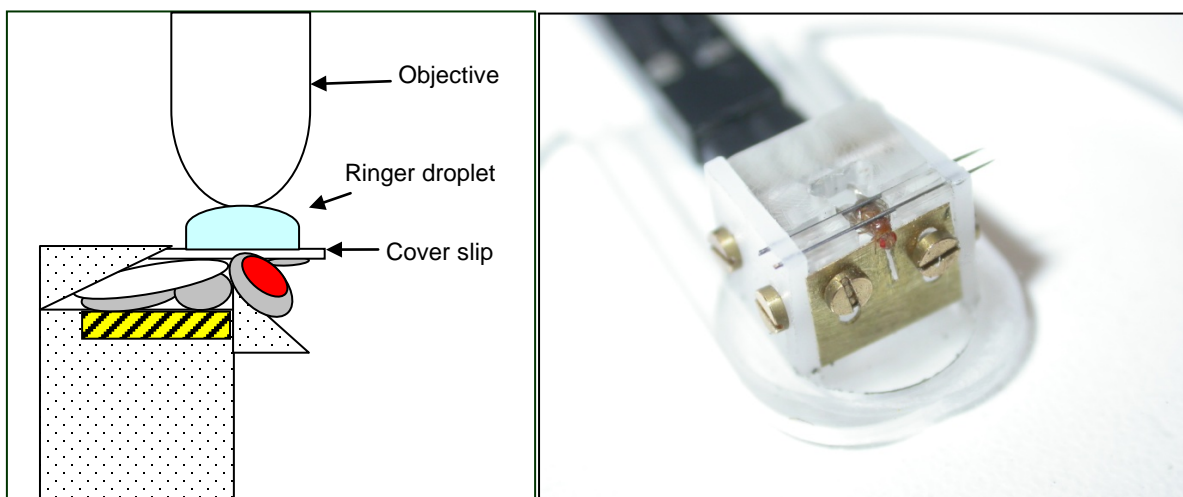


Figure 16: a) Schematic of the apparatus and fixation method for shock and odour application b) Foto of shock apparatus

Software

Utilised software included Metamorph (Molecular Devices Inc.) for live imaging. ImageJ (Freeware) for subsequent postprocessing and alignment of recorded images. Metafluor (Molecular Devices Inc.) for data readout of processed files, and Origin 8.1 (OriginLab Corporation) and Statistica 5.0 (Statsoft Inc.) for statistical calculation and handling of data readouts. Graphical processing of data was performed by Adobe Photoshop CS4 (Adobe Inc.)

The automatisisation of stimuli application was reached via the creation of Journals, sets of scripted trigger events and operations. Each experiment consisted of a defined number of cycles, each cycle corresponding to the capture of a single image in each of the fluorescence channels. The cycling frequency was set to 5 captures per second (5Hz).

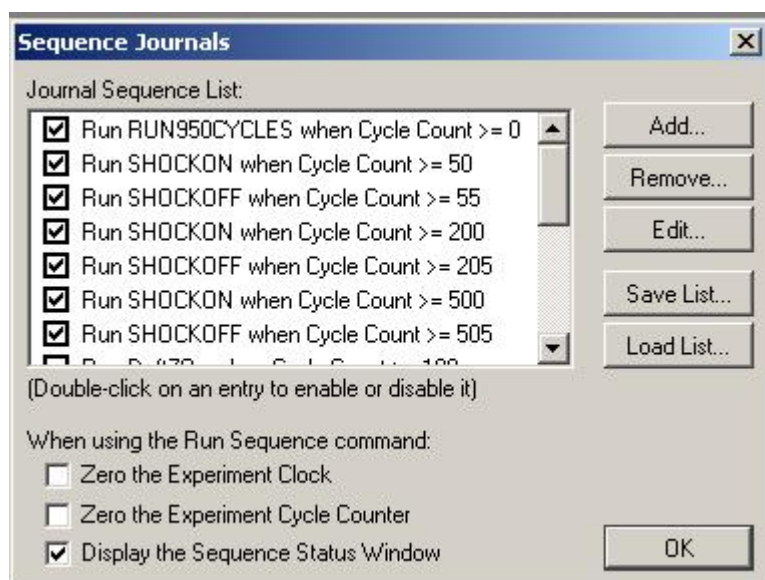


Figure 17: Creation of a Journal sequence for the automated stimulus application

Drug applications

200µl of pharmaceuticals were applied via direct introduction into the approx 200µl ringer droplet covering the brain, leading to an approximate 1:2 dilution of the applied solution, the application was done manually following an acoustic signal (50 cycles time stamp) by the recording software. Ringer and solvent applications were used as controls.

Methods

Both shock and odour were applied automatically via digital input output (DIO) signals to the olfactometer and shock apparatus generated via a predefined script embedded in the experimental journal and triggered by the recording software.

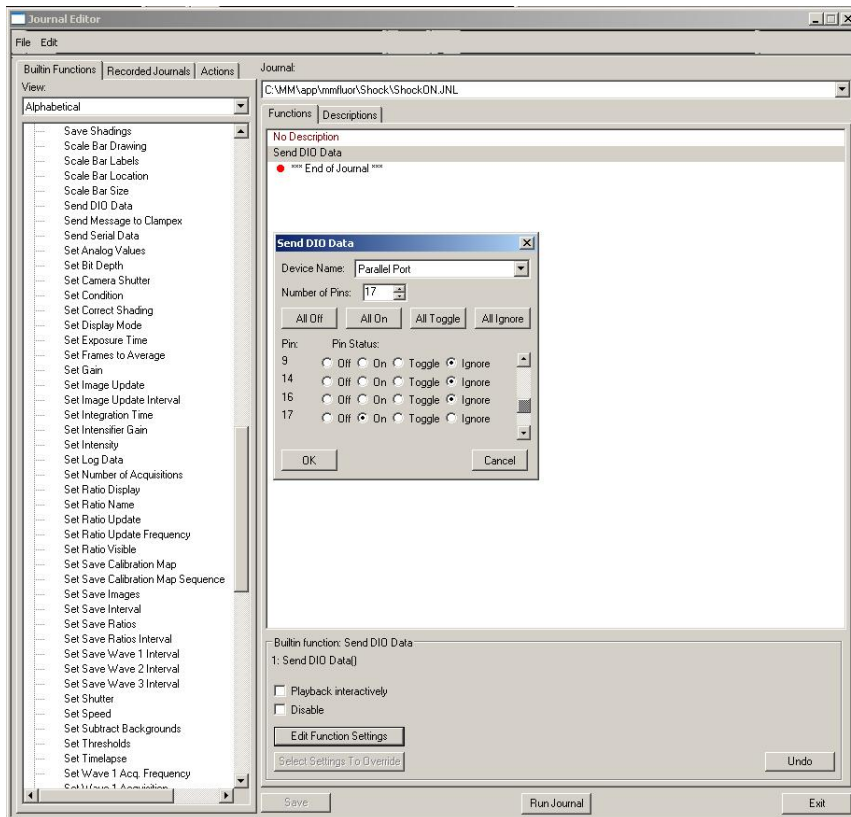


Figure 18: DIO Script creation for Metaflur journals

In case of electric shock a 1 sec application of a single 90V shock pulse was made, in case of odour a 1 second odour puff was given to the fly.

Two odours were selected for application: 3-Octanol (1:1000) and 4-Methylcyclohexanol (1:100) with applications of pure air and mineral Oil were used as controls.

IMAGE processing GUI

Movement correction via ImageJ

CalciumImageProcessor ,a GUI plugin for ImageJ (Völler, 2008) was utilised to reduce movement artifacts within recorded stacks. Its main component is the TurboReg plugin, providing methods to allign images with respect to each other (Thevenaz et al., 1998). TurboReq aligns the images by defining a transformation matrix, thus reducing the mean square difference of images.

The Calcium Imaging Processor provides the following funtctions:

Creation of Stacks

Transformation of the original CCD Images into .stk format, for further processing

Alignment of the EYFP stack with respect to ECFP Stack

To alleviate for small displacement in the channels, which stem from the microscop optics, causing intensity histogram differences between the two channels, an adaptation of the TurboReg module was used. It partitions the intensity information of the images in 5 intensity groups, hence allowing for easier alignment of respective intensity histograms between the two channels. Translation of this alignment matrix is computed by *Turboreg*, and subsequentially applied when aligning normal images thus reducing the displacment artifacts.

Movement correction

Due to small movements of the brain tissue either due to miniscule head movements or the pulsation of antennal hearts, displacements within the recorded images could occur. TurboReg utilizes the RigidBodyTransform method to allign the images with respect to each other. The ECFP stack is corrected by aligning all the images to the first image. EYFP stack is aligned to ECFP stack in a similar way.

Journal Evaluation

This option allows for averaging and intensity subtraction of three prestimulus cycles from three cycles during the stimulus application. The resulting image is recorded in false colours, translating 256 grey levels of intensity into the normal spectrum of 256 colors with colour 0 (lowest intensity) being black and colour 256 (highest intensity) white.

Averaging of multiple trials of a single fly

To reduce the measurement noise multiple trials can be run on the same animal, all the rotational and translational movements are again eliminated by the RigidBodyTransform method. The resulting stacks are averaged over the number of experimental trials.

Activation Movie

An averaged image from the first 5 cycles is subtracted from each individual cycle image, creating a stack which represents the difference from the initial fluorescence level prior to any stimulation. This stack can be viewed as a realtime movie showing the temporal dynamics of the response to the stimulus.

Calculations

Each individual intensity recording was corrected for background noise by subtraction of the background intensity from the ROI intensity for each channel, respectively. The standard activity level was determined by averaging of the corrected intensities during the initial 25 cycles of each experiment. This value was used as the reference baseline value R_0 or F_0 (for the Ratio value or the fluorescence intensity value) each value was then represented as the percentual difference.

$$EYFP_{corr} = EYFP - EYFP_{Background}$$

$$Ratio_{corr} = \frac{EYFP - EYFP_{Background}}{ECFP - ECFP_{Background}}$$

$$\Delta F / F_0 (EYFP_{corr}) = \left(\frac{EYFP_{corr}}{\left(\frac{\sum_{1-25} (EYFP_{corr})}{25} \right)} - 1 \right) * 100$$

$$\Delta R / R_0 (Ratio_{corr}) = \left(1 - \frac{Ratio_{corr}}{\left(\frac{\sum_{1-25} (Ratio_{corr})}{25} \right)} \right) * 100$$

Statistics

To investigate the difference between Applications a mean over the ratio change in the last 50 cycles of the application experiment (plateau phase) was calculated for each individual fly. A one-way-ANOVA was performed to check for significant differences in the application effects between groups.

4.2. Locomotor control

A new experimental setup for studying the impact of selective neuronal activation on the walking behaviour of the flies was designed and created. Preliminary experiments to study the effect of unilateral versus complete activation of neurons expressing Channelrhodopsin 2 (Chop2) within the protocerebral bridge were made. Since bright blue light is required to activate Chop2, visual response to this light had to be eliminated by using blind flies carrying a mutation in the *NorpA* gene (Hardie et al. 2003, Nuwal 2010).

Fly rearing

12 days before the experiment parent flies were put in a food vial with all-trans-retinal (150 µl, 250 mM dissolved in 100% ethanol) such that progeny will emerge 2 days before the experiment. Parents were removed after 2 days. Emerging flies were transferred to a new food vial with retinal (150 µl). 21-24 h before the experiment the flies were transferred to a new vial containing quarter of a tissue paper (Zetbox #165165) with 3 ml water and 30 µl retinal, in order to achieve starvation without desiccation. Then enhancer trap line 007y-Gal4 has previously been shown to drive strong expression in the protocerebral bridge (Poock et al., 2008) which can directly be visualised by the EYFP variety of the construct (Poock, unpublished).

Fly stocks

CS	$\frac{+}{-}; \frac{+}{-}; \frac{+}{-}$ $+ + +$
007y-GAL4,EYFP	$\frac{w^-}{w^-}; \frac{+}{+}; \frac{007y - GAL4, EYFP}{TM3}$
Chop	$\frac{w^-}{w^-}; \frac{UAS - chop}{UAS - chop}; \frac{UAS - chop}{UAS - chop}$
<i>norpA</i> ⁻ ; chop	$\frac{norpA^-}{norpA^-}; \frac{UAS - chop}{UAS - chop}; \frac{UAS - chop}{UAS - chop}$

Fly crosses

Experimental flies:	$P: \frac{w^-}{Y}; \frac{+}{+}; \frac{007y - GAL4, EYFP}{TM3} \times \frac{w^-}{w^-}; \frac{UAS - chop}{UAS - chop}; \frac{UAS - chop}{UAS - chop}$
	$F_1: \frac{w^-}{Y}; \frac{UAS - chop}{+}; \frac{007y - GAL4, EYFP}{UAS - chop}$

Blind flies control:	$P: \frac{norpA^-}{norpA^-}; \frac{UAS - chop}{UAS - chop}; \frac{UAS - chop}{UAS - chop} \times \frac{w^-}{Y}; \frac{+}{+}; \frac{007y - GAL4, EYFP}{TM3}$
	$F_1: \frac{norpA^-}{Y}; \frac{UAS - chop}{+}; \frac{007y - GAL4, EYFP}{UAS - chop}$

Dissection

Flies were anaesthetised on ice for 15 minutes, then glued on a perforated plastic coverslip prepared in the same way as for the imaging dissection. The depression in the cover slip was filled with the epoxy glue, the fly was placed dorsally on the glue and aligned perpendicularly to one of the coverslips sides, the head and thorax of the fly were gently pressed into the glue until the cuticula made immediate contact with the plastic wrap. The head of the fly was then slightly tilted until the proboscis touched was touching the thorax. Following this, three triangles of tissue paper were carefully placed on to the glue surface to the sides of the fly and over its head to prevent any future contact between the glue and the legs of the fly. Flies were left for 5 minutes in order to recover from anaesthesia and let the glue dry completely.

The head capsule of the fly was opened in a manner identical to the imaging dissection, the window was cut in the posterior part of the head capsule, just behind the ocelli.

Apparatus

The walking ball setup consisted of a styrofoam ball suspended in a laminar air stream within a glass pipe (Fig. 19). The movement of the ball was tracked via an optical mouse sensor where signals were transferred to a computer via an USB interface. The Data was recorded with an ASUS X57V notebook (ASUS Tek Computer Inc., China)

A custom made coverslip holder was attached to the microscope stage, allowing for alignment and fixation of the coverslip. The walking ball apparatus was placed in a dove tale fixture and slowly brought into the right position underneath the fly. Excitation light could be applied via apertures either to the whole visual field or to one side of it (see Fig. 19 in the Results section for an overview of stimulated brain regions).

Methods

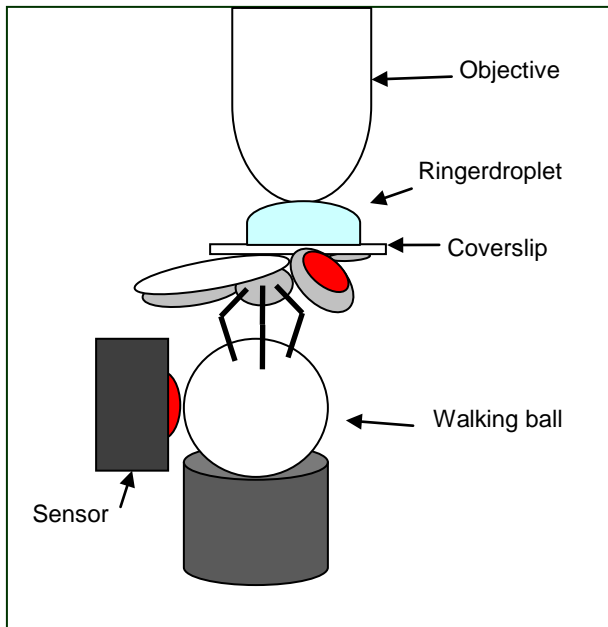


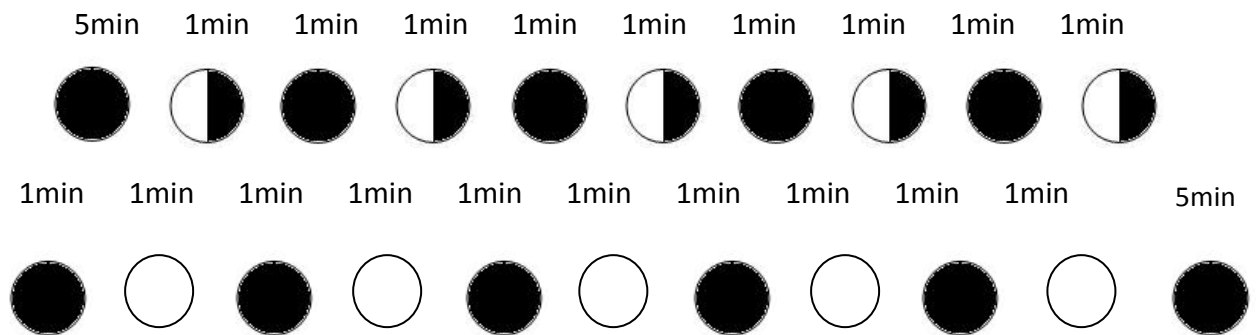
Figure19: Position of the animal in the walking ball apparatus

Software

The software was custom designed in house, and can read out movements of up to 5 walking balls simultaneously. It is controlled by experimental journals, each journal specifying parameters for each particular experiment, ranging from setting up the experimental timeframe, to defining the response sensitivity of additional stimuli, which can be given by devices controlled by the software. For these experiments however only the basic movement tracking function was utilized. The software code was primarily written in java, with an additional “manymouse” module written in C, this module allows not only for simultaneous tracking of several walking balls, but also allows for the readout of the movements into a constant recording independent of the standard driver routine incorporated in the operating system (OS).

Experimental Protocols

Two different stimulation protocols were applied. In the massed protocol, the stimulations of the same type occur subsequently, interrupted by long recovery phases. Flies were allowed to walk on the ball freely for 5 minutes during the pre test phase and in the post test phase, during the actual experiment the dissected brain region was illuminated either completely or just on one half for 1 minute, following 1 minute without any stimulation



In the fast mixed protocol, flies were allowed to walk on the ball freely for 2 minutes during the pre test phase and in the post test phase, during the actual experiment the dissected brain region was illuminated either completely or just on one half for 5, following 15 seconds of recovery without any stimulation, the sequence of full stimulation, recovery, half stimulation, recovery was repeated 14 times



Evaluation

The average of the recorded amount of rotational ball movement is plotted for each stimulus application.

4.3. Shockbox

A new experimental paradigm to study and constantly monitor the performance of individual flies was created. The paradigm allows one to set up classical olfactory conditioning experiments, as well as various operant and semi operant conditioning experiments for place learning and activity monitoring of the fly.

Fly rearing

In order to eliminate the effect of population density during development on the performance of the experimental flies, a special rearing method was applied. A spoon covered in approx. 1cm thick layer of food medium was placed vertically in a fly vial. Flies were introduced to the vial and allowed to lay eggs for 6 hours. After that flies were removed and the eggs left for development for additional 21 hours. Consecutively 100-200 larvae were collected from the spoon with a brush and placed on a thin layer of yeast in a fresh regular food vial.

Fly stocks

Canton S Flies were used in the tests

Apparatus

The setup consists of a small modular chamber made from acrylic glass (Fig. 20). Shock grids run along the roof and floor of the chamber. One long chamber side incorporates an infrared sensor from a bar code reader, while the opposite side is transparent in order to illuminate the fly and cast its shadow on the sensor to allow tracking. The ends of the chamber incorporate air input inlets, while the air output wells were made as a thin drilling in the middle of the roof and floor of the chamber. Modular design of the chamber allows for easy disassembly between experimental trials in order to clean the chamber of possible leftover markers from the previous experimental animal. A single chamber is enclosed in a non transparent plastic box with all electrical and olfactory access points covered to prevent illumination spill over from the outside.

Methods

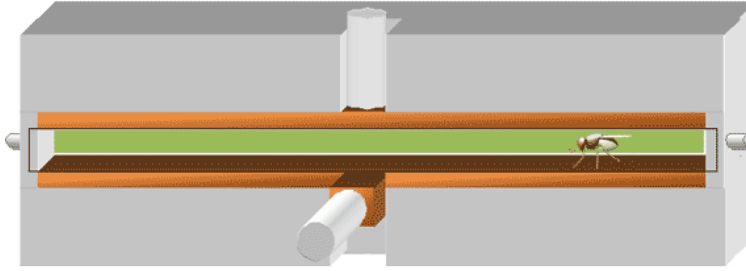
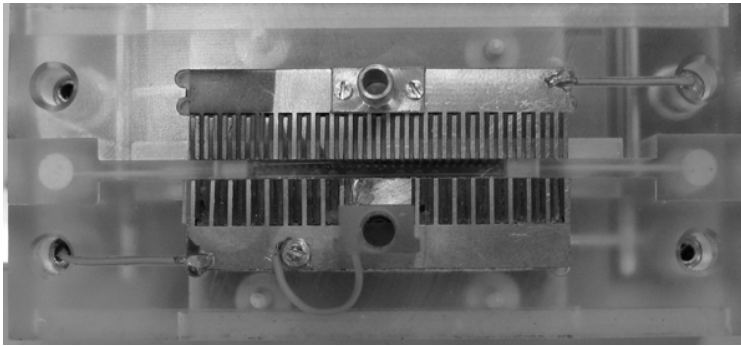
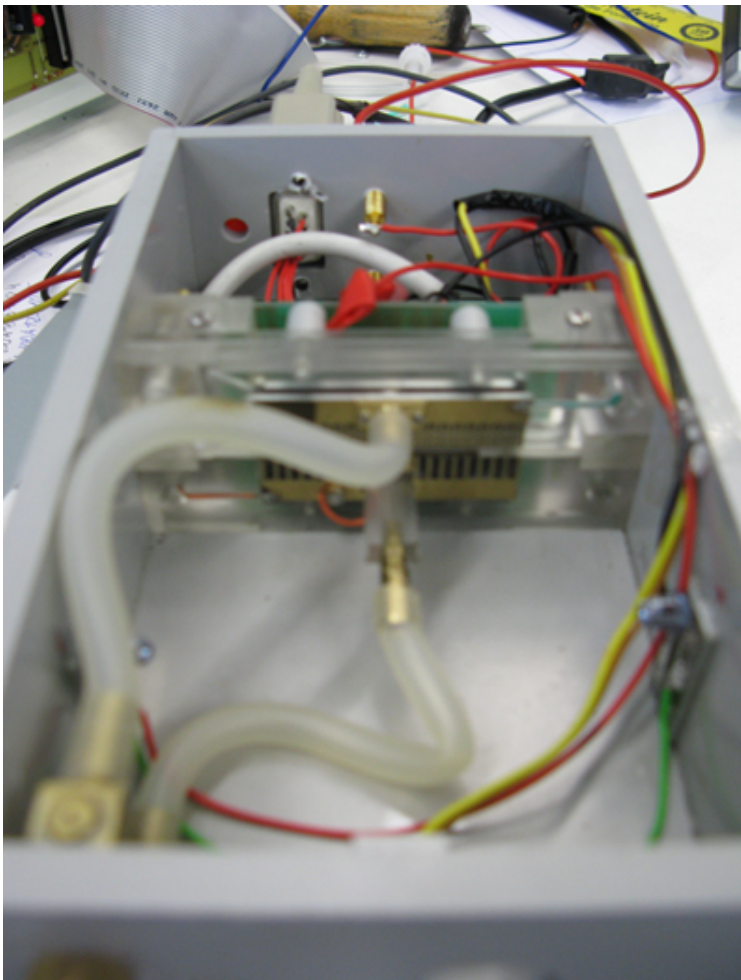


Figure 20: Shock box



Top: in scale schematic of the chamber

Middle: front view of the experimental chamber showing the electroshock grid and output air vents (lower one incorporates the loading tunnel)



Bottom: view of the complete chamber module with the top cover removed

Software

In the first set of experiments control software written for the Heat Box paradigm was used to track the position of the fly, due to design and circuitry similarities between the two paradigms. Application of electric shock was performed manually according to the rough position of the animal within the chamber. After the initial experimental phase new control software was developed specifically for the Shock Box paradigm, with automatic shock application by the software (Fig. 21).

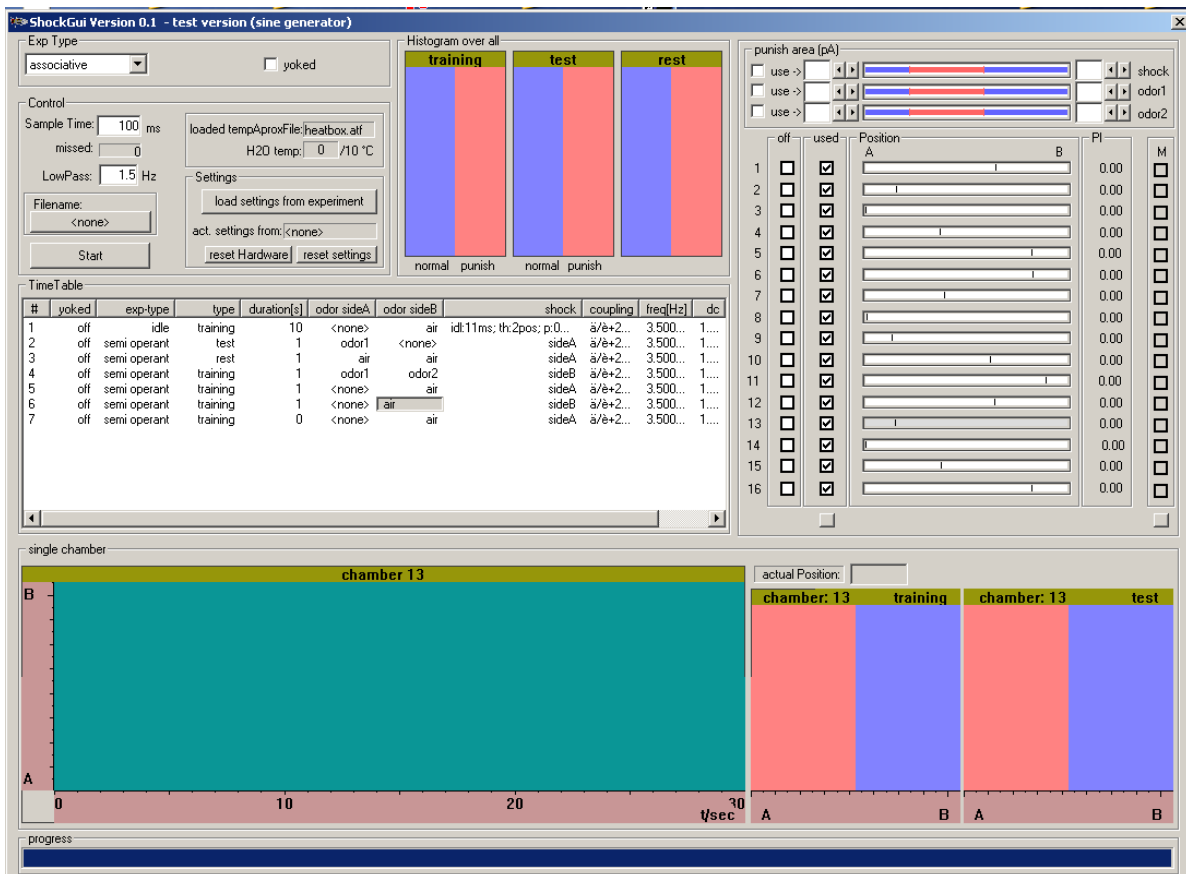


Figure 21: Shockbox control software (written by A. Eckart)

Multiunit software allowing for simultaneous control and monitoring of up to 16 shockbox modules

Preliminary place learning experiments

Flies were punished by 90V current constantly switched on while the fly was on the side of the chamber declared as “punished”. The experimental procedure consisted of 2 minutes pretest phase to get a base line walking activity and preference for a certain chamber side, this was followed by a 2 minutes training period, where the fly was punished while crossing the midline to the “punished” side and staying there, training was followed by a 2 minutes test phase, to see how the walking activity and side preference changed after training.

Place learning experiments

The experimental protocol was adjusted to a following scheme: pretest phase, three alternating training and test phases and a posttest phase to study possible memory extinction effects, each phase lasted for 1 minute.

Two sets of experiments were performed. In the first set dry air was blown into the chamber, during training flies were punished with 80V electric shock pulses delivered with a frequency of 2Hz for being at the punished side of the chamber; in the second set humidified air was blown into the chamber, the voltage of the punishment was increased to 100V . The punished side was alternated between the flies, to prevent possible accumulation of markers within the chamber between each tested animal and to eliminate the effect of chamber side preferences of individual flies. Two groups of flies were produced (Punished A, Punished B) according to the chamber side which was punished during the experiment. For each individual fly Preference Index towards the punished side (P_A or P_B) was calculated from the total time spent on each side of the chamber, ranging from -1 (100% avoidance) to 1 (100% attraction).

$$P_A = \frac{A - B}{A + B}$$

$$P_B = \frac{B - A}{B + A}$$

In order to quantify the effect of both reciprocal experiments a performance index PI was calculated from the mean preference indices of both groups (Punished A, Punished B), ranging from -1 (100% avoidance) to 1 (100% attraction).

$$PI = \frac{P_A + P_B}{2}$$

5. Results

5.1. cAMP Imaging

According to the present hypothesis on the cellular and molecular basis of olfactory conditioning cAMP levels in the mushroom body Kenyon cells are expected to increase after both, an olfactory stimulus or an electric shock and, very strongly, if both stimuli are given simultaneously. To test this hypothesis, cAMP levels in Kenyon cells had to be recorded under various stimulus conditions by employing genetically encoded sensors that change their fluorescence in the presence of cAMP.

Using the Gal4 line MB247 which strongly drives UAS-construct expression in the Kenyon cells of the mushroom bodies a number of lines with different insertion sites of the sensor constructs Epac1, Epac2, Epac2K390E and HCN2 generated by André Fiala, was tested for signal quality (Fig.22) The experiments revealed all lines featuring the Epac1 construct to be suitable for further investigation of cAMP dynamics. An effort was made to find at least one suitable line for each sensor type, however both Epac2K390E and HCN2 lines proved to be unusable due to low fluorescence signal strength (Fig. 23). Insertion line 5 featuring the Epac1 construct was deemed the best available sensor.

Results

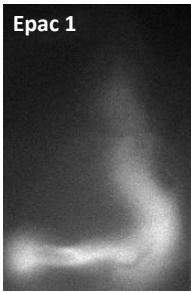
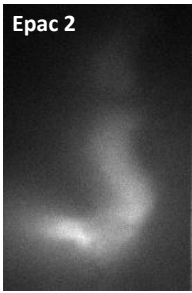
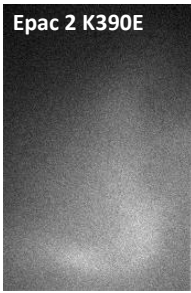

Fly line\Sensor	Epac2 K390E	Epac2	Epac1	HCN2
1	(2Chr.) tested	(2Chr.) tested	(3Chr.) tested	(2Chr.) tested
2	(2Chr.) tested	(3Chr.) tested	(2Chr.) tested	(3Chr.) tested
3	(3Chr.) tested	(2Chr.) tested	(3Chr.) tested	(3Chr.) tested
4	(2Chr.) tested	(2Chr.) tested	(3Chr.) tested	(3Chr.) tested
5	(2Chr.) tested	(3Chr.) tested	(2Chr.) tested	(3Chr.) tested
6	(2Chr.) tested	(2Chr.)		
7	(3Chr.) tested	(2Chr.) tested		
8	(2Chr.) tested	(3Chr.)		
9	(2Chr.) tested	(XChr.)		
10		(3Chr.) tested		

Figure 22: Sensor quality diagram, red space representing fly lines with unsuitable signal quality, green with acceptable one, panel in the lower right representing typical image quality for EYFP fluorescence of sensor types

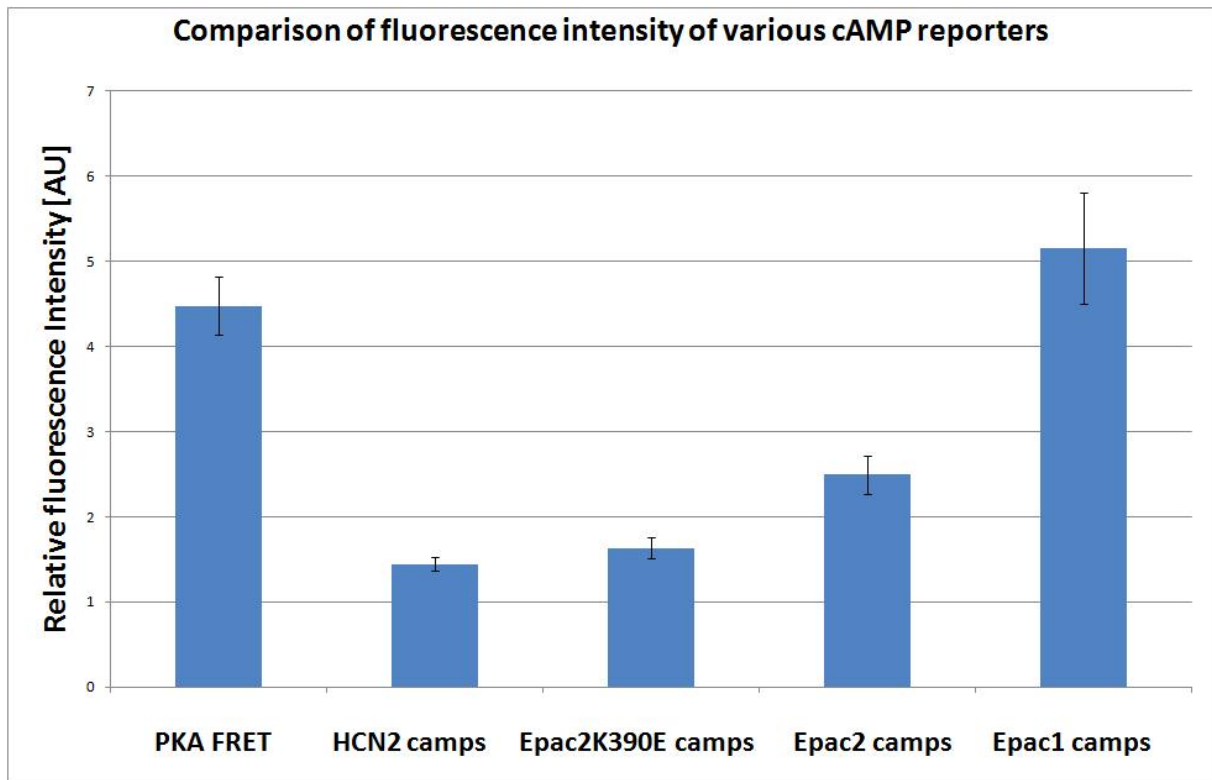


Figure 23: Comparison of fluorescence intensity of the EYFP channel for various sensor types

Relative fluorescence intensity measured as difference in intensity between background autofluorescence and sensor expressing fluorescent tissue. Columns representing mean relative intensity (n=10 for each group) in the EYFP channel, error bars representing the SEM. fluorescence in the EYFP channel for various sensor types utilizing the ECFP/EYFP fluorophore pair.

In order to demonstrate sensor functionality during pharmacological applications a series of experiments featuring application of two different concentrations (10 μ M and 50 μ M) of 8-Bromo-cAMP was performed. The sensor responded with different ratio values to application of both concentrations, the stronger response being recorded in the case of higher cAMP concentration. The temporal dynamics of the response proved to be rather slow with a rise time constant for the ratio in the range of hundred seconds, the ratio reaching its plateau phase between 100 and 200 seconds after the application (Fig. 24). The application artefact around the time point of application (10s, +/- 1s) due to the pipette tip insertion into the droplet is clearly visible in all cases of pharmacological applications.

Results

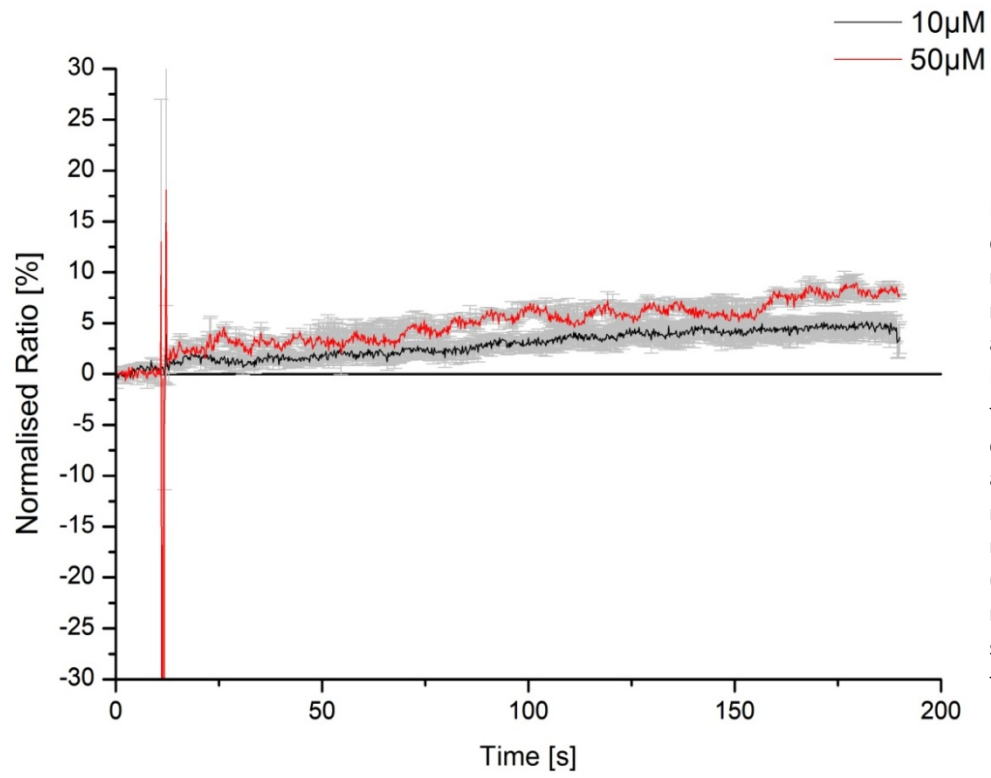


Figure 24: cAMP dynamics in the mushroom body in response to application of 8-Bromo cAMP of two different concentrations (10 and 50 μM). Lines representing the mean values ($n=12$). Error bars representing the standard error of the mean (SEM).

Results

In order to demonstrate sensor responsiveness to activity of adenylyl cyclases within the imaged cells, an application of Forskolin was performed. A strong response in form of approx. 20-30 % increase is visible in the ratio, as expected for near simultaneous activity of all cAMP producing cyclases within the imaged cells (Fig. 22).

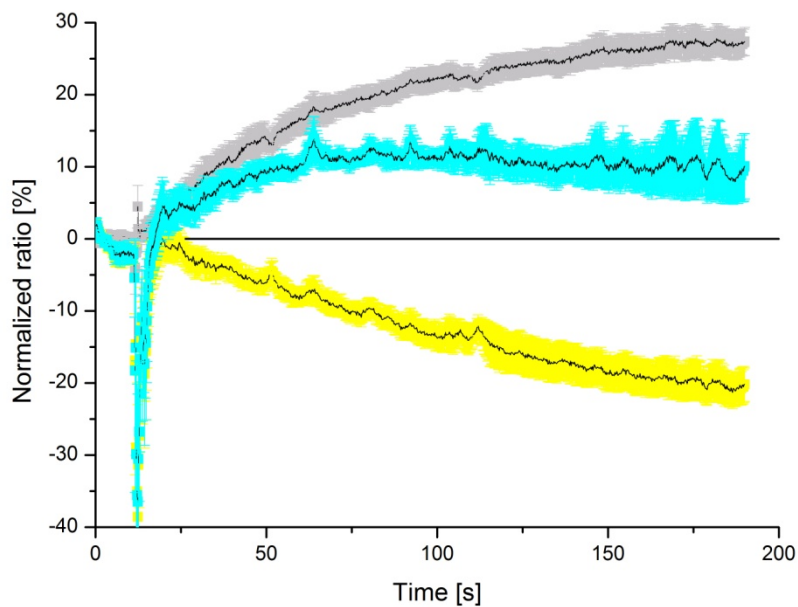


Figure 25: cAMP dynamics in response to the application of 10 μ M Forskolin, grey curve representing the change in the cAMP concentration, yellow and cyan curves, the change in respective fluorescence intensity). Lines representing the mean values (n=8). Error bars representing the standard error of the mean (SEM).

In order to provide pharmaceutical controls applications of physiological solution (Ringer in Fig. 23) and an inactive form of Forskolin (1,9-Dideoxyforskolin in Fig. 24) were performed both leading to negligible change in the ratio, and therefore deemed to present the approximate baseline of cAMP dynamics within the observed cells .

Results

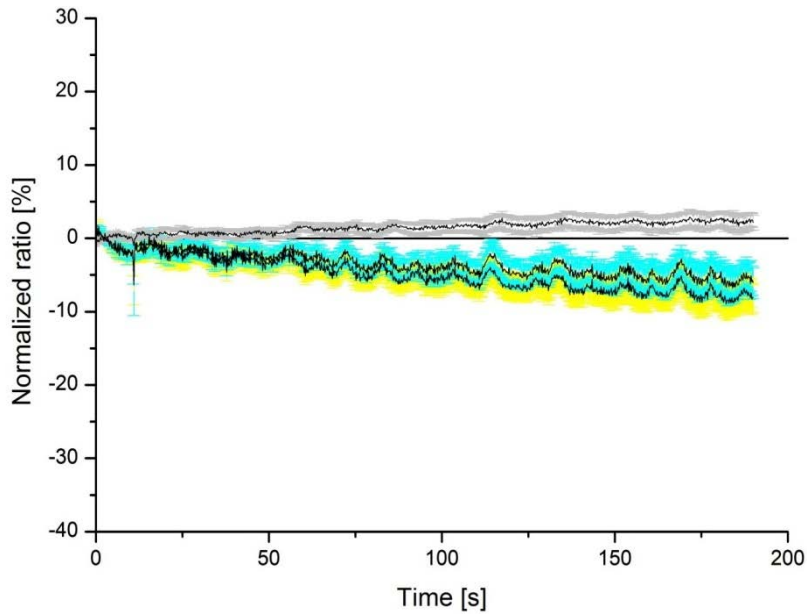


Figure 26: cAMP dynamics in response to the application of Ringer solution, grey curve representing the change in the cAMP concentration, yellow and cyan curves the change in respective fluorescence intensity. Lines representing the mean values (N=8). Error bars representing the standard error of the mean (SEM).

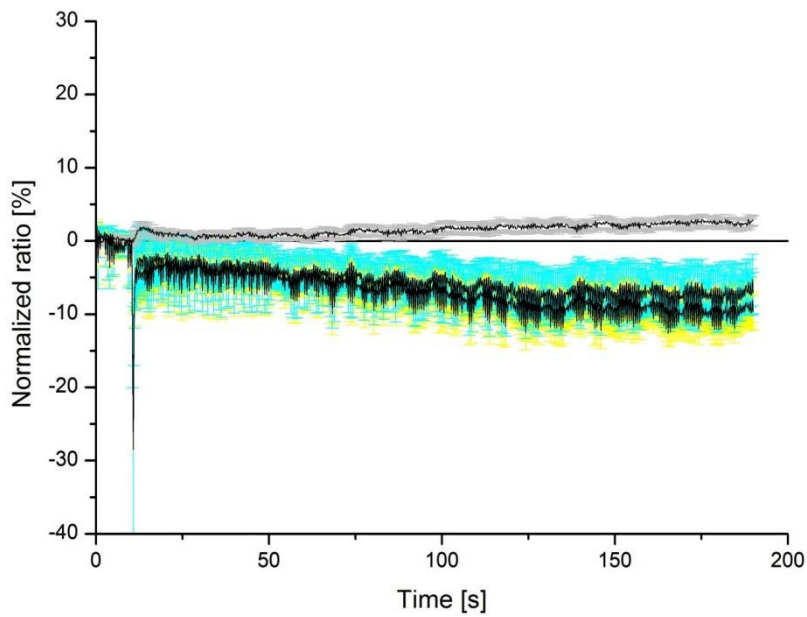


Figure 27: cAMP dynamics in response to the application of 10µM 1,9-dideoxyforskolin solution, grey curve representing the change in the cAMP concentration, yellow and cyan curves, the change in respective fluorescence intensity. Lines representing the mean values (n=8). Error bars representing the standard error of the mean (SEM).

Results

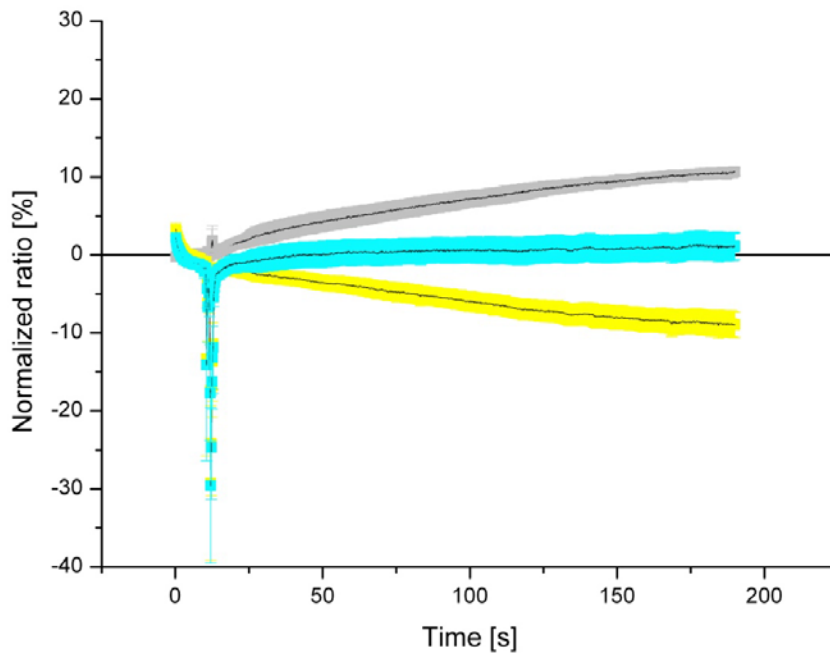


Figure 28: cAMP dynamics in response to the application of 10 μ M dopamine solution, grey curve representing the change in the cAMP concentration, yellow and cyan curves the change in respective fluorescence intensity. Lines representing the mean values (n=8). Error bars representing the standard error of the mean (SEM).

Several series of neurotransmitter applications featuring dopamine (Fig. 25), octopamine and acetylcholine, respectively, were performed to elucidate the effects of transmitter applications upon the cAMP dynamics within the imaged Kenyon cells. A comparative summary diagram of application effects was made, utilising the ratio intensity data within the last 50 cycles (10 seconds) for each individual pharmaceutical. The summary (Fig. 26) shows clear differences between the effects of control applications of carrier media and 1,9-dideoxyforskolin on one hand and applications of neurotransmitters on the other, with the response strengths to the applications of 8-Bromo-cAMP lying between the two groups.

Results

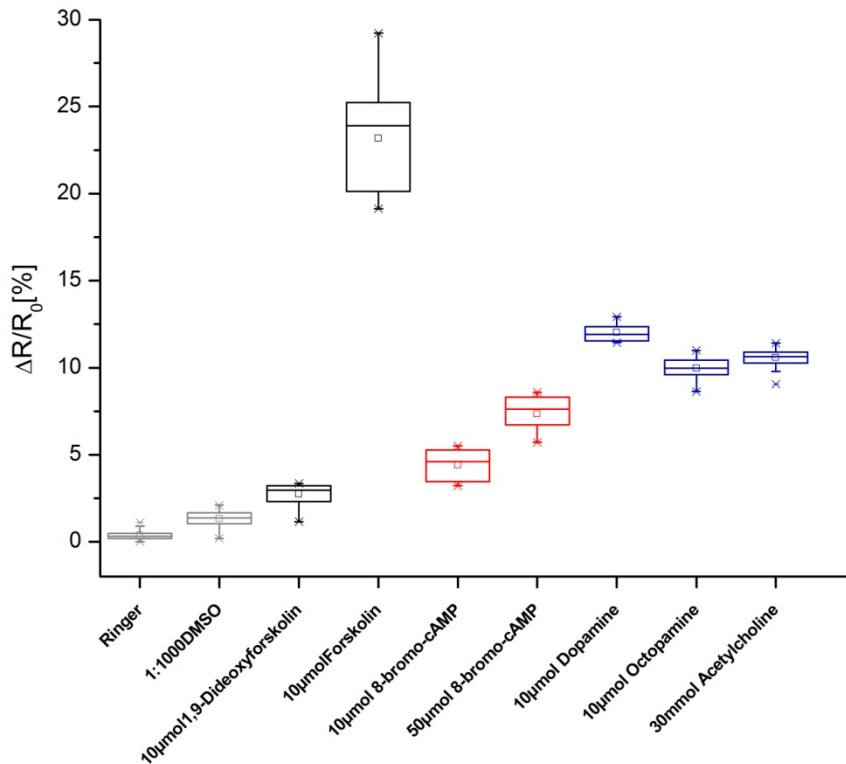


Figure 29: Summary of effects on cAMP dynamics induced by pharmacological applications, box plots represent the distribution of mean intensity in individual flies during the last 50 cycles of recording. Median (line), mean (square), 25th and 75th percentiles (box) and 10th and 90th percentiles (whiskers) are shown.

Several attempts to present olfactory and electroshock stimuli were made in the shock odour setup (Fig. 14). However, due to the accessibility difficulties of the antennae in this apparatus, the odour presentation shown here was performed using the fixation method as used for the application of pharmaceuticals (Fig. 13). Two series of experiments featuring the odorants methylcyclohexanol diluted 1:100 in paraffin oil (Fig. 27) and 3-octanol diluted 1:1000 in paraffin oil (Fig. 28) were performed. The concentrations used in the application experiments were chosen such that they would lead to similar learning scores in the T-Maze experiments (Niewalda 2011). These lead to distinctly different activation patterns in the antennal lobe (Völler 2007). Recorded ratio changes approximates to the baseline activity as recorded for application of control solutions.

Results

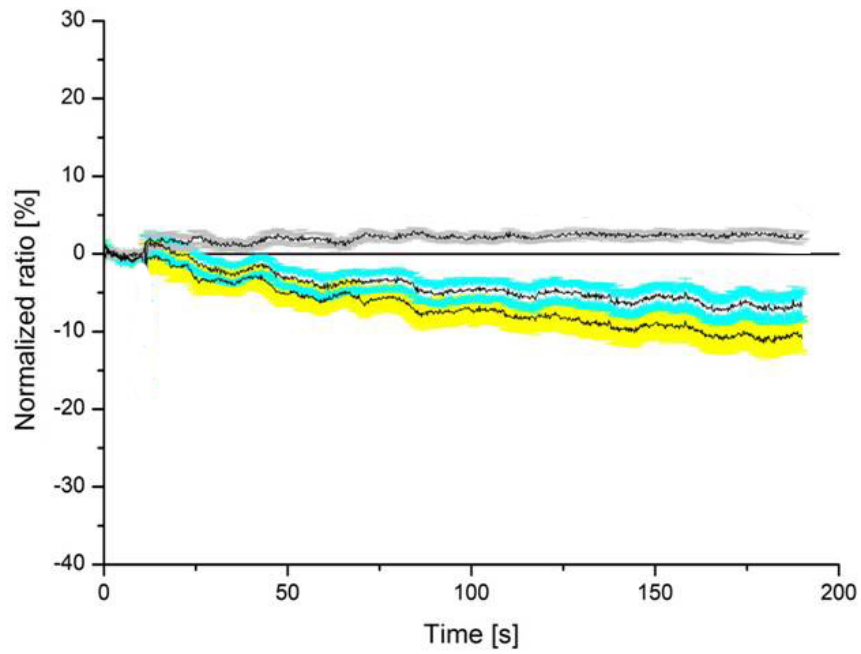


Figure 30: cAMP dynamics in response to the application of Methylcyclohexanol, grey curve representing the change in the cAMP concentration, yellow and cyan curves, the change in respective fluorescence intensity. Lines representing the mean values (n=8). Error bars representing the standard error of the mean (SEM).

Results

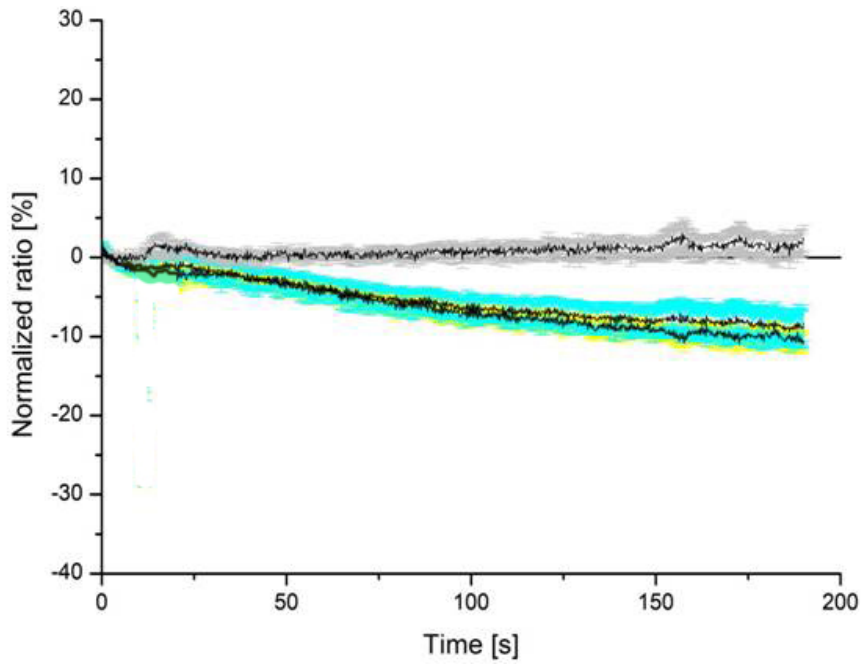


Figure 31: cAMP dynamics in response to the application of 3-Octanol, grey curve representing the change in the cAMP concentration, yellow and cyan curves, the change in respective fluorescence intensity. Lines representing the mean values (n=8). Error bars representing the standard error of the mean (SEM).

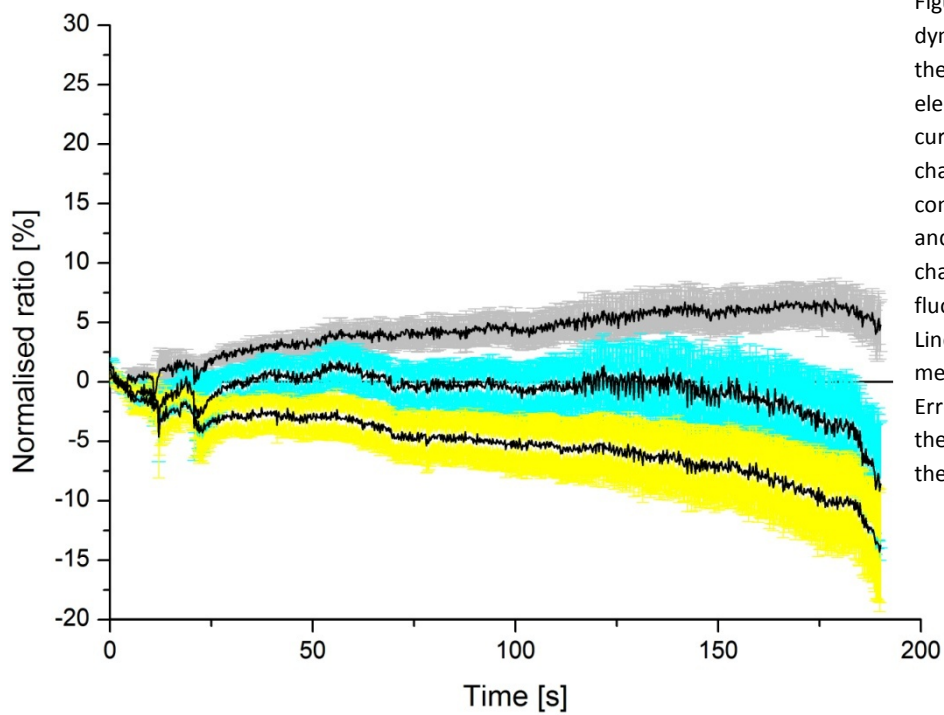


Figure 32: cAMP dynamics in response to the Application of electric shock, grey curve representing the change in the cAMP concentration, yellow and cyan curves, the change in respective fluorescence intensity. Lines representing the mean values (n=10). Error bars representing the standard error of the mean (SEM).

Results

Application of electric shock was performed in the shock apparatus (Fig. 14), leading to a reproducible maximal ratio change of about 5% at the plateau region of the recorded cAMP dynamics (Fig. 29)

Odorants, whether pure or mixtures, are assumed to activate only a small subset of Kenyon cells (Heisenberg 2003). Correspondingly cAMP increases in the MB lobes after odour application will be very small, and indeed no signals significantly different from controls could be recorded with MCH or 3Oct (Fig. 30). In order to stimulate a large number of Kenyon cells a cetylcholine was applied to the brain as a substitution stimulus for odorants, A clear cAMP response was observed (Fig. 26). In an attempt to demonstrate coincidence detection by adenylyl cyclases the combined effect of simultaneous Kenyon cell stimulation by acetylcholine induced activation) and electric shock was recorded, a summary diagram was created (Fig. 30) utilizing the same procedure as for the application of pharmaceuticals. Signal changes due to application of a single stimulus and the combined simultaneous application of acetylcholine and electric shock are shown. Comparing the latter response with the linear sum of the electroshock application and application of acetylcholine suggests a nonlinear summation of the cAMP production by the two stimuli in this particular case.

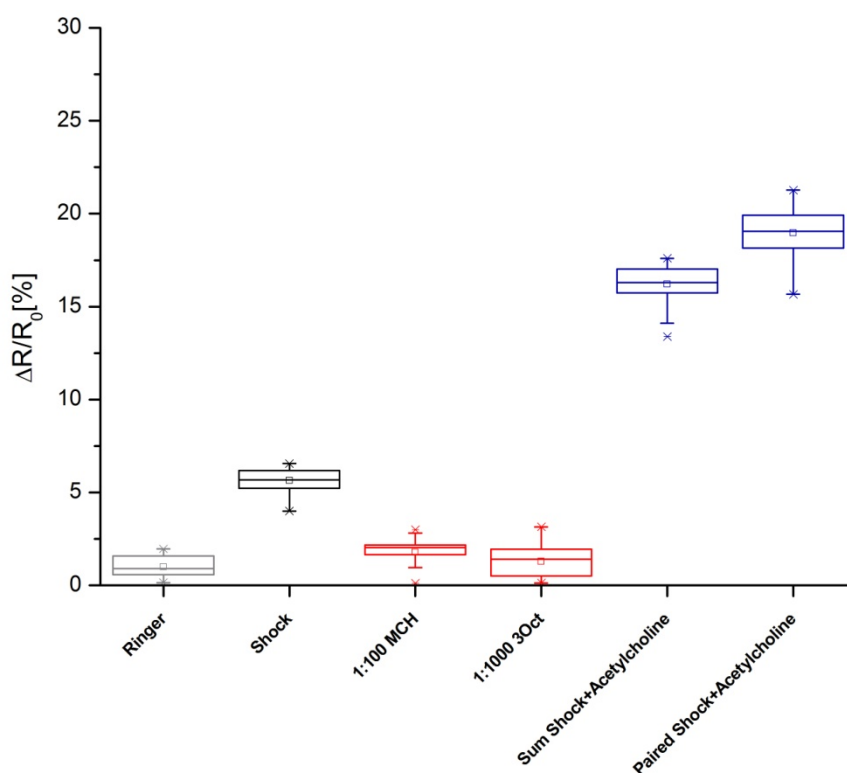


Figure 33: Summary of effects on cAMP dynamics induced by physiological applications of punishment (electric shock), odorants, or paired stimuli simulated odour signal (acetylcholin application to the mushroom body area, box plots represent the distribution of mean intensity in individual flies during the last 50 cycles of recording. Median (line), mean (square), 25th and 75th percentiles (box) and 10th and 90th percentiles (whiskers) are shown.

Results

Since signal-to-noise levels of optogenetic imaging can be improved by increasing the expression of the sensors. In an attempt to combine multiple copies of the UAS-Sensor construct in the same animal and to produce higher fluorescence intensity in lines featuring either Epac2K390E or the HCN2 sensor, as well as to generate an Epac1 featuring line by the combination of two sensor copies, several genetic crossings were made. For the sake of emission strength comparison a line featuring two copies of the PKA-FRET (Fig. 34), sensor construct which utilises the same number and type of fluorophores, and the Epac1.5 (Fig. 35) line were used. Mean emission strength images from various application experiments were utilised to get a representation of the signal strength quality in the respective lines. Combining two sensor copies proved to reliably increase the signal quality over the quality in the parental lines (Fig. 35) Due to the combination of two sensor copies it was not possible however, to establish a line featuring the Epac 1 sensor, showing a better signal quality than the Epac1.5 line (Figs. 23 and 36). Establishing a viable line featuring the Epac2K390E was a success (Fig. 35) adding this sensor type to the list of viable sensors. Due to extremely low signal strength it was not possible to establish a suitable line featuring the HCN2 construct.

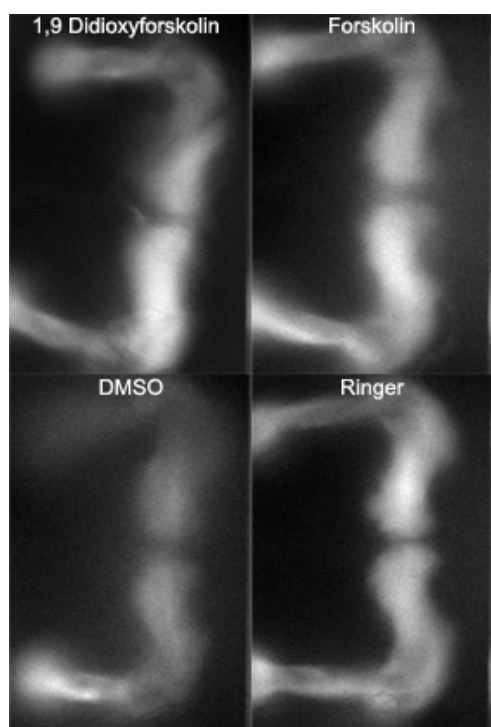


Figure 34 : **PKA-based cAMP sensor (PKA-FRET)**

Initial CFP emission of the mushroom bodies of four individual flies featuring two UAS-copies of the sensor construct, the images were taken prior to application of the indicated pharmaceuticals, showing individual variability of the fluorescence intensity between flies featuring the same sensor construct.

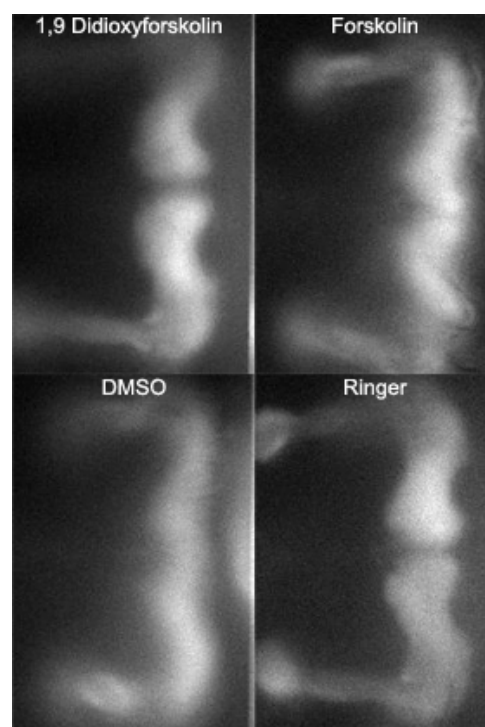


Figure 35 : **Epac1-based cAMP sensor (Epac1.5)**

Initial CFP emission of the mushroom bodies of four individual flies featuring a single UAS-copy of the sensor construct, the images were taken prior to application of the indicated pharmaceuticals, showing individual variability of the fluorescence intensity between flies featuring the same sensor construct.

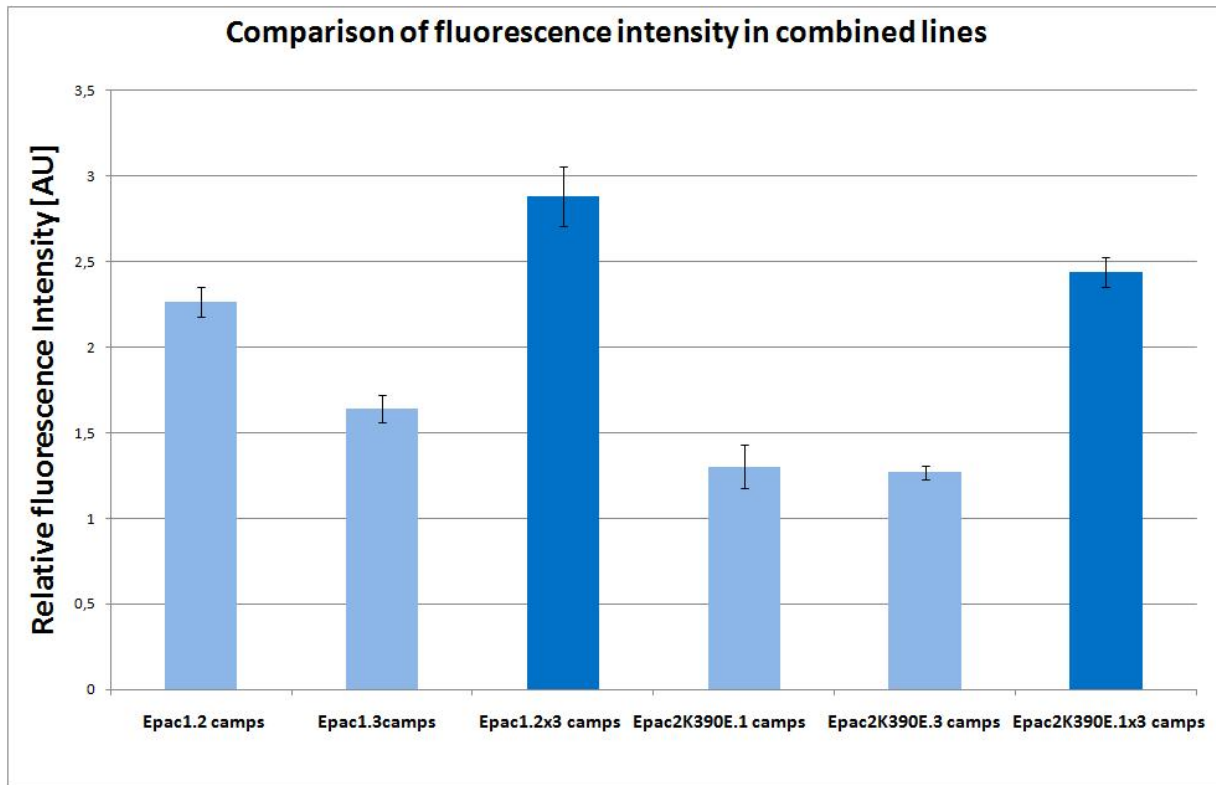


Figure 36: Comparison of fluorescence intensities in combined fly lines.

Means of relative fluorescence intensities are presented as columns, with error bars representing the SEM. Lines featuring multiple copies of the sensor construct show a significantly increased fluorescence intensities both for the Epac1 camps (T-test for independant samples $p < 0,01$, $n = 10$) and the Epac2K390E (T-test for independant samples

5.2. Imaging and optical activation of neurons in walking flies

In order to elucidate the validity of Strauss model for locomotor control in *Drosophila* described in the introduction part, an optogenetic attempt to visualise and activate parts of the protocerebral bridge in walking animals was made. Utilising the UAS-Chop (ChR2) and 007y-Gal4 constructs, as well as Fluorophore-tagged UAS-ChR2-YFP and 007y-Gal4GFP constructs, combined with a careful dissection of the animal, to make parts of its brain accessible for light activation (Fig. 36). While this line showed strong expression outside of the protocerebral bridge, particularly in the area of mushroom body calices it, the expression pattern was deemed suitable for further neuronal activation experiments.

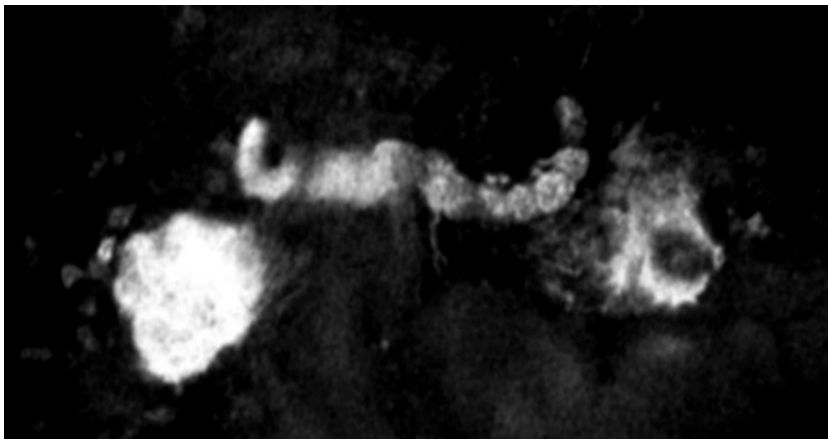


Figure 37: confocal image of 007y-Gal4 mcd8GFP expression pattern

The viability of the new dissection method was confirmed by fluorescent microscopy of the dissected animal. A bridge-like structure was reproducibly made both visible and accessible by the dissection procedure, while being detectable by naked eye as a faint outline only, its distinct shape could be made more pronounced by post processing and contrast enhancement of the recorded images (Fig. 37). However it was difficult to positively identify it as a protocerebral bridge without an anatomical comparison, which was performed, utilising images of paraffin slices (Fig. 38). Due to positive identification of the observed, pilot walking ball experiments were performed, which revealed a reliable walking duration of the dissected animals being at least 30 minutes long. This duration was used in all subsequent activation experiments.

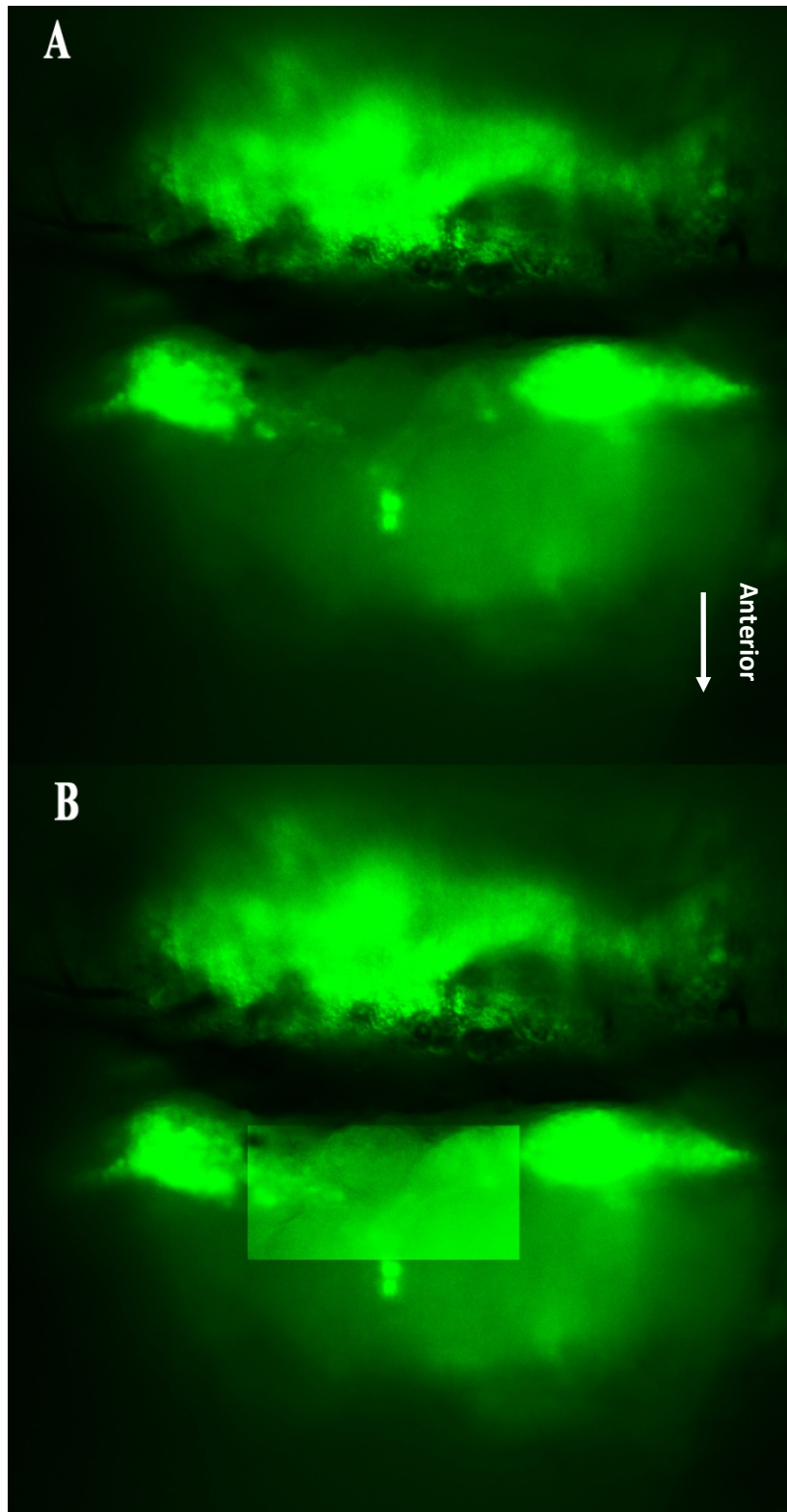


Figure 38:

Top: Direct view on the brain of a dissected fly fastened in the apparatus

Bottom: Same image with a contrast enhanced area around the protocerebral bridge. Light stimulation was focused either on the whole area or its right half, depending on the experimental protocol (Fig. 40)

Results

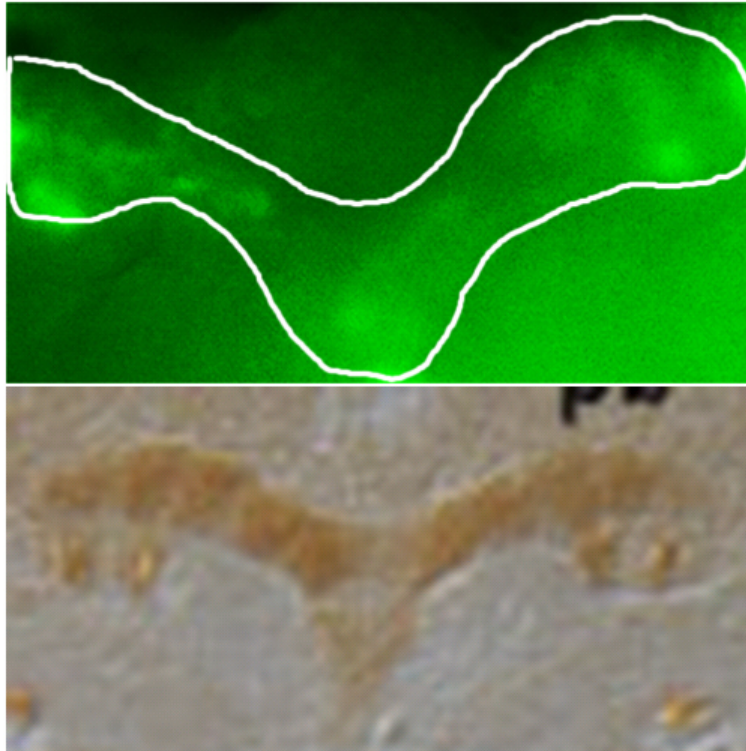


Figure39: Confirmation of driver and dissection viability

The fluorescent image observed in the brain of dissected fly fastened in the apparatus, white outline indicating the structure of the protocerebral bridge (top), compared to a paraffin slice (Poeck et. al 2007) (bottom). The structure of the protocerebral bridge is discernable and can be easily identified as such, allowing for selective stimulation

Results

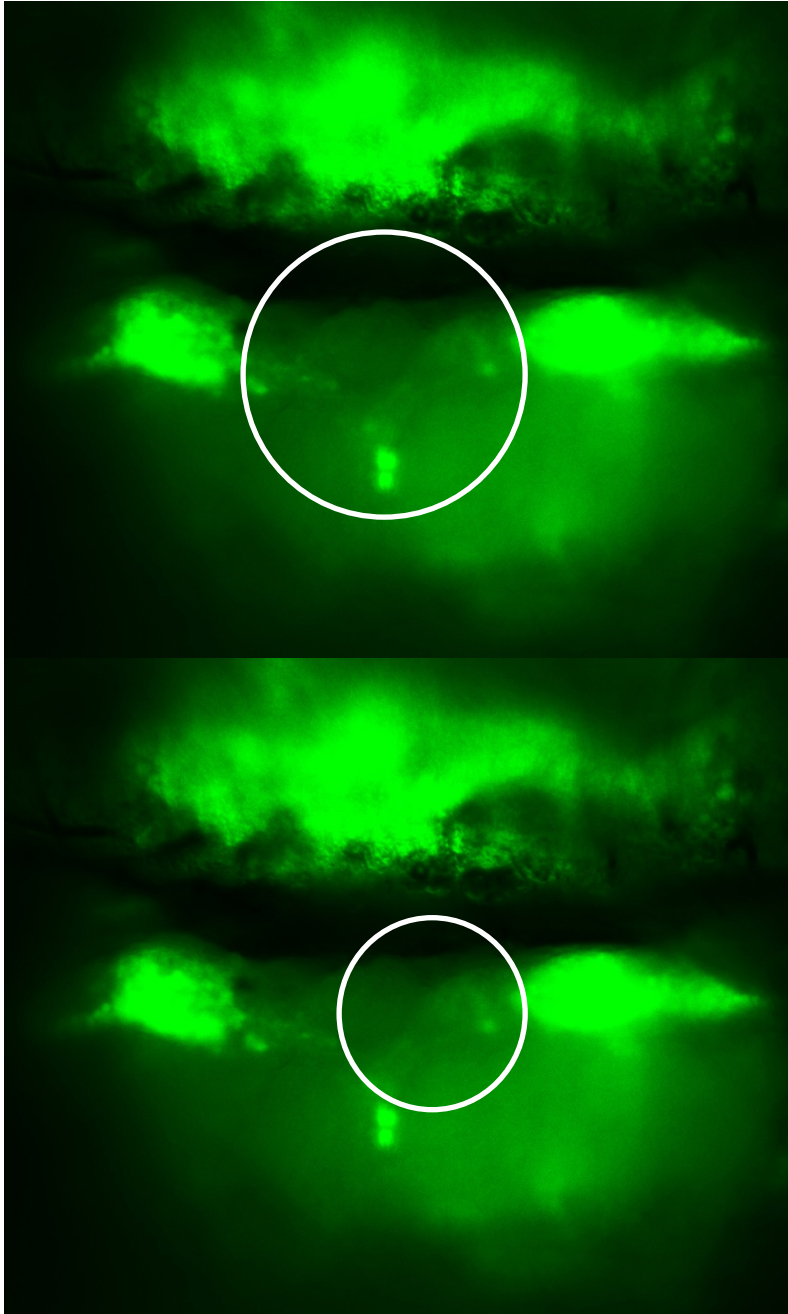


Figure40: Stimulation areas

Aperture focusing was used for selective stimulation of either the whole, or only half of the protocerebral bridge. The relative positions of the stimulated areas are indicated by the circles (top image representing the aperture focus for full bridge stimulation, bottom image representing the aperture focus for half bridge stimulation).

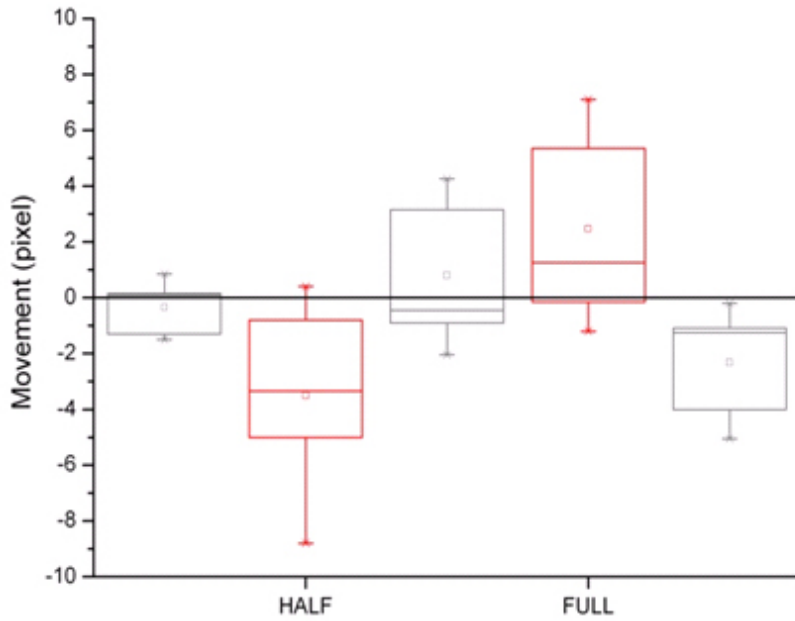
Results

Stimulation was always performed either on the left side of the protocerebral bridge or on the entire bridge area. The recorded walking behaviour with positive values indicating ball rotation to the right and negative rotation to the left was plotted as a box plot in two different ways, first one (Fig. 39A, 40A) showing overall direction of movement for each respective phase of the experiment (all movement in the phases of half bridge activation, all movement in phases without activation and so on) the second way of presentation (Fig. 39B, 40B) shows the combined movement in the first minute interval of either all half bridge or all full bridge activations.

Although the interpretation of recorded walking behaviour is very difficult, a difference in the walking behaviour between the control (CS wildtype) and experimental group (007y-Gal4 x UAS-Chop-eYFP) flies can be observed. Interestingly the flies in which the protocerebral bridge was stimulated by light showed no clear preference for the walking direction, whereas the control flies always showed a trend (T-test, $p > 0,05$, $n=10$) in side preference during both the activation phases and the intermittent phases between activations.

Results

A



B

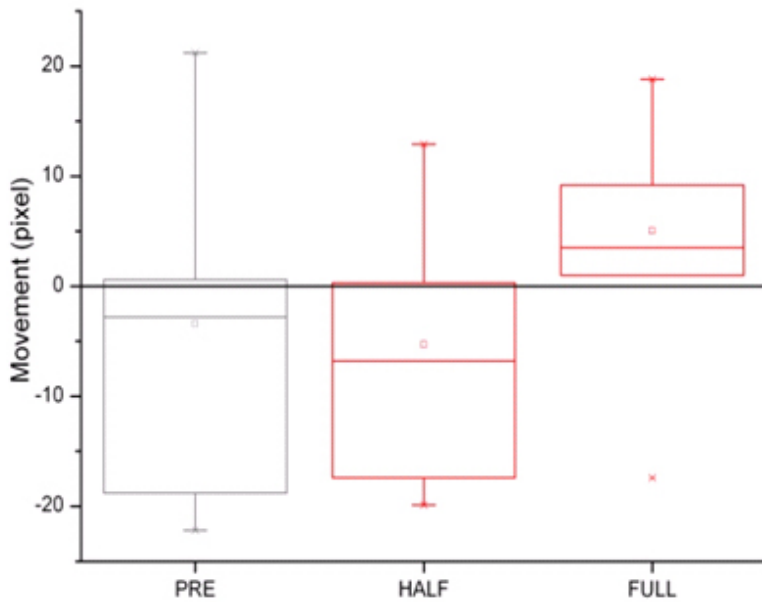


Figure 41: CS flies

A: leftmost grey box plot representing 5 minutes pretest without stimulation; leftmost red boxplot represents the sum of movement during 1 minute activation bouts of half bridge stimulation; middle grey boxplot representing the sum of movement during 1 minute pauses of half bridge stimulation; rightmost red box plot representing sum of movement during 1 minute activation bouts of full bridge stimulation; rightmost grey box plot representing the sum of movement during 1 minute pauses of full bridge stimulation (N=10).

B: leftmost grey box plot representing 5 minutes pretest without stimulation; red boxplots represent the pooled movement data during first 10 seconds of activation of all half stimulation and full stimulation parts of the experiment respectively (N=10).

Results

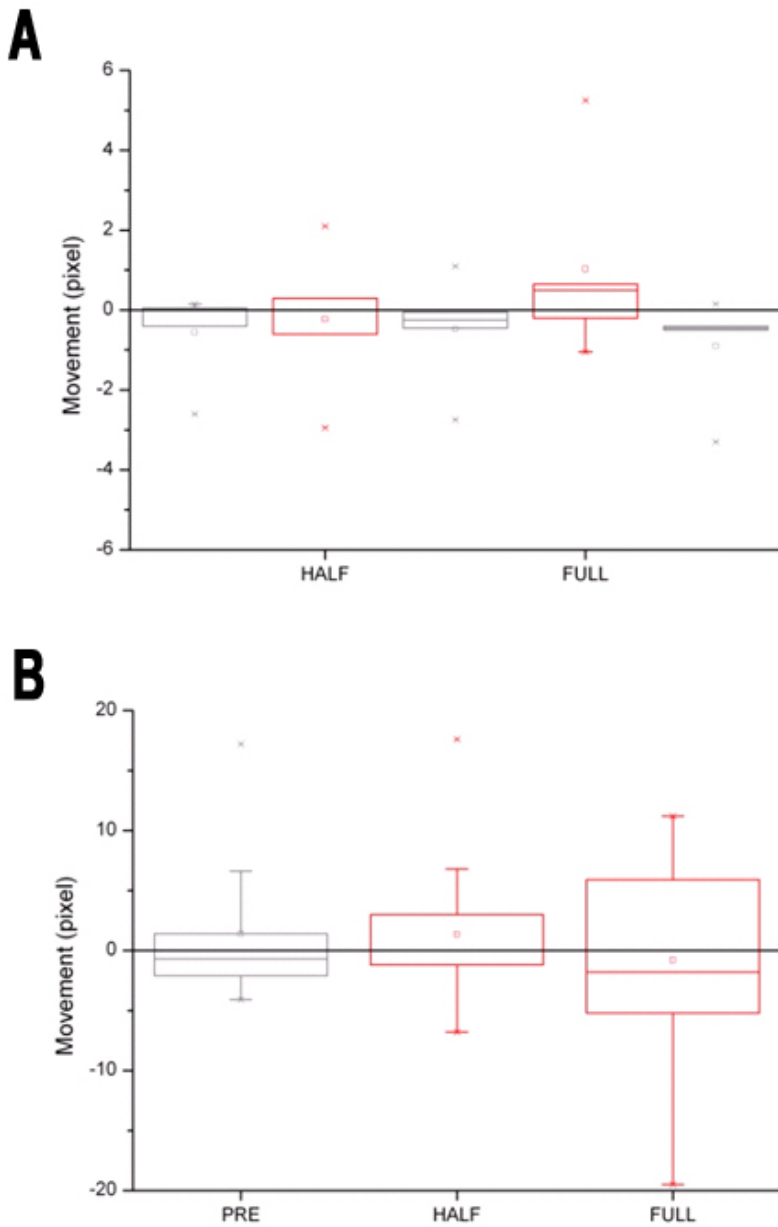


Figure 42 : 007Y-GAL4 x CHOP-eYFP flies

A: leftmost grey box plot representing 5 minutes pretest without stimulation; leftmost red boxplot represents the sum of movement during 1 minute activation bouts of half bridge stimulation; middle grey boxplot representing the sum of movement during 1 minute pauses of half bridge stimulation; rightmost red box plot representing sum of movement during 1 minute activation bouts of full bridge stimulation; rightmost grey box plot representing the sum of movement during 1 minute pauses of full bridge stimulation (N=10).

B: leftmost grey box plot representing 5 minutes pretest without stimulation; red boxplots represent the pooled movement data during first 10 seconds of activation of all half stimulation and full stimulation parts of the experiment respectively (N=10).

Results

After improvements in the ball tracking device and evaluation software a new set of experiments was performed, apparatus inherent ball movement noise (Fig. 43) was determined by recording of 1 minute constantly observed fly inactivity bout. Recordings with wild type Canton S flies were performed to determine normal activity pattern under experimental condition, showing severe differences between extremely active flies (Fig. 45) and flies displaying sporadic activity bouts only (Fig. 44). However the fixation procedure still has an impact on the fly performance when compared to the activity pattern of a fly fixed in a clamp by a small needle glued to its thorax (Fig. 46).

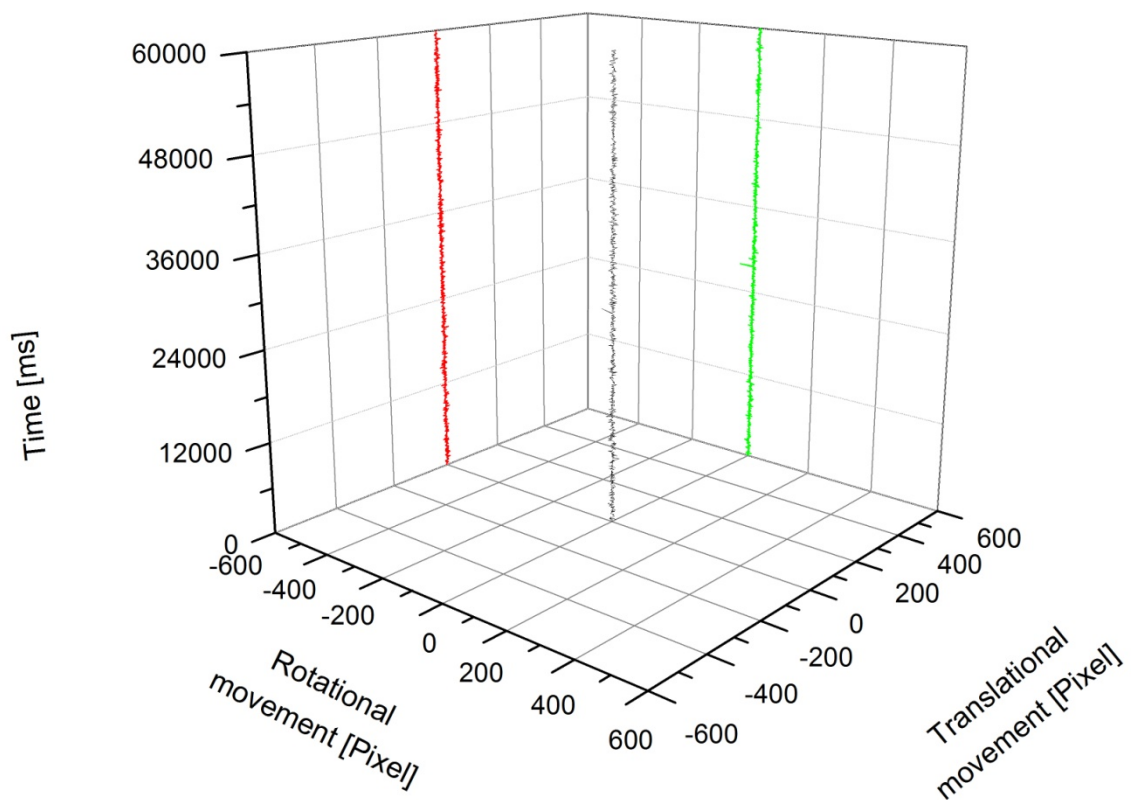


Figure 43: Spatiotemporal noise pattern

Ball movement noise with the fly standing on the ball, recorded over a 1 minute interval, without any movement activity of animal. Temporal dynamics are represented in the vertical axis, spatial dynamics in the horizontal; green line representing rotational activity with rotation to the left represented by negative values, rotation to the right by the positive ones, red line representing translational activity, with forwards translation represented by positive and backwards translation by negative values; three dimensional black line represents the trajectory of the ball movement in space and time.

Results

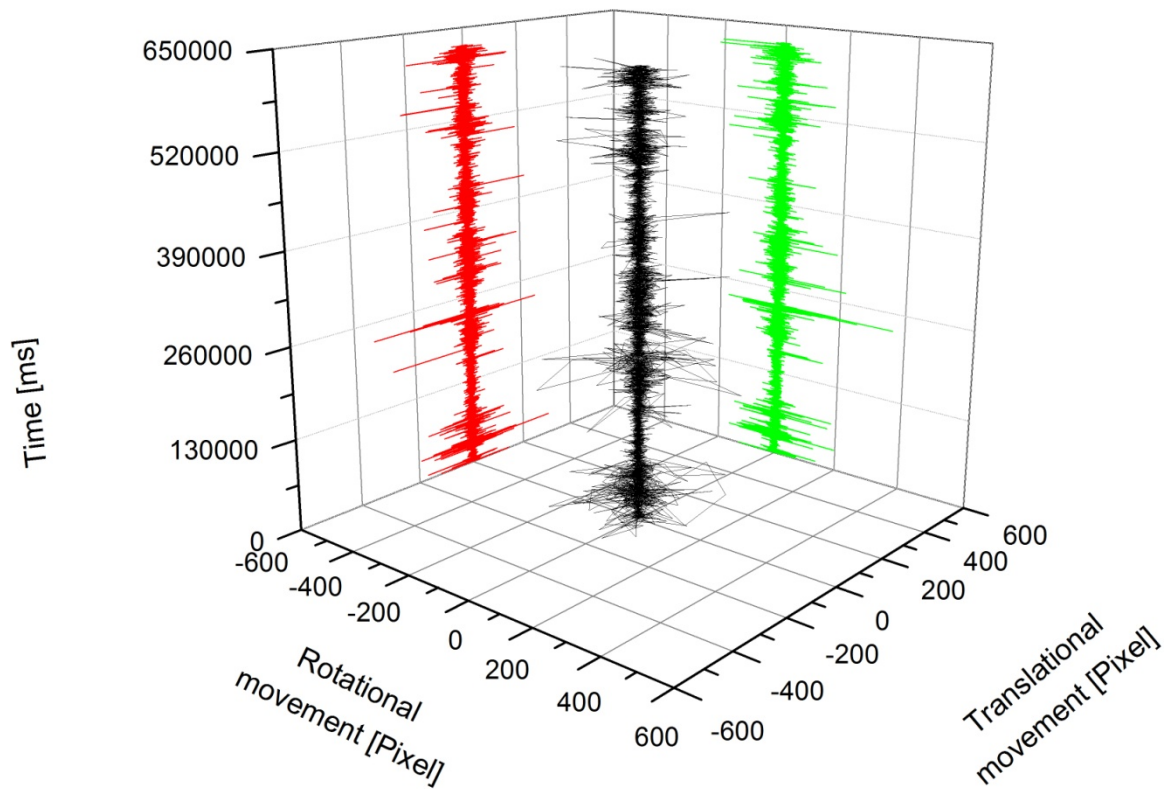


Figure 44: Spatiotemporal activity pattern of a normal active wild type CantonS fly

Activity pattern of a typical CantonS fly. Data is recorded over 650 seconds of mixed stimulus application, with 2 minutes pre test phase, 14 subsequent activation bouts of 40 seconds each and a post test phase of 2 minutes. Temporal dynamics are represented in the vertical axis, spatial dynamics in the horizontal; green line representing rotational activity with rotation to the left represented by negative values, rotation to the right by the positive ones, red line representing translational activity, with forwards translation represented by positive and backwards translation by negative values; three dimensional black line represents the trajectory of the ball movement in space and time.

Results

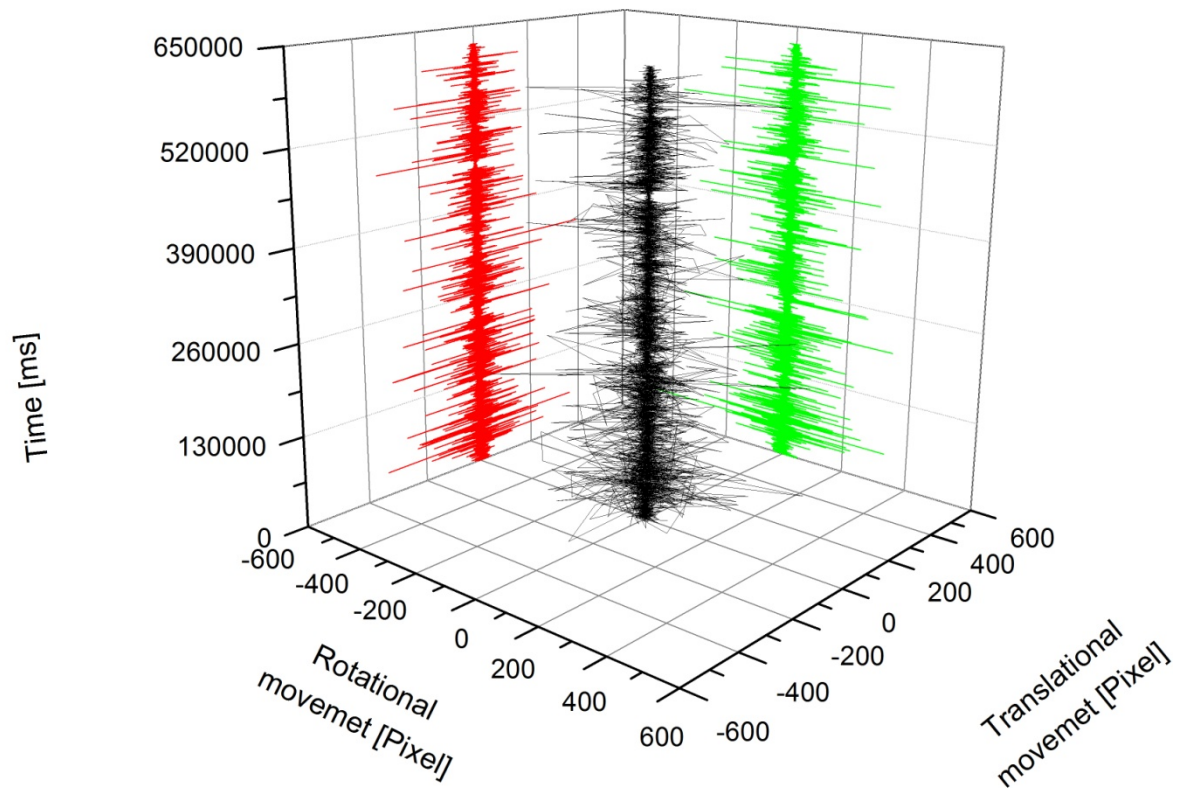


Figure 45: Spatiotemporal activity pattern of a hyperactive CantonS fly

Typical activity pattern of an extremely active CantonS fly. Average unidirectional movement speed approximates to 7,6 mm/s. Temporal dynamics are represented in the vertical axis, spatial dynamics in the horizontal; green line representing rotational activity with rotation to the left represented by negative values, rotation to the right by the positive ones, red line representing translational activity, with forwards translation represented by positive and backwards translation by negative values; three dimensional black line represents the trajectory of the ball movement in space and time, all values in the diagram have been multiplied by -1 to represent the actual movement direction of the fly.

Results

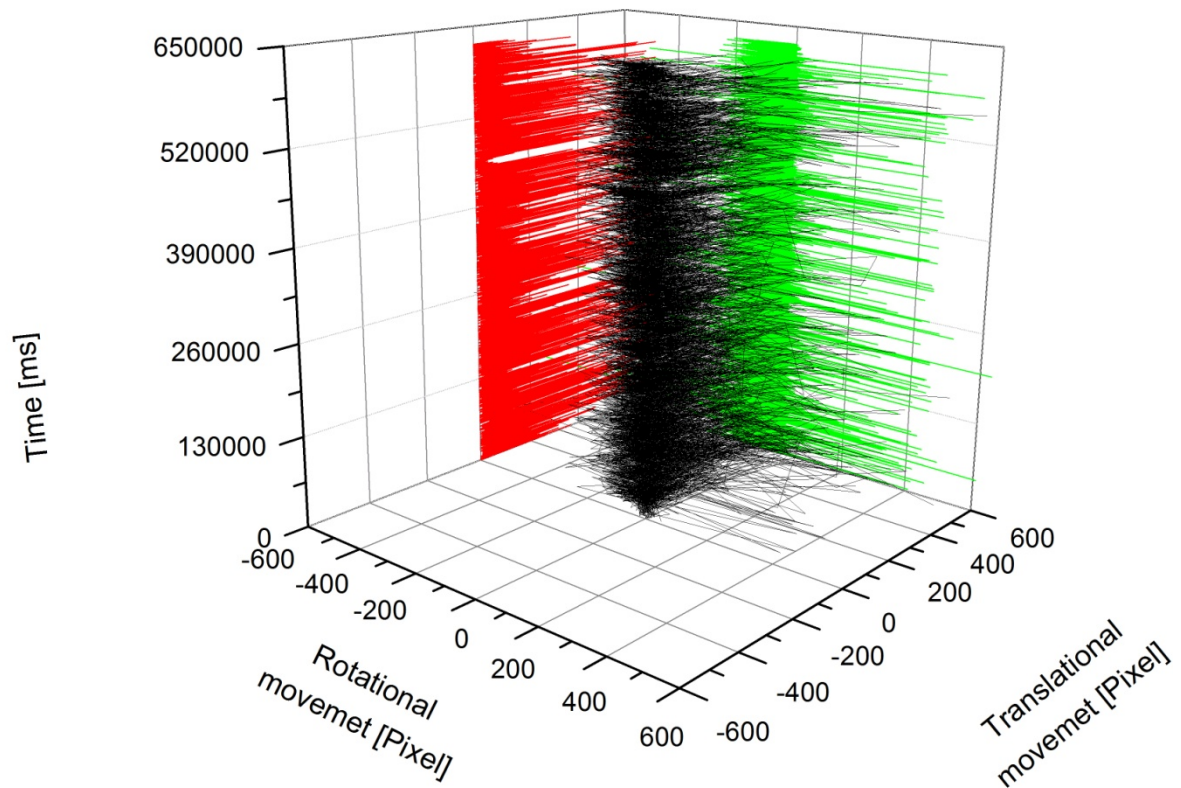


Figure 46: Spatiotemporal activity pattern of a hyperactive CantonS fly

Typical activity pattern of an CantonS fly with an unglued head, tethered to a holding clamp by a small needle glued to the flies thorax only. Temporal dynamics are represented in the vertical axis, spatial dynamics in the horizontals; green line representing rotational activity with rotation to the left represented by negative values, rotation to the right by the positive ones, red line representing translational activity, with forwards translation represented by positive and backwards translation by negative values; three dimensional black line represents the trajectory of the ball movement in space and time.

5.3. Conditioning in the “Shock Box”

For imaging molecular changes related to learning and memory it would be of great advantage if one could train individual flies and test their performance prior to the imaging experiment described in the previous chapter. With this goal in mind a new behavioural paradigm was developed that should permit classical, operant or semi-operant conditioning. This paradigm has been described in detail in methods.

Preliminary testing of the chamber was performed in form of a place learning experiment, utilizing manual punishment application, while tracking the fly with the tracking utility implemented in the Heat Box software. Upon entry into the chamber flies were given 1 minute habituation time, after which recording of the fly movement commenced. Most flies were patrolling the chamber from left to right and back throughout the entire recording period and reacted to the punishment sporadically. A large proportion of flies apparently ignored the punishment stimulus and continued patrolling the chamber (Fig. 47). Some flies however displayed visible avoidance behaviour of the punished chamber side, spending most of the time on the unpunished chamber side with only brief forays into the punished area both during the training and the test phase. An example of such fly is shown in Fig. 48. However the majority of the flies showed no immediate response towards punishment in the training phase, or a subsequent avoidance behaviour in the test phase.

Results

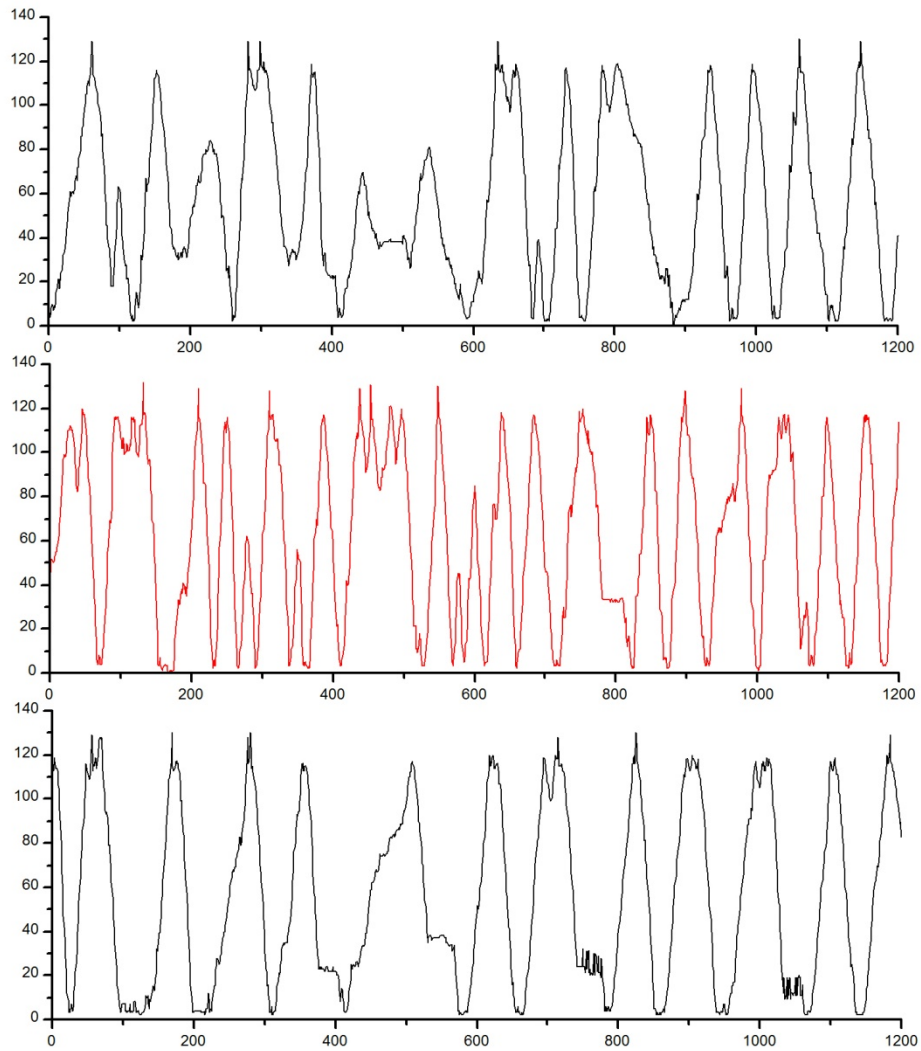


Figure 47: Typical spatiotemporal dynamics of fly movement within the Shock box

Movement and dwelling behaviour of 5 typical CS flies, during the place learning experiment. Punishment was applied upon entering of the left chamber side (Position 0-65). The absolute position of the fly during each time step is plotted on the ordinata, while the abscissa displays the time in 100ms steps. Upper black graph represents the pretest phase, middle red graph represents the training phase and lower black graph represents the test phase. Phase duration was set to two minutes with phases following each other in immediate succession.

Results

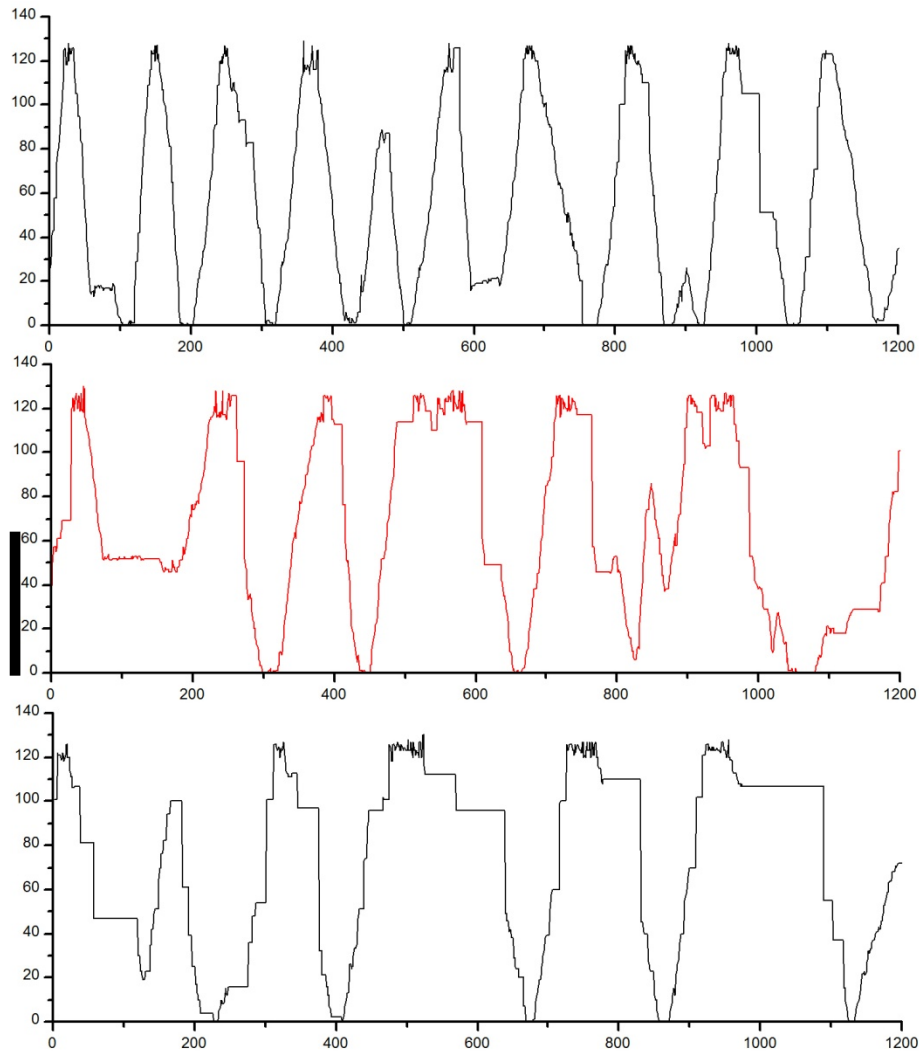


Figure 48: Spatiotemporal dynamics of the movement of a fly showing avoidance of one chamber side (punished side marked by black bar)

Typical case, displaying avoidance behaviour, the fly patrols in the pretest phase and starts to avoid the punished side during training, avoidance behaviour is persistent in the test phase. Punishment was applied upon entering of the left chamber side (Position 0-65). The absolute position of the fly during each time step is plotted on the ordinata, while the abscissa displays the time in 100ms steps. Upper black graph represents the pretest phase, middle red graph represents the training phase and lower black graph represents the test phase. Phase duration was set to two minutes with phases following each other in

Introducing a new tracking and control software specifically designed for the shock box paradigm a series of pilot experiments featuring 80V voltage strength for punishment and dry air circulation in the chamber. Novel experimental protocol was used, switching from 2 minutes pretest, 2 minutes training, 2 minutes test routine, to 1 minute duration of all phases, as well introduction of several alternating training and test periods, and a posttest phase, which might serve as an indicator of memory extinction. Flies appeared nonresponsive to punishment, irrespective of the punished side

Results

(Figs. 49, 50) flies showed no specific reaction towards application of electric shock and were patrolling the chamber throughout all phases of the experiment.

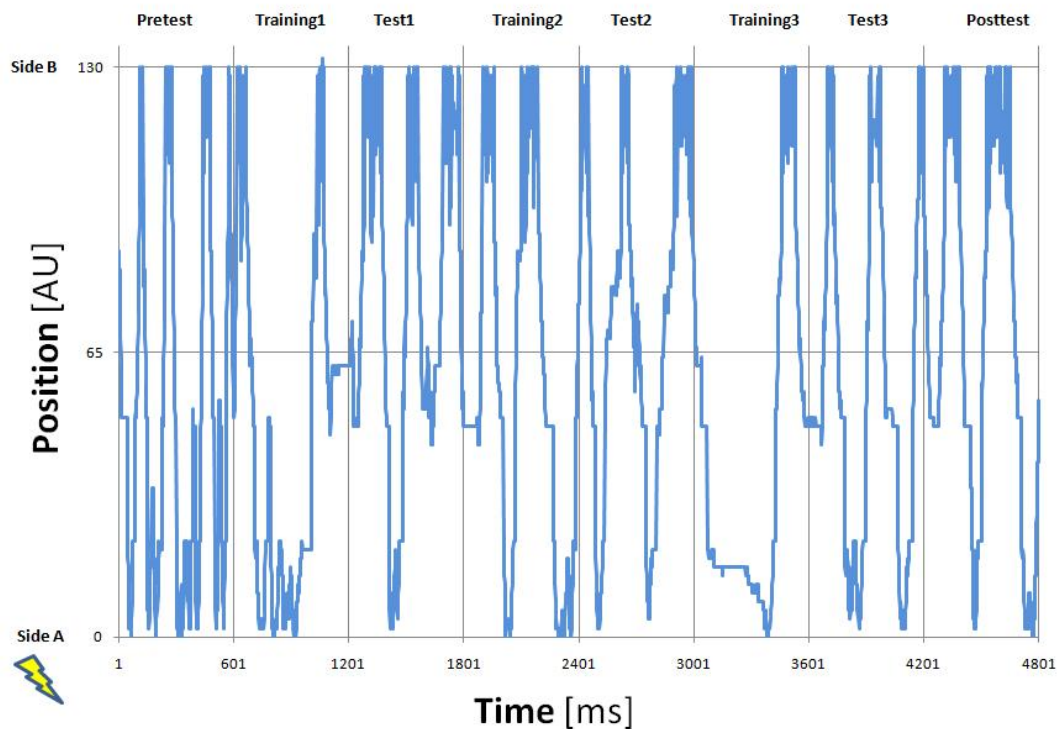


Figure 49: Spatiotemporal dynamics of fly movement under dry air conditions (punished side A)

Typical case displaying lack of avoidance behaviour. during training, avoidance behaviour is persistent in the test phase. Punishment was applied upon entering of the left chamber side (Position 0-65) subsequently called side A. The absolute position of the fly during each time step is plotted on the ordinata, while the abscissa displays the time.

The calculated performance index clearly demonstrates a lack of any avoidance behaviour in the training phases or any type of learning or memory dependent effects in the test phases for both reciprocal groups (Fig. 50). Therefore two changes were made to the experimental conditions: an increase in the punishment voltage, and a change in the air circulation within the chamber from dry to humidified air. These changes had an immediate effect both on the behaviour during the training phases, as flies responded to the application of electric shock by movement to the unpunished chamber side, as well as on the performance in the test phases, where flies tended to either patrol the previously unpunished side or sit their displaying only short bouts of movement (Figs. 52,53). These avoidance and putative learning effects can be clearly observed in the graph displaying the

Results

performance index of both reciprocal groups (Fig. 54), increasing in strength after the first training/test pair and reaching a plateau of approximately 60-80% avoidance in the subsequent training/test pairings.

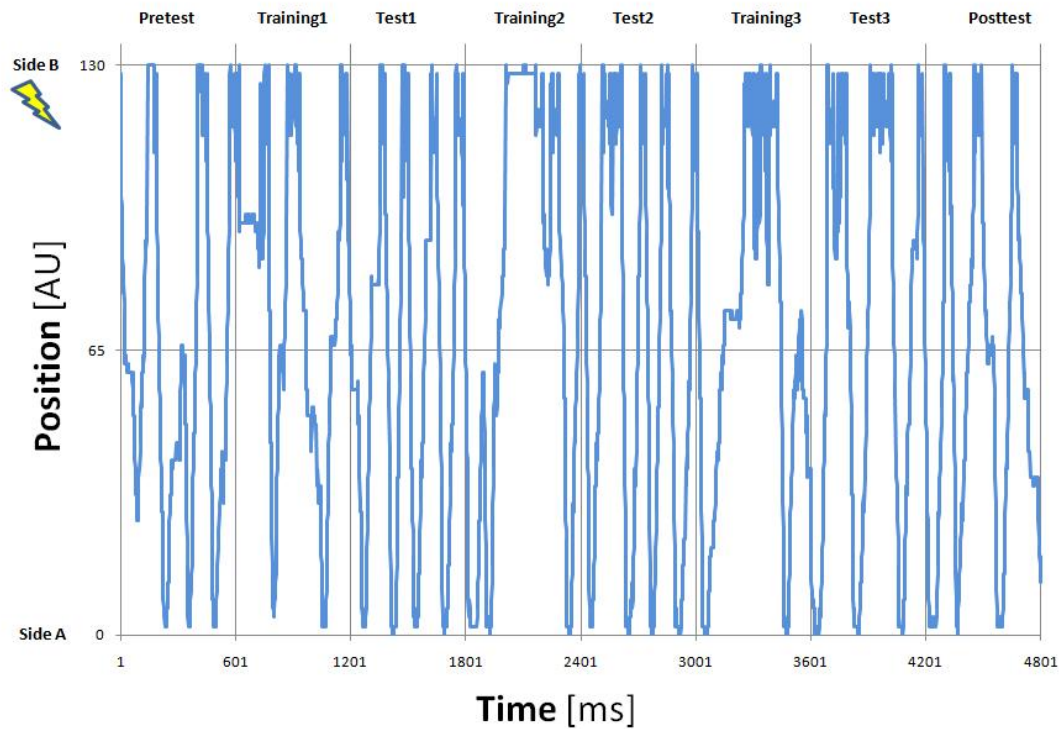


Figure 50: Figure 49: Spatiotemporal dynamics of fly movement under dry air conditions (punished side B)

Typical case displaying lack of avoidance behaviour. during training, avoidance behaviour is persistent in the test phase. Punishment was applied upon entering of the left chamber side (Position 0-65) subsequently called side A. The absolute position of the fly during each time step is plotted on the ordinata, while the abscissa displays the time.

Results

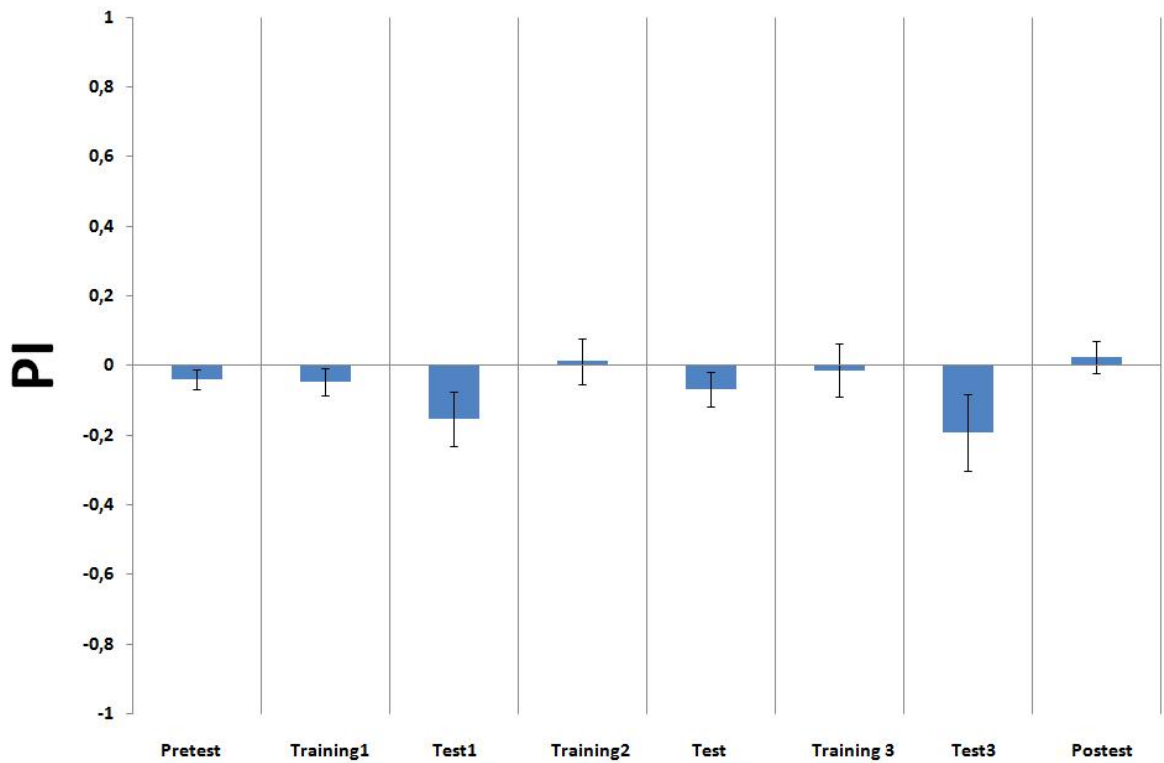


Figure 51: Performance Index of the tested fly group (dry air conditions)

A performance index was calculated for the fly group (ranging from -1 for 100% avoidance, to 1 for 100% attraction towards the punished side) for each phase of the experiment respectively. Performance index incorporates reciprocal preference experiments, in order to eliminate naive side preference of individual flies. In each phase of the experiment the flies showed no significant (One-sample-t-test, fixed value=0, $p > 0,05$, $n=10$) divergence from chance level preference (0).

Results

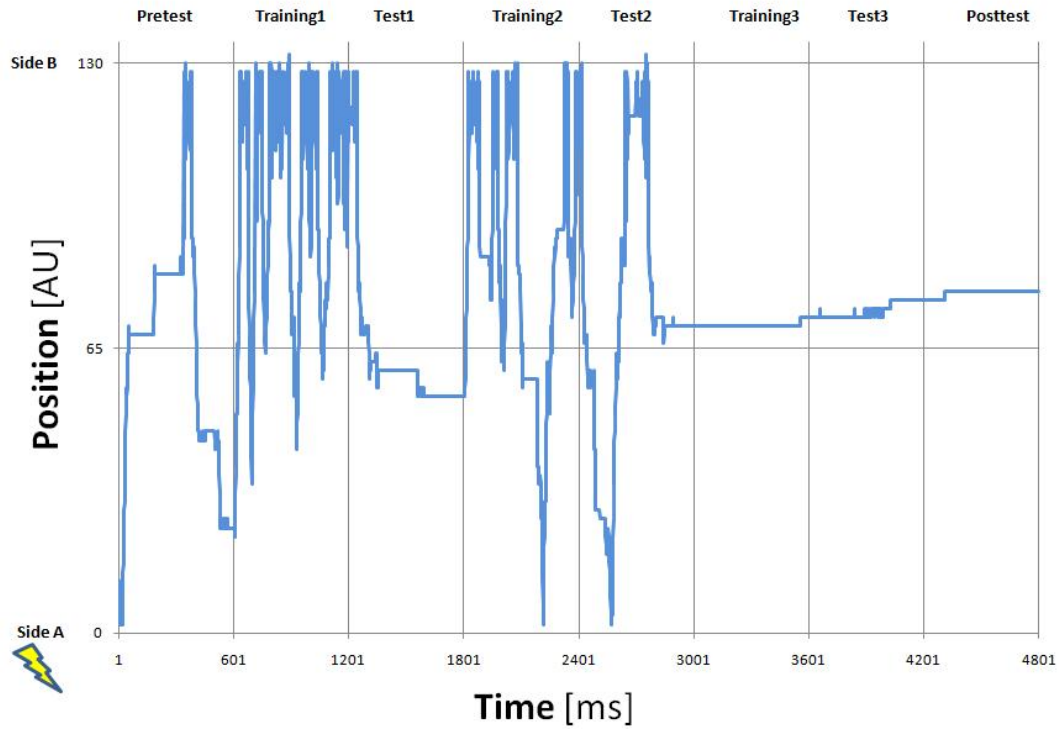


Figure 52: Spatiotemporal dynamics of fly movement under humid air and increased voltage conditions (punished side A)

Typical case, displaying avoidance behaviour, the fly patrols in the pretest phase and starts to avoid the punished side during training, avoidance behaviour is persistent in the test phase. Punishment was applied upon entering the chamber side A (Position 0-65). The absolute position of the fly during each time step is plotted on the ordinata, while the abscissa displays the time.

Results

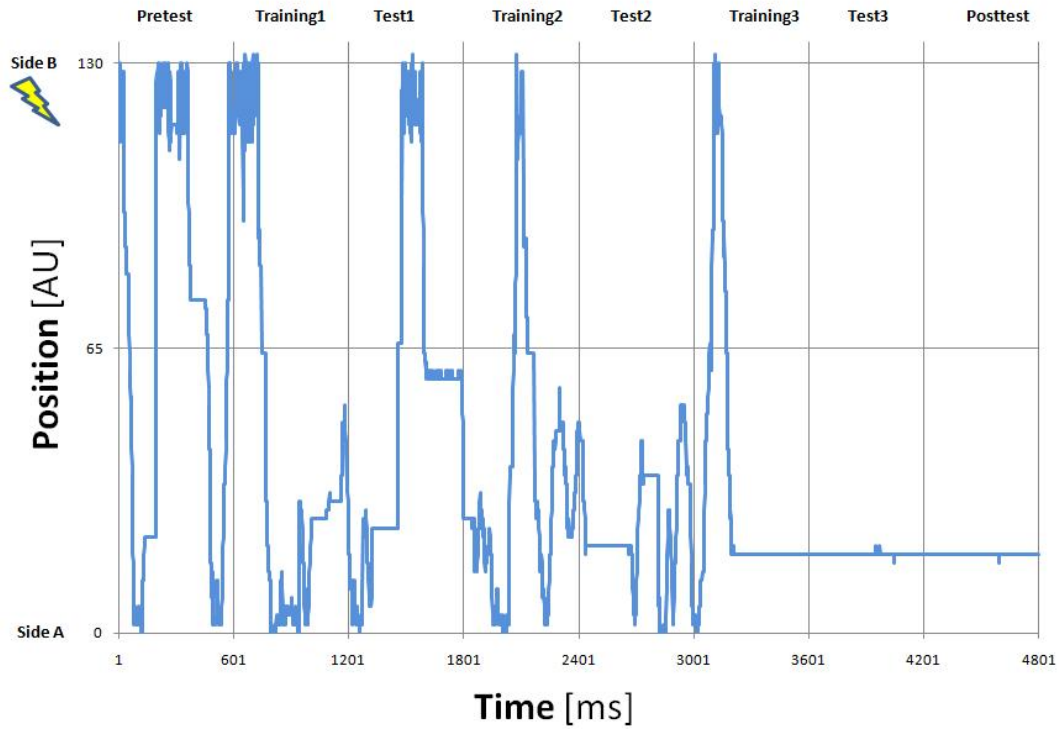


Figure 53: dynamics of fly movement under humid air and increased voltage conditions (punished side B)

Typical case, displaying avoidance behaviour, the fly patrols in the pretest phase and starts to avoid the punished side during training, avoidance behaviour is persistent in the test phase. Punishment was applied upon entering the left chamber side B (Position 0-65). The absolute position of the fly during each time step is plotted on the ordinata, while the abscissa displays the time.

Results

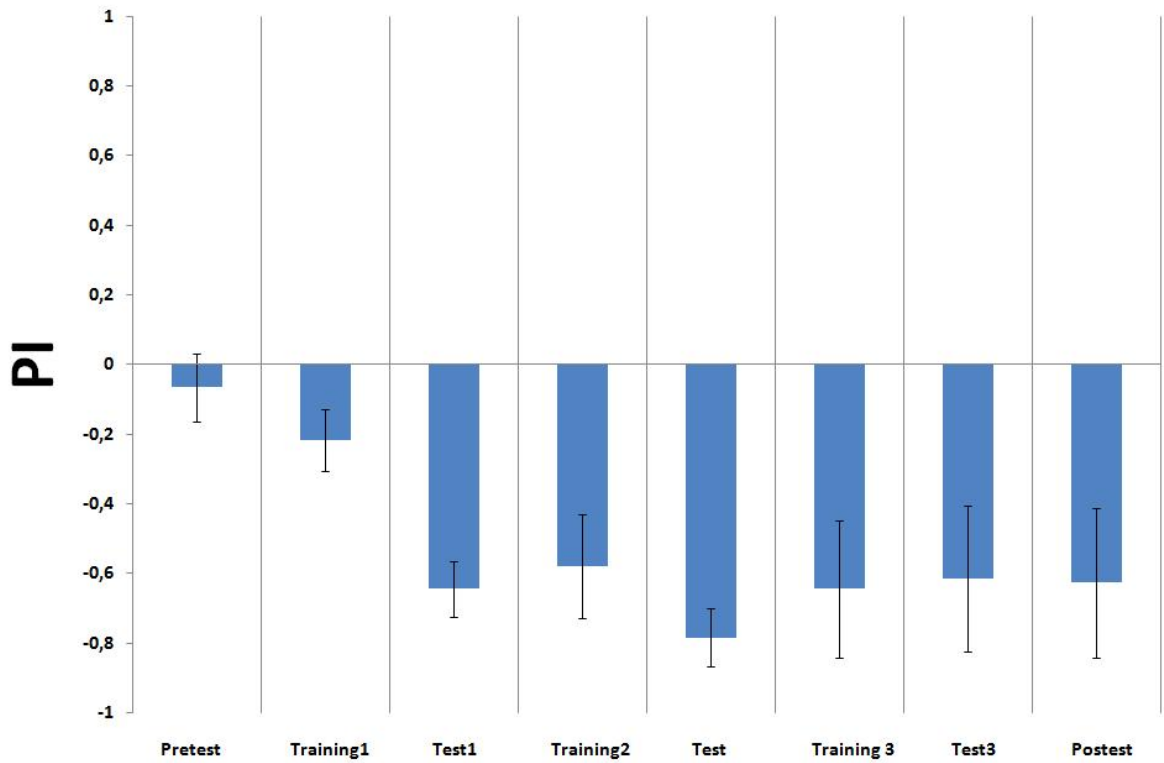


Figure 54: Performance Index of the tested fly group (humid air increased voltage conditions)

A performance index was calculated for the fly group (ranging from -1 for 100% avoidance, to 1 for 100% attraction towards the punished side) for each phase of the experiment respectively. Performance index incorporates reciprocal preference experiments, in order to eliminate naive side preference of individual flies. In each phase of the experiment, excluding the pretest phase, the flies showed avoidance of the punished side, significantly (One-sample-t-test, fixed value=0, $p < 0,05$, $n=10$) diverging from chance level preference (0).

6. Discussion

6.1. cAMP Imaging

Results presented in this study support the current working model of STM acquisition via a cAMP dependent Pathway

The greatest advantage of genetically encoded fluorescent reporters is the possibility to selectively monitor distinct populations of cells in which the probes can be selectively expressed. Such an endeavour would be extremely difficult by conventional imaging utilising dyes. The main goal of this study was visualising and monitoring the intracellular activity, leading to formation of short term memory and thus underlies the learning behaviour. To be meaningful, these experiments had to be done in an as intact as possible animal, able to react towards external stimuli. Novel sensor proteins are usually tested in cell culture or thin slices of tissue, which allow for easy application of pharmaceuticals and can be done under very controlled optical conditions when compared to application to *in vivo* specimens. Such sensor characterisation experiments usually give first data about the signal strength, fluorescence intensity and bleaching qualities of the sensor proteins.

Optical recordings in an intact, behaving animal, are prone to a whole set of complicating issues, like movements of the imaged tissue, induced by muscle contractions or fluid movements. The three dimensional nature of the live specimen furthers the problems of the method, restricting access to particular cell clusters, which is not the case in an approximately two dimensional cell culture setting. In addition such characterisation studies often record strong responses because they work with concentrations of pharmaceuticals exceeding the physiological ranges by several orders of magnitude, whereas the cellular responses to physiological stimuli can be comparatively low. Therefore experiments performed in cell culture, while providing important information about the quality and various properties of sensors used, give little relevant information, about the actual processes within the intact organisms. In addition the basis fluorescence intensity of the sensor has to be strong enough to permeate intervening tissue and still be discernable from auto-fluorescent sources and be robust enough towards fluctuations of fluorescence intensity and movement artefacts within the experimental specimen, thus requiring a high signal to noise ratio. Furthermore sensor sensitivity towards concentration changes of the observed molecules and ions has to

Discussion

correspond to physiological range. Whereas studies involving fluorescent reporters are meanwhile very common in cell culture, isolated tissue, and even dissected brains, the technique of *in vivo* imaging is still relatively new.

In this study a comparative analysis of *in vivo* suitability of several transgenic fly lines featuring various sensor types was performed. The sensor types used were Epac1, Epac2, Epac2 K390E and HCN2. The Epac based sensors feature a cAMP binding domain of the Epac-Protein (exchange protein activated by cAMP) fused to two fluorophores eYFP and eCFP. The HCN2 based sensor in turn features the cAMP binding domain of a channel protein usually found in pacemaker cells of the heart, fused to the same fluorophores. Upon a cAMP binding event the sensor undergoes a conformational change resulting in a loss of FRET between the two fluorophores, discernable in the ratio of fluorescence intensities. *Drosophila melanogaster* represents an ideal model organism to test the sensor under *in vivo* conditions, because it provides a powerful tool by transgenic probe expression in form of the Gal4-UAS System (Duffy 2002), which allows for a relative ease of comparative testing of various sensor lines. Multiple transgenic fly lines featuring the respective sensor constructs fused to a UAS sequence were generated by A.Fiala. Due to the random nature of transgene insertion, the quality of the sensor fluorescence can vary between transgenic lines. For each group of fly lines featuring the same sensor type, an attempt was made to find at least one line with a signal quality suitable for further *in vivo* experiments (Fig. 22). This was not possible for the fly lines featuring Epac2K390E and HCN2 constructs respectively, as the signal quality in those fly lines was far below the quality required to provide images suitable for further post processing by the alignment software.

To circumvent this issue an attempt was made to generate fly lines featuring several copies of the transgenes in the same animal, as it was previously reported, that multiple copies of the UAS-transgene lead to an increase in fluorescence intensity and hence to an increase in the signal strength. This was verified for flies featuring the tetrameric cAMP sensor PKA FRET (Figs 23,34). Utilising balancer chromosomes and transgenic lines with construct insertions on different chromosomes, several lines featuring two copies of the respective sensor construct were generated. This attempt was successful for all transgenic constructs with the exception of the lines featuring two copies of the HCN2 sensor transgene, as those still displayed signal strengths far below acceptable levels and thus were not used in further experiments. While a general signal strength improvement was detected in flies combining two sensors in comparison to the parental lines featuring single sensor constructs, a particular improvement was registered for the recombinants of Epac2K390E,

Discussion

whereas the recombinant Epac1 line stemming from the Epac1.2 and Epac1.3 (Fig. 36) lines showed no significant increase in signal strength, when compared to the best candidate of the preliminary screening, the Epac1.5 line (Fig. 23). Functional viability of the sensor in recombinant lines was verified by means of pharmacological application of Forskolin (Data not shown).

Based upon these qualitative screening experiments the fly line number 5 featuring the Epac1 construct (Epac1.5) was used in all further studies, due to the strongest reproducible signal strength. To characterise both the sensor viability and the cyclase activity *in vivo* a series of experiments featuring application of various pharmaceuticals was performed. Upon applying two different concentrations of 8-Bromo-cAMP, a membrane permeable and comparatively stable cAMP variant, different response strengths of the sensor were recorded (Fig. 24). Dose-dependent responses are generally considered proof for the specificity of the effects.

Via pharmacological application of Forskolin it was possible to record the putative maximal change in the cAMP concentration, as Forskolin leads to activation of all adenylyl cyclase types in the cell (de Souza et. al 1983). Upon application of 50 μ M Forskolin solution, decrease in FRET of 20%-30% could be recorded which, assuming a linear relation between FRET and cAMP concentration, indicates a net increase of 20-30% in the level of cAMP(Fig. 25). Interestingly these results correspond to findings related to cAMP activity not only in the Kenyon cells of the mushroom bodies (Tomchick et al., 2009) but also in a subset of clock neurons (Shafer et al. 2008). Therefore it was expected that applications of pharmaceuticals and stimuli activating only a single or a subset of cyclase types, would lead to comparatively smaller change in the cAMP level. This was indeed observed (Figs. 26,30). Carrier controls (Figs. 26,27) demonstrated the specificity of the effects.

In general the dynamics of changes in cAMP concentration in response to application of pharmaceuticals interacting with the adenylyl cyclases either directly as in the case of Forskolin or indirectly via G-protein coupled receptors (dopamine, octopamine) (Schwärzel et al., 2003), correspond with the previously reported cAMP dynamics in cases of similar pharmacological stimulation (Tomchik et al., 2009, Gervasi et al., 2010). Similar low speed of the change in cAMP concentration was reported both in the mushroom body Kenyon cells (Gervasi et al., 2010) and circadian clock neurons (Schafer et al. 2008). In both studies pharmaceuticals were applied to the brain via baths. In the case of the more targeted application via micropipettes (Tomchik et al., 2009) changes in cAMP concentration occurred slightly faster. The cAMP concentration in the specimen

Discussion

gradually increases until reaching an asymptotic state, with the exact amount of the increase depending heavily upon the applied substance.

In each case of pharmacological application an application artefact was observed, probably caused by the shadow of the pipette tip crossing the dissected area and blocking the optical path for the fluorescence.

The recorded images were focused on the medial lobes of the mushroom bodies as especially the γ -lobes have been reported to play an important role in the memory acquisition phase (Zars et al., 2000; Mc Guire et al. 2001, Mc Guire et al. 2003). Therefore results of this study reflect primarily the cAMP dynamics within the medial lobes, whereas recent studies focus primarily on cAMP dynamics in the vertical lobes (Tomchik et al., 2009; Gervasi et al., 2010).

Octopamine and dopamine were applied pharmacologically, as those substances are well known to act as aversive or appetitive reinforcers able to produce associative memory (Hammer 1997; Hammer & Menzel 1998). In accordance with the proposed model of short term memory formation (Heisenberg, 2003; Gerber et al. 2004), it was expected that the animals respond to physiological punishment in form of electric shock by an increase of cAMP concentration, due to mediation of punishment to the adenylyl cyclase of the Kenyon cells via the dopaminergic system (Schwärzel et al. 2003), whereas a physiological olfactory stimulus mediated to the region of the mushroom body calyx might result in stimulation of the cyclase only in a limited number of Kenyon cells. Application of electric shock (Fig. 32) leads to a clear increase in the cAMP levels, however the increase is prolonged and displays the dynamics similar to those observed for applications of pharmaceuticals, at the moment reasons for such prolonged activation are unclear, as there are no comparable in vivo studies with application of physiological stimuli so far, only experiments using pharmacological baths (Gervasi et al., 2010) and microinjections (Tomchik et al., 2009) have been published. To check whether this effect is due to the death of the fly by electrocution, as large portions of fly body were in contact with the shock wires during application, after the application of electric shock flies were removed from the apparatus and checked for tactile responsiveness by gently touching the flies feet with a brush. Data from nonresponsive flies was discarded. Therefore it can likely be excluded, that the prolonged increase in cAMP concentration after the application of electric shock is produced by lethal damage to the fly.

Application of simple odorants like methylcyclohexanol (Fig. 30) and 3-octanol (Fig. 31) did not result in an increase in the cAMP level when compared to the pooled controls (Fig. 33). This fact is not in

conflict with the current working model however. Although the sensor expression driven by the MB-247 Gal4 driver does not mark all of the Kenyon cells, it encompasses about a half of them (Gerber et al., 2004). Therefore according to the sparse code model (Heisenberg, 2003) a Ca^{2+} influx due to presentation of an odorant is expected in just a small subset of Kenyon cells (Wang et al., 2004), probably not more than 10 or 20 (Heisenberg personal communication). An odour evoked increase in the cAMP level, due to the cyclase activation in those cells would therefore be expected only in a signal of about 1-2% of that, if all observed neurons expressing the sensor would be activated. Such a small signal would in most cases be below the noise level of the setup, thus it is not surprising, that no clear response to the application of odorants could be observed. A much higher signal to noise ratio would be required in order to show the actual impact of simple odorant presentation on the cAMP levels in the Kenyon cells. Previously discussed improvement in the form of introducing several UAS-sensor constructs into the experimental animals, as well as utilizing imaging setups allowing for greater observation precision, like two photon microscopy (Gervasi et al., 2010), might help to alleviate the limitations imposed by the approach used in this study.

To circumvent the fact odour application probably stimulates only a few Kenyon cells, a pharmacological approach was taken once again. Because the main input to the Kenyon cells is cholinergic, acetylcholine was applied to the brain in an attempt to simulate broad activation of the mushroom body via the olfactory pathway, producing a FRET signal comparable to that of dopamine and octopamine applications (Fig. 26). Finally pharmacological application of acetylcholine was combined with application of electric shock (Fig. 30). Effects of simultaneous application of both the simulated CS in form of acetylcholine and the US in form of the electric shock seem to undergo nonlinear summation in regards to changes in cAMP concentration, as the FRET signal of the combined simultaneous application is larger, than the sum of responses to application of the individual stimuli. This *in vivo* result corresponds with the findings of the Davis group (Tomchik et al. 2009), where both the US and CS were simulated via microinjections to a dissected brain. It is extremely difficult to adjudicate the temporal proximity of both US and CS on the level of the Kenyon cells, as the diffusion speed of acetylcholine to the calyx region of the mushroom bodies is unknown. Thus it is possible that in this case a situation encountered in backwards conditioning (Hammer 1997) So far the results from both pharmacological and physiological stimulation support the current working model for olfactory memory formation in *Drosophila*, and correspond to pharmacological studies of cAMP dynamics in dissected brains (Shafer et al. 2008; Tomchik et al. 2009). *In vivo* it is only possible to compare our results with a study by the Preat group (Gervasi et al. 2010), where the

Discussion

effects of pharmacological applications on PKA levels suggest cAMP dynamics similar to the presented results

To expand on the present results in the future it will be crucial to improve the fixation of the fly in the shock apparatus in order to allow reliable delivery of the odorants to the antennae of the experimental animal, thus allowing for application of both the US and the CS physiologically. In addition it is feasible to perform the experiments on *rutabaga* and *dunce* mutants to study the relevance of the calcium- and calmodulin responsive adenylyl cyclase and the cAMP phosphodiesterase for the cAMP level in Kenyon cells under CS and US application on several levels of the cAMP-PKA pathway. Of particular importance for further learning and memory studies would be the investigation of the effects of temporal changes of CS/US pairings on cAMP levels, to shed some light upon trace conditioning, backwards learning and pain relief situations (Yarali et al. 2008).

6.2. Imaging and optical activation of neurons in walking flies

Optogenetic approaches towards studying physiological processes and reactions in the experimental animals allows for an elegant solution to various problems and questions previously accessibly only through complex electrophysiological or biochemical studies. Whereas recording of intracellular activity and concentration dynamics of various molecules in response to external stimuli can be monitored to a great extent, as shown in the previous chapter, manipulation of intra and intercellular events can also be achieved by optogenetic means (Schroll et al., 2006). According to the protocerebral bridge model presented by Strauss (Stauss et al., 2010), localised neuronal activity in the glomeruli on just one side of the protocerebral bridge should lead to the shortening of steps on the contralateral body side. In the presented experiments, an attempt was made to activate one side of protocerebral bridge, dissecting the head of the fly and thus making the bridge neurons accessible for optical activation. Dissected flies showed reliable activity up to 30 minutes after the dissection procedure.

This study shows that by selective expression of ChR2 tagged with a fluorescent protein as a marker in the neurons of interest, direct application of light to specific parts of the brain under visual control is possible. However multiple copies of the UAS-construct may be necessary for improved signal strengths (Riemensperger, 2006).

The results presented here may be biased by or prone to several possible artefacts. The most pronounced problem stems from the fact that introducing the fly to the walking ball after dissection represents for the animal a stressful situation, which the flies need to habituate to. Habituation time varies immensely between individuals, and the time until the flies start to display normal walking behaviour, ranges from several minutes to up to 24 hours. The preliminary apparatus design utilised in the initial experiments proved to be prone to erroneous tracking of ball movements resulting in reduced sensitivity and sporadic data fluctuations. These tracking artefacts were eliminated by repositioning the styrofoam ball closer to the sensor. The evaluation and recording software was also subsequently redesigned, providing an uncluttered data stream. The recordings show both relatively low noise of the basic condition without movement (Fig. 43) and fast, precise responsiveness of the apparatus towards actual movements of the fly (Fig. 44).

In the second set of experiments the protocol was changed to 11 minutes of mixed application, in order to accommodate for shorter stimulation and recovery times. As reported by studies in

Discussion

C. elegans and cell culture (Nagel et al. 20, Lin et al., 2009), the recovery time of Channel Rhodopsin 2 lies between 10-15 milliseconds, whereas prolonged stimulation leads to desensitisation of the channel. In addition, the mixed stimulation approach could reduce the effects of fatigue, and tissue damage allowing one to compare behavioural effects on the same time scale. On the other hand, however, neurophysiological studies on *Drosophila* neuromuscular junctions (Schroll et al., 2006) have revealed that light stimulation of neurons expressing ChR2 can cause a prolonged spiking pattern in motor neurons over several seconds of activation.

Although the averaged speeds of unidirectional movement (Fig. 45) approximated those reported by other studies (Nuwal N.,2010, Seelig et al., 2010) the observed flies did not display continuous walking behaviour, but rather short activity bouts often reversed in their direction. Putative reasons for such behaviour are probably both the stress and the novelty of the situation experienced by the experimental animal which dedicates large amounts of its activity towards exploring the limits of its impeded mobility. Therefore it is feasible to record the movement activity only after the animal is habituated to its situation, and starts to display either constant or frequent bouts of forward walking. Though in principle sporadic burst-like activity of the fly might be influenced by activation of protocerebral bridge, the model proposed by Strauss et al. addresses only cases of goal oriented forward walking and approach behaviour. Thus interpreting any effects appearing due to neuronal manipulation outside of this modus operandi is therefore difficult.

One possibility to instigate walking behaviour in the fly was recently addressed in the literature (Seelig et al., 2010) as flies with dissected heads can be forced to display optomotor behaviour while walking on the ball. It may be very worthwhile to pursue a similar approach in order to control walking bouts of the fly. As an alternative, flies can be entrained to walking by constant, long term (12h plus) exposure to the walking ball situation. The reduced impact of handling stress coupled with a long period of starvation (Buchner, personal communication) elicits reliable walking behaviour. This approach however, requires additional handling while transferring the fly to the microscope, and a drastic increase in handling stress due to the subsequent dissection, this issue can be circumvented, however, by dissecting flies prior to the walking ball exposure, and constantly refreshing the physiological solution covering the dissected area, as well as supplying it with oxygen, by a perfusion setup. As tested for a small number of animals, flies dissected by similar methods can reliably survive up to 8 hours, provided the Ringer solution is periodically exchanged every 30 minutes to prevent evaporation.

Repetition of the mixed application protocol, with habituated flies displaying frequent bouts of walking activity, could therefore be attempted. An additional asset might be utilisation of blind

Discussion

mutants such as *NorpA*⁻ (Hardy et al., 2003), such animals would not visually react to the activation stimulus, and were already successfully used in walking ball experiments (Nuwal N., 2010). Obviously, it would not be possible to instigate walking activity of such animals in the optomotor experiments. Making the necessity of alternate habituation and entraining procedures, in order to get higher number of flies showing reliable walking activity, even more pronounced.

This study has therefore provided the combined experimental groundwork and crucial preliminary testing ground for the application of optical activation, dissection, fixation, recording and evaluation of behavioural data. Further experiments are needed, however, to demonstrate the viability of the proposed model *in vivo*. In addition the described method allows for simultaneous recording of neuronal activity, if used in combination of calcium reporters coupled to fluorophores, with excitation and emission wavelengths not overlapping with the activation wavelength of ChR2. A second stimulation option could be introduced via utilisation of IR light for stimulation (Zurberg et al., 2007) while expressing heat sensitive TRP1 cation channels in the flies.

6.3. Conditioning in the “Shock Box”

One of the main disadvantages of various behavioural paradigms is their lack of flexibility in respect to the kind of learning, which can take place within the constraints of the paradigm. The paradigms allowing to monitor and subsequently quantify various kinds of behaviour and to implement both operant and classical conditioning are relatively rare, one of the prime examples being the flight simulator/torque meter paradigm (Brembs 2000, Brembs & Heisenberg 2003). For years the general trend in learning and memory research in *Drosophila* has gravitated towards mass assays such as the meanwhile classical Tully Quinn T-Maze setup (Tully & Quinn, 1985) in the case of olfactory learning, while this paradigm has repeatedly proven itself as a robust learning situation for the olfactory learning and memory, it cannot be excluded that it is prone to behavioural group effects influencing the observed learning performance.

Furthermore such paradigms tend to be functional “black-boxes”, presenting the experimenter with a binary yes/no information about the performance of the animals before and after the experiment, but withholding information about behaviour taking place during training and test phases. Although such results are well suited for statistical hypothesis tests, continuous behavioural monitoring of the experimental animals throughout the experiment may provide helpful information, allowing for better understanding of the processes of learning and memory formation, as well as for screening the experimental animals, dividing them into distinct groups, based on their individual performance and subsequently isolating them for further physiological studies.

In addition should one desire to study the influence of previous experience and conditioning upon future performance in a different conditioning and learning situation, it is crucial to reduce handling and external influence during the inter trial phases. The modular setup and differential operation modes of the Shock Box allows for application of such tiered paradigms (featuring several subsequent experiments involving different types of learning), to an even higher degree than its design predecessor the Heat Box (Wustmann et al. 1996, Putz & Heisenberg 2002).

Preliminary experiments in the Shock box without an addition of air circulation demonstrated that place learning though in principle displayed by some flies, was not reproducible on a large scale. While the majority of flies displayed no clear side preference in the test phase, and showed only sporadic reaction towards punishment during training (Fig. 47), some flies reacted aversively towards the punishing stimulus and displayed clear avoidance behaviour in the subsequent test phase (Fig.

48). Although it cannot be excluded, that flies deposited some kind of chemical signal within the punished chamber side, or marked it in some different way, utilizing the mark as a cue for further avoidance, cleaning the chamber with alcohol and drying it had no visible effect on the performance and behaviour of flies, when compared to testing flies in an uncleaned chamber. It appears that the behaviour and performance of flies varies for each individual, which is not surprising in itself. It is therefore crucial however to find a set of suitable experimental parameters including strength of electric shock, humidity, entrainment duration, number of entrainment trials, strength of the air flow within the apparatus, to produce best possible and reproducible results in a large number of individuals. In the case of humidity and shock strength it is well known, that those can heavily influence learning performance in the Tully Quinn olfactory learning paradigm (Schwärzel personal communication). It may very well be however, that the situation in the Shock Box is not particularly well suited for place learning, as the immediate onset of maximal punishment strength upon crossing into the punished chamber side is not directly comparable to the comparatively slow increase in temperature occurring in the place learning experiment in the Heat Box (Putz & Heisenberg, 2002). In addition, regarding the application of electric shock, in vertebrates it has been shown, that prolonged punishment substantially degrades not only overall performance but also specifically the learning ability (Jackson et al. 1979). Some of the tested flies were affected by the shock severely and were subsequently not able to leave the punished chamber side for some time. In such animals the disorientation due to and inescapability of such a prolonged drastic punishment might have led to a severe decrease in learning performance. It is also worth considering increasing the number of training intervals spaced by test intervals, as a single training often leads to significantly lower training performance, when compared to repetitively mixed training and test intervals (Beck et al., 2000).

After implementation of most of the mentioned experimental improvements, in a second series of place learning experiments conditioned avoidance of the punished side could be achieved both in the training and in the test phases of the experiment. Giving first indications, that place learning might indeed work with electric shock posing as a negative reinforcer (Fig. 54), additional experiments are needed however to assess the observed effects. The main asset of this study was the creation of a paradigm paving the way for additional studies on various aspects of learning ability, thus additional future experiments involving different types of learning (purely associative, purely operant).

Several new avenues are now directly open for future investigations. One is to try and find the framework requirements to reliably elicit place learning in the experimental animals. The second behavioural experiment, easily achieved without further setup modification, would be the no

Discussion

idleness paradigm, where animals are punished in case of inactivity over defined time periods, thus entraining flies to be constantly active. This particular kind of experiment proved to be extremely difficult to perform in the Heat Box paradigm, as there fly performance takes a huge hit in the course of the experiment, due to constant heat conditions (Yang, Heisenberg personal communication). The animals, however, could be more robust towards shock punishment, as the temporal dynamics of application of electric shock are much more precise than those of temperature changes in the Heat Box. Additional care should be taken in the clear division between sexes during testing, as it has been previously reported, that spatial learning performance can be gender specific (Conrad et al., 2004).

Meanwhile a paradigm based upon similar principles has been developed by the Miesenböck group, in their setup clear cases of successful olfactory learning and memory formation have been shown, it would therefore be an ideal proof of principle to repeat their experiments in the Shock Box, in order to see the functional comparison of both paradigms (Claridge-Chang et al., 2009).

Should at least two different types of learning be successfully established in the Shock Box, it would pose a very promising platform to model and to further the study depression and learned helplessness in *Drosophila*, pioneered by Brown (Brown et al., 1996) after reporting this phenomenon in the cockroach (Brown, Stroup 1988). The successful establishment of olfactory learning and memory formation in individual flies, combined with the possibility to study those animals, which showed distinctly high or low memory scores, physiologically by odour application in an imaging setup, as introduced by the Fiala group (Fiala 2002; Fiala & Spall, 2003), could finally shed some light upon the neuronal activity underlying the differences in the olfactory learning performance. In addition the application of light could easily be achieved by adding an array of diodes or a laser to the setup, which would in turn allow for immediate (in contrast to the Heat Box) heat punishment, or neuronal activation experiments utilizing ChR2, which utilises blue light, while the tracking sensor of the Shock Box is sensitive to light in the long wavelength part of the spectrum.

7. Literature

Adams MD (2000) The genome sequence of *Drosophila melanogaster*. *Science* 287:2185-2195.

Beck CDO, Schröder B & Davis RL. (2000). Learning performance of normal and mutant *Drosophila* after repeated conditioning trials with discrete stimuli. *Jour. Neurosci.* 20, 2944-2953.

Bockaert J & Pin JR. (1999). Molecular tinkering of G-Protein-coupled receptors: an evolutionary success. *EMBO Jour.* 18, 1723-1729.

Brembs B. (2003). Operant conditioning in invertebrates. *Curr Opin Neurobiol* 13:710-717.

Brembs B, Heisenberg M. (2000) The operant and the classical in conditioned orientation of *Drosophila melanogaster* at the flight simulator. *Learn Mem* 7:104-115.

Brown GE, Mitchell AL, Percy AM, Robertson CL. (1996) Learned helplessness in *Drosophila melanogaster*? *Psychol Rep* 78:962.

Brown GE, Stroup K. (1988) Learned helplessness in the cockroach (*Periplaneta americana*). *Behav Neural Biol* 50:246-250.

Buchner E. (1974) Bewegungserperzeption in einem visuellen System mit gerastertem Eingang. Thübingen 1974.

Claridge-Chang A, Roorda RD, Vrontou E, Sjulson L, Li H, Hirsh J, Miesenbock G. (2009) Writing memories with light-addressable reinforcement circuitry. *Cell* 139:405-415.

Conrad CD, Jackson JL, Wiczorek L, Baran SE, Harman JS, Wright RL, Korol DL. (2004) Acute stress impairs spatial memory in male but not female rats: influence of estrous cycle. *Pharmacol Biochem Behav* 78:569-579.

Cruse H. (2007) *Neural Networks as Cybernetic systems.* Ebook 2nd Ed. urn:nbn:de:0009-3-6153

de Souza NJ , Dohadwalla AN, Reden J (1983) Forskolin: a labdane diterpenoid with antihypertensive, positive inotropic, platelet aggregation inhibitory, and adenylate cyclase activating properties, *Med. Res. Rev.*, pp. 201–219

Duffy JB. (2002). GAL4 system in *Drosophila*: a fly geneticist's Swiss army knife. *Genesis* 34:1-15.

Fiala A, Spall T, Diegelmann S, Eisermann B, Sachse S, Devaud JM, Buchner E & Galizia CG. (2002). Genetically expressed cameleon in *Drosophila melanogaster* is used to visualize olfactory information in projection neurons. *Curr. Biol.* 12:1877-1884.

Fiala A & Spall, T. (2003). In vivo calcium imaging of brain activity in *Drosophila* by transgenic cameleon expression. *Sci. STKE* 174:PL6.

Fischer JA, Giniger E, Maniatis T, Ptashne M. (1988) GAL4 activates transcription in *Drosophila*. *Nature* 332:853-856.

von Frisch K, (1914) *Zool Jahrb. Abt. Allg. Zool. Physiol Tiere* 35, 1-182.

Gerber B, Tanimoto H & Heisenberg M. (2004). An engram found? Evaluating the evidence from fruit flies. *Curr. Opin. Neurobiol.* 14, 737-744.

Gervasi N, Tche´nio P, Preat T (2010) PKA Dynamics in a *Drosophila* Learning Center: Coincidence Detection by Rutabaga Adenylyl Cyclase and Spatial Regulation by Dunce Phosphodiesterase. *Neuron* 65, 516–529

Griesbeck O. (2004). Fluorescent proteins as sensors for cellular functions. *Curr. Opin. Neurobiol.* 14:636-641.

Hammer M. (1997). The neural basis of associative reward learning in honeybees. *Trends Neurosci.* 20 (6): 245-52.

Hammer M & Menzel R. (1998). Multiple sites of associative odor learning as revealed by local brain microinjections of octopamine in honeybees. *Learn. Mem.* 5(1-2): 146-156.

Hanesch U, Fischbach KF, and Heisenberg M. “Neuronal architecture of the central complex in *Drosophila melanogaster*,” *Cell Tissue Res.*, vol. 257, pp. 343-366, 1989.

Hardie RC, Martin F, Chyb S, Raghu P.(2003) Rescue of light responses in the *Drosophila* "null" phospholipase C mutant, *norpAP24*, by the diacylglycerol kinase mutant, *rdgA*, and by metabolic inhibition. *J Biol Chem* 278:18851-18858.

Heisenberg M. (2003). Mushroom body memoir: from maps to models. *Nat. Rev. Neurosci.* 4 (4): 266-275.

Jackson RL, Maier SF, Coon DJ. (1979) Long-term analgesic effects of inescapable shock and learned helplessness. *Science* 206:91-93.

Kandel ER (1976) Cellular basis of behavior: An introduction to behavioral neurobiology, W. H. Freeman , San Francisco

Kandel ER, Schwartz JH & Jessel TM. (2000). Principles of Neuroscience (Fourth Edition), Raven Press, New York.

Knöpfel T, Diez Garcia J & Akeman W. (2006). Optical probing of neuronal circuit dynamics: genetically encoded versus classical fluorescent sensors. *Trends in Neurosci.* 29, 3, 160-166.

Kreidl A. (1895) Ueber die Perception der Schallwellen bei den Fischen . *Archiv für die gesammte Physiologie des Menschen und der Thiere (Pflügers Archiv)* 61:450-464.

Lai SL, Lee T. (2006) Genetic mosaic with dual binary transcriptional systems in *Drosophila*. *Nat Neurosci* 9:703-709.

Lin JY, Lin MZ, Steinbach P, Tsien RY. (2009) Characterization of engineered channelrhodopsin variants with improved properties and kinetics. *Biophys J* 96:1803–1814.

Mank M, Reiff DF, Heim N, Friedrich MW, Borst A & Griesbeck O. (2006). A FRET-based calcium biosensor with fast signal kinetics and high fluorescence change. *Biophys Jour.*; 90(5):1790-6.

Martin JR, Ernst R, and Heisenberg M. “Temporal pattern of locomotor activity in *Drosophila melanogaster*,” *J. Comp. Physiol. A*, vol. 184, pp. 73-84, 1999.

McGuire SE, Le PT, Osborn AJ, Matsumoto K & Davis RL. (2003). Spatiotemporal rescue of memory dysfunction in *Drosophila*. *Science* 302, 1765-1768.

Miesenböck G. (2004). Genetic methods for illuminating the function of neural circuits. *Curr. Opin. Neurobiol.* 14, 395-402.

Miyawaki A, Griesbeck O, Heim R & Tsien RY. (1999). Dynamic and quantitative Ca²⁺ measurements using improved cameleons. *Proc. Natl. Acad. Sci. USA* 96(5), 2135-40.

Miyawaki A. (2003). Fluorescence imaging of physiological activity in complex systems using GFP-based probes. *Curr. Opin. Neurobiol.* 13, 591-596.

Nagel G, Szellas T, Huhn W, Kateriya S, Adeishvili N, Berthold P, Ollig D, Hegemann P, Bamberg E. (2003) Channelrhodopsin-2, a directly light-gated cation-selective membrane channel. *Proc Natl Acad Sci U S A* 100:13940-13945.

Neuser K, Triphan T, Mronz M, Poeck B, Strauss R. (2008) Analysis of a spatial orientation memory in *Drosophila*. *Nature* 453:1244-1247.

Nikolaev VO, Bünemann M, Hein L, Hannawacker A, Lohse MJ. (2004). Novel single chain cAMP sensors for receptor-induced signal propagation. *J Biol Chem.* 279:37215-8.

Nikolaev VO, Bünemann M, Schmitteckert E, Lohse MJ, Engelhardt S. (2006). Cyclic AMP imaging in adult cardiac myocytes reveals far-reaching beta1-adrenergic but locally confined beta2-adrenergic receptor-mediated signaling. *Circ Res.* 99:1084-91.

Nikolaev VO, Lohse MJ. (2006). Monitoring of cAMP synthesis and degradation in living cells. *Physiology (Bethesda).* 21:86-92.

Pavlov I. (1927). *Conditioned Reflexes.* (trans. Anrep GV). Oxford: Oxford Univeristy Press.

Putz G, Heisenberg M. (2002) Memories in *Drosophila* Heat-box Learning. *Learn Mem* 9:349-359.

Riemensperger T, Völler T, Stock P, Buchner E & Fiala A. (2005). Punishment Prediction by Dopaminergic Neurons in *Drosophila*. *Curr. Biol.* 15, 1953-1960.

Riemensperger T. (2006) Untersuchung prädiktiver Eigenschaften des dopaminergen Systems von *Drosophila melanogaster* mittels genetisch kodierter Calcium Sensoren.

Schwärzel M, Monastirioti M, Scholz H, Friggi-Grelin F, Birman S & Heisenberg M. (2003). Dopamine and octopamine differentiate between aversive and appetitive olfactory memories in *Drosophila*. *J. Neurosci.* 23 (33), 10495-10502.

Seelig JD, Chiappe ME, Lotti GK, Duttar A, Osborne J, Reiser MB, Jayaraman V. (2010) Two-photon calcium imaging from head-fixed *Drosophila* during optomotor walking behavior. *Nature Methods* 7, 535–540

Skinner BF. (1950) Are theories of learning necessary? *Psychol Rev* 57:193-216.

Schroll C, Riemensperger T, Bucher D, Ehmer J, Voller T, Erbguth K, Gerber B, Hendel T, Nagel G, Buchner E, Fiala A. (2006) Light-induced activation of distinct modulatory neurons triggers appetitive or aversive learning in *Drosophila* larvae. *Curr Biol* 16:1741-1747.

Spall T. (2004). Optische Visualisierung neuronaler Aktivität: Etablierung des in vivo Imaging mit dem genetisch codierten Sensor Yellow Camleon 2.1 und Untersuchung der olfaktorischen Codierung im Gehirn von *Drosophila melanogaster*. Dissertationsschrift, Fakultät: Biologie, Bayerische Julius Maximilians Universität zu Würzburg.

Strauss R, Pichler J. (1998) Persistence of orientation toward a temporarily invisible landmark in *Drosophila melanogaster*. *J Comp Physiol A* 182:411-423.

Strauss R, Berg C. (2010) The Central Control of Oriented Locomotion in Insects - Towards a Neurobiological Model. WCCI 2010 IEEE World Congress on Computational Intelligence July, 18-23, 2010 - CCIB, Barcelona, Spain

Thevenaz, P., Ruttimann, U. E. und Unser, M. (1998). "A pyramid approach to subpixel registration based on intensity." *IEEE Trans Image Process* 7(1): 27-41.

Thorndike E. (1898) Some Experiments on Animal Intelligence. *Science* 7:818-824.

Tomchik SM, Davis RL. (2008) Behavioral neuroscience: Out of sight, but not out of mind. *Nature* 453:1192-1194.

Tsien RY. (1998). The green fluorescent protein. *Annu. Rev. Biochem.* 67:509-44.

Tully T & Quinn WG. (1985). Classical conditioning and retention in normal and mutant *Drosophila melanogaster*. *Jour. Comp. Physiol. [A]*. 157 (2), 263-277.

Völler T. (2008) Visualisierung und Manipulation neuronaler Aktivitäten im Gehirn von *Drosophila melanogaster*

Wang Y, Guo HF, Pologruto TA, Hannan F, Hakker I, Svoboda K & Zhong Y. (2004). Stereotyped odor-evoked activity in the mushroom body of *Drosophila* revealed by green fluorescent protein-based Ca²⁺ imaging. *Jour. Neurosci.* 24, 6507-6514.

Wustmann G, Rein K, Wolf R, Heisenberg M. (1996) A new paradigm for operant conditioning of *Drosophila melanogaster*. *J Comp Physiol A* 179:429-436.

Zars T, Fischer M, Schulz R & Heisenberg M. (2000). Localization of a short-term memory in *Drosophila*. *Science* 288, 672-675.

Zurborg S, Yurgionas B, Jira JA, Caspani O, Heppenstall PA (2007) Direct activation of the ion channel TRPA1 by Ca²⁺. *Nat Neurosci* 10:277-279.

8. Curriculum Vitae

Persönliche Daten

Vor- und Zuname: Alexander Kapustjansky (geb. Kapustjanskij)

Adresse: Hauptstrasse 80, 97218 Gerbrunn

Telefon:

e-mail-Adresse:

Staatsangehörigkeit: deutsch

Geburtsdaten: 01. Januar 1979 in Winnica/Ukraine

Berufliche Qualifikation

seit 03/2007 Diplombiologe (Mag. rer. nat.)

Schulische Ausbildung

1985 – 1988 Grundschule, Winnica/Ukraine

1988 – 1994 Allgemeinbildende Schule, Winnica/Ukraine

1994 – 1994 Mönchsberg Volksschule, Würzburg

1994 – 1999 Deutschhaus Gymnasium, Würzburg
Abschluss: Abitur

Studium

1999 – 2004	Diplomstudium der Biologie, Universität Würzburg
2004 – 2006	Studium der Biologie/Chemie für das Gymnasiallehramt, Universität Würzburg
2006 – 2007	Diplomstudium der Biologie, Universität Wien Abschluss: Diplom (Mag. rer. nat.)

Berufserfahrungen

1999 – 2000	Mitarbeiter für Technik und Vertrieb bei Comtech GmbH
2000-2006	Wissenschaftliche Hilfskraft im Bereich der Soziobiologie und Tierphysiologie an der Universität Würzburg
2006-2007	Wissenschaftliche Hilfskraft im Bereich der Evolutionsbiologie an der Universität Wien
2007-2011	Wissenschaftliche Hilfskraft im Bereich der Genetik und Neurobiologie an der Universität Würzburg
2005-2011	Freiberuflicher Übersetzer und Dolmetscher für Deutsch/Englisch/Russisch auf Honorarbasis
2006-2011	Freiberuflicher Web und Grafik Designer auf Honorarbasis

Sprachkenntnisse

Deutsch fließend

Englisch fließend

Russisch fließend

Ukrainisch fließend

Polnisch in Wort und Schrift

9. Acknowledgements

I would like to express my sincere gratitude to some people, who were crucial for the completion of this work.

First of all, to Prof. Dr. Erich Buchner for providing unparalleled support and supervision throughout the whole project. Sharing ideas and insights, nudging me in the right direction and always taking time and effort, to provide me with the best possible answers to my innumerable questions and queries. Without him, this thesis would not be possible.

I would like to thank Prof. Dr. Martin Heisenberg not only for being my co-supervisor and creating an incredibly stimulating scientific working environment I am truly proud to have been part of, for numerous discussion rounds, opportunities to develop new ideas and for introducing me to the world of fly cognition, but also for providing support, when everything seemed grim and hopeless.

To Prof. Dr. Wolfgang Rössler for showing genuine interest in the scientific principles of my work to and agreeing to bridge the gap to a different model organism and become my second supervisor and referee of this manuscript.

I would like to extend my thanks to Prof. Dr. André Fiala, who provided the core idea of this project and introduced me to important techniques and methods in the initial phase of my thesis and always had helpful suggestions guide my work.

I would like to give my special thanks to Prof. Dr. Henrike Scholz, who introduced me to the world of fly neurobiology, and allowed me to start as a PhD student in Würzburg.

To Prof. Dr. Charlotte Förster for interest in my ongoing work and for giving me a chance to continue, what I started under the guidance of others, as a member of her new institute.

My very special thanks to the often unsung heroes of the scientific progress, the people whose input, work and efforts, made many of the experimental setups possible in the first place: Konrad Öchsner, Hans Kaderschabek, Benjamin Schmid and Andreas Eckart.

To Benjamin, yet again, Birgit, Claire, Narendra, Nidhi and Tulip, it just seems right to mention you together despite alphabetical order, Marlene, Partho, Sophie, Sven, Tilman, Yi Chun, and all the other members of the Institute, both old and new, the list would be just too long, to mention everybody explicitly, all of you have contributed to a working environment, which yet has to find its equal, thank you.

Last but not least, I would like to thank my parents for always being there for me, both through the bright and very dark moments of those 3 years. It is only due to them, that I was ever able to reach the point of my life, I am currently at.